DEVELOPMENT OF THE SIMPLIFIED METHOD FOR INTERNAL STABILITY DESIGN OF MECHANICALLY STABILIZED EARTH WALLS

by

Tony Allen, PE
Washington State Department of Transportation
FOSSC Materials Laboratory Geotechnical Branch
Olympia, Washington

Barry Christopher, Ph.D., PE
Consultant
Roswell, Georgia

Victor Elias, PE
Consultant
Bethesda, Maryland

Jerry DiMaggio, PE
Federal Highway Administration
Office of Bridge Technology
Washington, DC

Prepared for

Washington State Department of Transportation
and in cooperation with
US Department of Transportation
Federal Highway Administration

June 2001

TECHNICAL REPORT STANDARD TITLE PAGE

1. REPORT NO. WA-RD 513.1	2. GOVERNMENT ACCESSION NO.	3. RECIPIENT'S CATALOG NO.
4. TITLE AND SUBTITLE Development of the Simplified Method for Internal Stability Design of Mechanically Stabilized Earth Walls		5. REPORT DATE July 2001
		6. PERFORMING ORGANIZATION CODE
7. AUTHOR(S) Tony Allen, Barry Christopher, Victor Elias, Jerry DeMaggio		8. PERFORMING ORGANIZATION REPORT NO.
9. PERFORMING ORGANIZATION NAME AND ADDRESS Washington State Department of Transportation Transportation Building, MS 47370 Olympia, Washington 98504-7370		10. WORK UNIT NO.
		11. CONTRACT OR GRANT NO.
12. SPONSORING AGENCY NAME AND ADDRESS Research Office Washington State Department of Transportation Transportation Building, MS 47370 Olympia, Washington 98504-7370		13. TYPE OF REPORT AND PERIOD COVERED Research report
		14. SPONSORING AGENCY CODE
15. SUPPLEMENTARY NOTES This study was conducted in cooperation with the U.S. Department of Transportation, Federal Highway Administration.		

16. ABSTRACT

In 1994, a technical working group under the auspices of the T-15 Technical Committee on Substructures and Walls of the American Association of State Highway and Transportation Officials (AASHTO) Bridge Subcommittee, was formed to reevaluate the design specifications for mechanically stabilized earth (MSE) walls contained in the AASHTO Standard Specifications for Highway Bridges (1996). One of the areas of focus was the internal stability design of MSE walls. Several methods for calculating the backfill reinforcement loads were available at that time in the AASHTO Standard Specifications, and the intent was to unify the design methods to simplify and clarify the specifications. To accomplish this, full-scale MSE wall case history data were gathered and analyzed so that the unified method developed could be calibrated to the empirical data, since all of the methods available were empirical in nature. The effect of simplifications in the method, such as how vertical soil stresses are calculated and how reinforcement stiffness is considered in the design, could also be evaluated with these full-scale wall data to ensure that the unified method developed was adequately accurate. From this effort, the AASHTO Simplified Method was developed.

This report summarizes the development of the Simplified Method. It uses a number of full-scale MSE wall case histories to compare the prediction accuracy of the Simplified Method to that of the other methods currently available and focuses primarily on steel reinforced MSE walls. The theoretical assumptions used by the Simplified Method, as well as the other methods, are also evaluated and compared in light of the empirical evidence. This evaluation showed that the prediction accuracy of the Simplified Method is at least as good as that of the other methods, while the Simplified Method still simplifies calculations. This evaluation also showed, however, that all of the methods have limitations that must be considered.

17. KEY WORDS Soil reinforcement, mechanically stabilized earth walls, MSE walls, earth pressure, stability, sands, loads	18. DISTRIBUTION STATEMENT No restrictions. This document is available to the public through the National Technical Information Service, Springfield, VA 22616		
19. SECURITY CLASSIF. (of this report) None	20. SECURITY CLASSIF. (of this page) None	21. NO. OF PAGES	22. PRICE

DISCLAIMER

The contents of this report reflect the views of the authors, who are responsible for the facts and the accuracy of the data presented herein. The contents do not necessarily reflect the official views or policies of the Washington State Transportation Commission, Department of Transportation, or the Federal Highway Administration. This report does not constitute a standard, specification, or regulation.

TABLE OF CONTENTS

FIGURES

TABLES

EXECUTIVE SUMMARY

In 1994, a Technical Working Group under the auspices of the T-15 Technical Committee on Substructures and Walls of the American Association of State Highway and Transportation Officials (AASHTO) Bridge Subcommittee, was formed to reevaluate the design specifications for mechanically stabilized earth (MSE) walls contained in the AASHTO Standard Specifications for Highway Bridges (1996). One of the areas of focus was the internal stability design of MSE walls. Several methods for calculating the backfill reinforcement loads were available at that time in the AASHTO Standard Specifications, and the intent was to unify the design methods to simplify and clarify the specifications. To accomplish this, full-scale MSE wall case history data were gathered and analyzed so that the unified method developed could be calibrated to the empirical data, since all of the methods available were empirical in nature. The effect of simplifications in the method, such as how vertical soil stresses are calculated and how reinforcement stiffness is considered in the design, could also be evaluated with these full-scale wall data to ensure that the unified method developed was adequately accurate. From this effort, the AASHTO Simplified Method was developed.

This paper summarizes the development of the Simplified Method. It uses a number of full-scale MSE wall case histories to compare the prediction accuracy of the Simplified Method to that of the other methods currently available and focuses primarily on steel reinforced MSE walls. The theoretical assumptions used by the Simplified Method, as well as the other methods, are also evaluated and compared in light of the empirical evidence. This evaluation showed that the prediction accuracy of the Simplified Method is at least as good as that of the other methods, while the Simplified Method still simplifies calculations. This evaluation also showed, however, that all of the methods have limitations that must be considered.

THE PROBLEM

In 1994, a Technical Working Group (TWG) under the auspices of the T-15 Technical Committee on Substructures and Walls of the American Association of State Highway and Transportation Officials (AASHTO) Bridge Subcommittee, was formed to reevaluate the design specifications for mechanically stabilized earth (MSE) walls contained in the AASHTO Standard Specifications for Highway Bridges (1996). A number of state transportation departments were having difficulty evaluating a rapidly increasing variety of new proprietary MSE wall systems because of a the lack of adequate technical guidance in the AASHTO design code at that time, especially as some of the wall systems did not seem to agree with the technical code requirements. The need to update the design specifications increased as a result of recommendations provided by Christopher et al. (1990), which documented the results of a major FHWA project to evaluate this very issue. This study provided a new approach to designing the internal stability of MSE walls, utilizing the global stiffness of the soil reinforcements to estimate the reinforcement loads. At that time, and up through the 1996 AASHTO specifications, the tieback wedge or Coherent Gravity approaches were used to estimate stresses in MSE walls, with some variation to account for different reinforcement types (Mitchell and Villet, 1987; Berg et al., 1998), although the FHWA Structure Stiffness Method was added to the AASHTO Standard Specifications in 1994 as an acceptable alternative method.

The AASHTO Bridge T-15 Technical Committee wanted to incorporate the new developments in the internal stress design of MSE walls with the previous technology and to adapt the design code requirements to the new MSE wall systems. Accomplishing this required the involvement of the major MSE wall suppliers, as well as national technical experts on MSE wall design. Concurrent to the AASHTO effort, the FHWA developed a training manual for the design of MSE walls and reinforced slopes (Elias and Christopher, 1997). Resources were combined to address the needs of both AASHTO and the FHWA to produce a consistent design protocol for MSE wall design. One of the key areas of controversy to be resolved was the calculation of internal reinforcement stresses. Data from full-scale MSE wall case histories were gathered and analyzed for

this combined effort to evaluate existing methods of calculating reinforcement stresses and to modify or develop a new combined approach to estimating reinforcement stresses. This resulted in the Simplified Method provided in the current AASHTO Standard Specifications for Highway Bridges (1999).

This paper summarizes the development history and basis for the Simplified Method. It also discusses a comparison of the method to other methods found in US design codes and guidelines. The case history data used to develop the Simplified Method include wall geometry, material properties, reinforcement details, construction details, and measured reinforcement loads. The primary focus of this paper is on steel reinforced MSE walls with granular backfills. Though the Simplified Method does include the design of geosynthetic reinforced systems, only general aspects of geosynthetic wall design using the Simplified Method will be addressed to keep the scope of the paper manageable.

BACKGROUND ON INTERNAL STABILITY DESIGN METHODS

The three primary methods existing in design codes and guidelines at the time of the development of the Simplified Method included the Coherent Gravity Method (AASHTO, 1996), the Tieback Wedge Method (AASHTO, 1996), and the FHWA Structure Stiffness Method (Christopher et al., 1990). These three empirical methods were the focus of the TWG and FHWA efforts. The differences in the predictions from these methods are the result of both differences in the case studies used to develop each method and differences in the assumptions for each method. All three methods also use limit equilibrium concepts to develop the design model but working stress observations to adjust the models to fit what has been observed in full-scale structures. Small-scale gravity and centrifuge models taken to failure have been used to evaluate design models at true limit equilibrium conditions (Juran and Schlosser, 1978; Adib, 1988; Christopher, 1993).

COHERENT GRAVITY METHOD

This method was originally developed by Juran and Schlosser (1978), Schlosser (1978), and Schlosser and Segrestin (1979) to estimate reinforcement stresses for steel strip reinforced precast panel-faced MSE walls. They utilized the concepts developed by Meyerhof (1953) to determine the vertical pressure beneath an eccentrically loaded concrete footing. Meyerhof's approach was applied to the reinforced soil mass at each reinforcement level and the wall base by assuming that the reinforced soil mass behaves as a rigid body, allowing the lateral load acting at the back of the reinforced soil zone to increase the vertical stress by overturning the moment to greater than γZ. The lateral stress carried by the reinforcement was determined by applying to the vertical stress a lateral earth pressure coefficient calculated from the soil friction angle. The stress carried by each reinforcement was assumed to be equal to the lateral soil stress over the tributary area for each reinforcement. This was based on the assumption that the reinforcement fully supports the near vertical face of the wall, that it is, in essence, a tieback.

This lateral earth pressure coefficient was assumed to be K_o at the top of the wall, decreasing to K_a at a depth of 6 m below the wall top. K_o conditions were assumed at the

wall top because of potential locked-in-compaction stresses, as well as the presence of lateral restraint from the relatively stiff reinforcement material, which was assumed to prevent active stress conditions from developing. With depth below the wall top, the method assumes that these locked-in-compaction stresses are overcome by the overburden stress, and deformations become great enough to mobilize active stress conditions. These assumptions were verified at the time, at least observationally, on the basis of measurements from full-scale walls, as shown in Figure 1. All walls were steel strip reinforced with precast concrete facing panels (Schlosser, 1978). The data in Figure 1 are presented as a K_r/K_a ratio, and from this, as well as the theoretical concepts mentioned above, Schlosser (1978) concluded that K_o and K_a could be used directly as lateral earth pressure coefficients for the design of MSE walls. Note, however, that the equation typically used to calculate K_o was derived for normally consolidated soils, and compaction would tend to make the soil behave as if it were overconsolidated.

The design methodology is summarized in equations 1 through 6, and figures 2 and 3. Other MSE wall systems such as bar mat reinforced walls (Neely, 1993) and geogrid reinforced walls (from 1983 to 1987) (Netlon, 1983) adopted this design methodology. Welded wire MSE wall systems initially used a pseudo tieback-wedge method (Mitchell and Villet, 1987; Anderson et al., 1987). Welded wire MSE wall systems typically used a higher lateral stress than the Coherent Gravity model based on full-scale instrumented structures (Mitchell and Villet, 1987). However, once AASHTO adopted the Coherent Gravity model without distinction for reinforcement type, the welded wire wall systems shifted to that methodology.

$$T_{\max} = S_v R_c \left(\boldsymbol{s}_v \ K_r \ \right) \tag{1}$$

$$\boldsymbol{s}_v = \frac{V_1 + V_2 + F_T \sin \boldsymbol{b}}{L - 2e} \tag{2}$$

$$e = \frac{F_T (\cos \boldsymbol{b}) h / 3 - F_T (\sin \boldsymbol{b}) L / 2 - V_2 (L / 6)}{V_1 + V_2 + F_T \sin \boldsymbol{b}} \tag{3}$$

$$K_o = 1 - \sin \boldsymbol{f} \tag{4}$$

$$K_a = Tan^2 (45 - \boldsymbol{f}/2) \tag{5}$$

$$H_1 = H + \frac{Tan\boldsymbol{b} \times 0.3H}{1 - 0.3Tan\boldsymbol{b}} \tag{6}$$

where T_{max} is the peak reinforcement load at each reinforcement level, S_v is vertical spacing of the reinforcement, R_c is the reinforcement coverage ratio (reinforcement unit width/horizontal spacing of reinforcements), σ_v is the vertical stress at each reinforcement level as determined from equations 2 and 3, K_r varies from K_o to K_a based on the reinforcement zone soil properties as shown in Figure 3 (K_a is determined by assuming a horizontal backslope and no wall friction in all cases), ϕ is the reinforced backfill peak soil friction angle, e is the resultant force eccentricity, and all other variables are as shown in Figure 2.
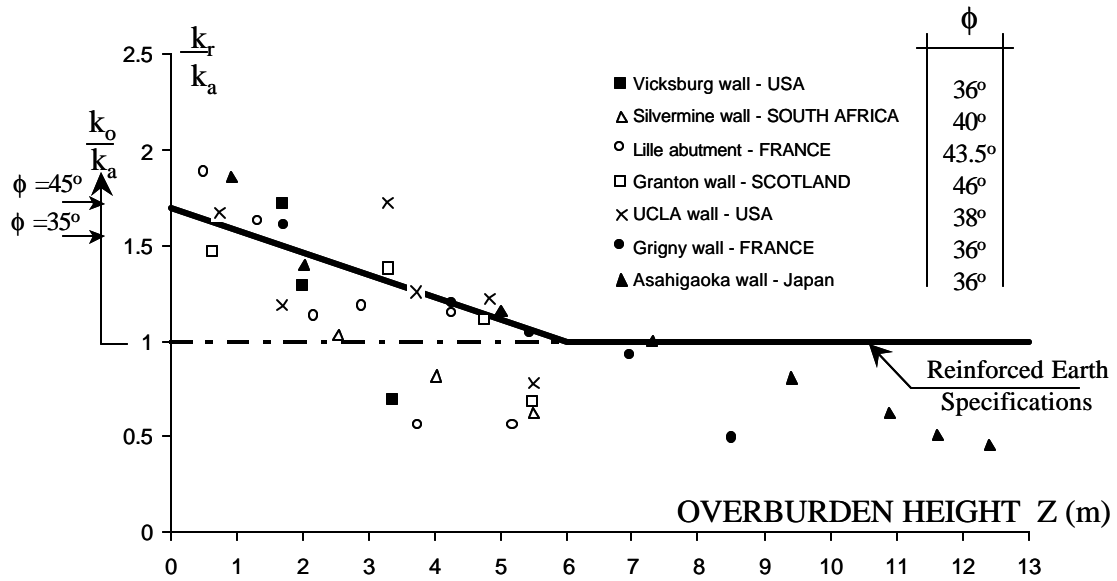
Figure 1. Variation of K_r/K_a for steel strip reinforced walls (adopted from Schlosser, 1978).

5
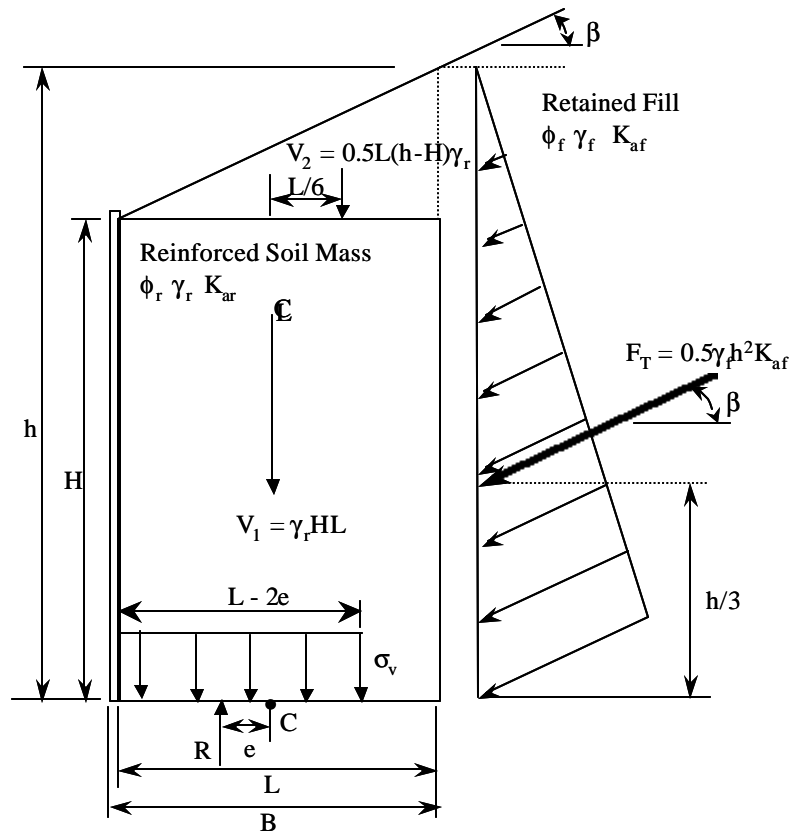
Figure 2. Forces and stresses for calculating Meyerhof vertical stress distribution in MSE walls (adopted from AASHTO, 1999).
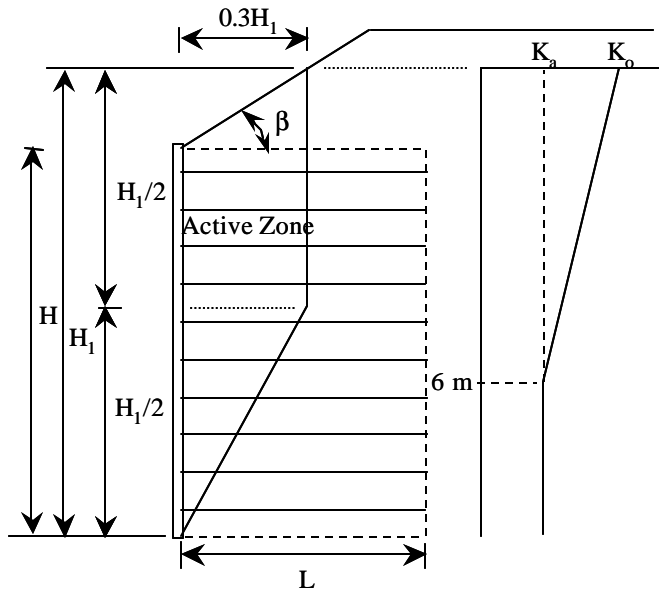
Figure 3. Determination of lateral earth pressure coefficients failure plane location for internal stability design using the Coherent Gravity Method (adopted from AASHTO, 1996).

6

TIEBACK WEDGE METHOD

Originally developed by Bell et al. (1975) and the US Forest Service (Steward et al., 1977), the Tieback Wedge Method has been applied to geosynthetic walls and welded wire systems. This method was developed as an adaptation of the earliest work done by Lee et al. (1973), which summarized the basis for steel strip reinforced MSE wall design. Reduced scale laboratory model walls (Bell et al., 1975) were used to attempt to verify the validity of the model developed by Lee et al., (1973), and some early attempts were made to verify design assumptions using full-scale walls (Steward et al., 1977; Bell et al., 1983).

In the Tieback Wedge Method, the wall is assumed for internal design to be flexible. Therefore, the lateral soil stresses behind the wall reinforcement have no influence on the vertical stresses within the reinforced wall zone, and vertical stress within the wall is simply equal to γZ. Because this has mainly been applied to extensible geosynthetic reinforcement, the method assumes that enough deformation occurs to allow an active state of stress to develop. Hence, the lateral earth pressure coefficient, K_a, is used to convert vertical stress to lateral stress. Though initially K_o was recommended for use with these walls (Bell et al., 1975), Bell et al. (1983) found that this was likely to be too conservative given full-scale wall performance, and K_a was recommended instead. K_a is determined by assuming a horizontal backslope and no wall friction in all cases, given an active zone defined by the Rankine failure plane.

T_{max} is determined as shown in Equation 7:

$$T_{max} = S_v R_c K_a \left(\gamma Z + S + q \right) \tag{7}$$

where γ is the soil unit weight, Z is the depth to the reinforcement level relative to the wall top at the wall face, S is the average soil surcharge depth above the wall top, q is the vertical stress due to traffic surcharge, and all other variables are as defined previously.

As is true in the Coherent Gravity Method, each reinforcement layer is designed to resist the lateral stress within its tributary area, treating the reinforcement layer as a tieback.

FHWA STRUCTURE STIFFNESS METHOD

The Structure Stiffness Method was developed as the result of a major FHWA research project in which a number of full-scale MSE walls were constructed and monitored. Combined with an extensive review of previous fully instrumented wall case histories (Christopher et al., 1990; Christopher, 1993), small-scale and full-scale model walls were constructed and analytical modeling was conducted (Adib, 1988).   This method is similar to the Tieback Wedge Method, but the lateral earth pressure coefficient is determined as a function of depth below the wall top, reinforcement type, and global wall stiffness, rather than using K_a directly.   Furthermore, the location of the failure surface is the same as is used for the Coherent Gravity Method (Figure 3) for MSE walls with inextensible soil reinforcement. It is a Rankine failure surface for MSE walls with extensible soil reinforcement.   The design methodology is summarized in equations 8, 9, and 10.   Note that because the reinforcement stress, and the strength required to handle that stress, varies with the global wall stiffness, some iteration may be necessary to match the reinforcement to the calculated stresses.

$$T_{max} = S_v R_c K_r \left(\boldsymbol{g} Z + S + q \right) \tag{8}$$

$$K_r = K_a \left(\Omega_1 \left(1 + 0.4 \frac{S_r}{47880} \right) \left(1 - \frac{Z}{6} \right) + \Omega_2 \frac{Z}{6} \right) \qquad \text{if } Z \le 6\,\text{m} \tag{9a}$$

$$K_r = K_a \Omega_2 \qquad \text{if } Z > 6\,\text{m} \tag{9b}$$

$$S_r = \frac{EA}{(H/n)} \tag{10}$$

where K_r is the lateral earth pressure coefficient, S_r is the global reinforcement stiffness for the wall (i.e., the average reinforcement stiffness over the wall face area), Ω_1 is a dimensionless coefficient equal to 1.0 for strip and sheet reinforcements or equal to 1.5

for grids and welded wire mats, Ω_2 is a dimensionless coefficient equal to 1.0 if S_r is less than or equal to 47880 kPa or equal to Ω_1 if S_r is greater than 47880 kPa, EA is the reinforcement modulus times the reinforcement area in units of force per unit width of wall, H/n is the average vertical spacing of the reinforcement, and n is the total number of reinforcement layers. This stiffness approach was based on numerous full-scale observations that indicated that a strong relationship between reinforcement stiffness and reinforcement stress levels existed, and it was theoretically verified through model tests and numerical modeling.

DEVELOPMENT OF THE SIMPLIFIED METHOD

The development of the Simplified Method was an attempt to combine the best and simplest features of the various methods that were allowed by the AASHTO Standard Specifications together into one method. For example, one desire was to somehow account for the differences among the various reinforcement types and their typical global stiffnesses, yet simplify the calculation by avoiding the need to reiterate each time the reinforcement density was adjusted to match the reinforcement stresses to the reinforcement capacity available for the wall. Furthermore, the Coherent Gravity method did not provide a way to account for the differences in reinforcement type, since K_a and K_o were used directly in that method to calculate reinforcement stresses regardless of the reinforcement type. A method was needed that could easily be adopted to new MSE wall reinforcement types as they became available. Hence, a goal for this method was to develop a single K_r/K_a curve for each reinforcement type based on reinforcement type alone. Note that the concept of using of a K_r/K_a ratio for MSE wall system internal stress determination was not new to the FHWA Structure Stiffness Method, as Schlosser (1978) provided an early summary of MSE wall reinforcement stresses using this K_r/K_a ratio approach to establish Reinforced Earth wall design specifications (see Figure 1).

Another significant difference among the methods was how the vertical soil stress was calculated. The issue was whether the wall should be treated internally as a rigid body, allowing overturning moment to be transmitted throughout the reinforced soil mass, elevating the vertical stress in the wall. This calculation approach adds a significant complication to internal stress computations, and the validity of this

assumption was considered questionable by the TWG as well as by the FHWA (data discussed later in this paper provide the basis for this conclusion). Furthermore, the FHWA Structure Stiffness Method, allowed by the AASHTO Standard Specifications, did not consider this overturning moment for internal vertical stress computations. Given this supporting information, it was decided to not consider the overturning moment for internal vertical stress computations but to retain it only for external bearing stress computations as a conservative measure.

An important step in the development of this method was to calibrate the method relative to available full scale MSE wall data. Details of this calibration are provided.

The design methodology for the Simplified Method is similar to that of the FHWA Structure Stiffness and Tieback Wedge Methods. Equation 8 can be used for the determination of T_{max}, except that K_r/K_a is determined directly from Figure 4 rather than from equations 9 and 10.
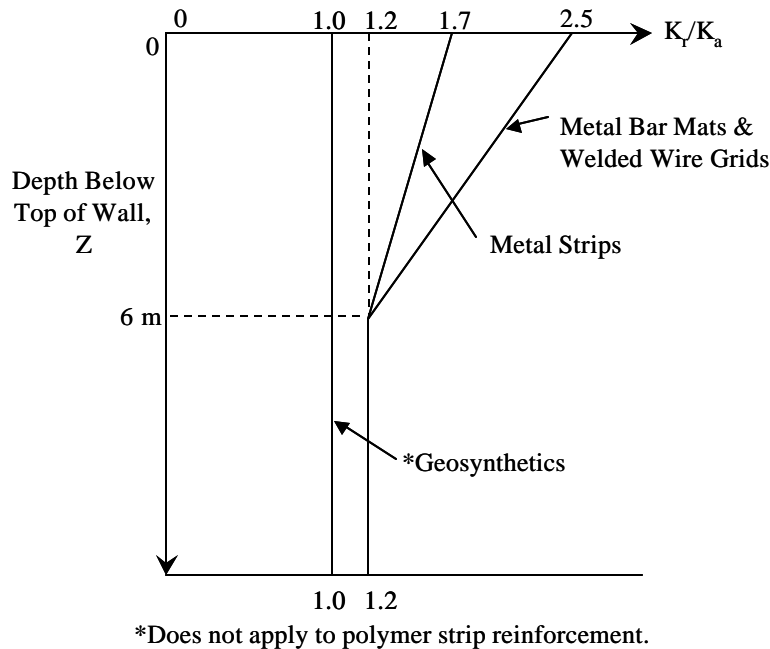
Figure 4. Determination of K_r/K_a for the Simplified Method (after AASHTO, 1999).

SUPPORTING CASE HISTORY DATA

For the purpose of assessing the ability of a given method to predict internal reinforcement stresses accurately, a case history must include adequate material property information, such as backfillspecific soil friction angles and unit weights, reinforcement geometry and spacing, overall wall geometry, some idea of the compaction method used, and some understanding of foundation conditions. All of the case histories selected for this analysis had adequate information for this assessment. Wall geometry and material properties are summarized for all of the walls in tables 1, 2, and 3, and in figures 5 through 21. Note that the properties of the soil backfill behind the reinforced soil zone were assumed to be the same as the reinforced zone backfill, unless otherwise noted.

The following is a description of each of these case histories.

LILLE, FRANCE, STEEL STRIP MSE WALL, 1972

A reinforced earth bridge abutment wall 5.6 m high was constructed in 1972 near Lille, France (Bastick, 1984). Precast reinforced earth concrete facing panels and steel reinforcing strips were used for the entire wall. The overall geometry and wall details are shown in Figure 5. The wall backfill was a gravelly sand (red schist). The type of test used to determine the soil shear strength for the backfill was not reported, and only the resulting measured soil friction angle was provided. The soil backfill behind the wall was reported to have a soil friction angle of 35°, but it is not clear whether this was a backfill-specific measured value. The foundation conditions beneath the wall were also not reported. Tensile strength (F_u = 440 MPa) and modulus (200,000 MPa) of the steel were estimated on the basis of typical minimum specification requirements for the steel.

Bonded resistance strain gauges were attached in pairs (top and bottom of the reinforcement) at each measurement point to account for any bending stresses in the reinforcement. Only reinforcement loads, converted from strain gauge readings, including their distribution along the reinforcement, were reported (Bastick, 1984).

Table 1. Summary of wall geometry and material properties for steel strip reinforced walls.

Case No.	Case Description and Date Built	Backfill ϕ	Backfill γ (kN/m³)	K_a	*Typical S_v (m)	S_h (m)	Reinforcement Coverage Ratio, R_c	Reinforcement Geometry (mm)	Reinforcement Area/Unit (mm²)	Global Wall Stiffness, S_r (kPa)
SS1	Lille, France Steel Strip Wall, 1972	44°	18.1	0.18	0.75	0.50	0.16	1.5 x 80 (smooth steel strip)	120	64,000
SS2	UCLA Steel Strip Test Wall, 1974	38°	19.8	0.24	0.76	0.76	0.105	80 x 3 (smooth steel strip)	240	103,538
SS3	WES Steel Strip Test Wall, 1976	36°	18.5	0.26	0.61	0.77	0.13	101.6 x 0.635 (smooth steel strip)	64.5	29,477
SS4	Fremersdorf Steel Strip Wall, 1980	37°	19.6	0.25	0.76	0.76	0.079	60 x 5 (ribbed steel strip)	300	102,791
SS5	Waltham Cross Steel Strip Wall, 1981	56°	22.6	0.09	0.76	0.76 for top 6 layers, 0.51 for 7th layer, 0.38 for layers 8 and 9, and 0.31 for layers 10 and 11	0.053, 0.079, 0.105, and 0.131 respective of S_h	40 x 5 (ribbed steel strip)	200	105,274
SS6	Guildford Bypass Steel Strip Walls, Sections A & B, 1981	48°	22.3	0.15	0.30	0.90	0.083	75 x 5 (smooth steel strip)	375	264,021
SS7	Asahigaoka, Japan Steel Strip MSE Wall, 1982	36°	17.7	0.26	0.75	0.75 for top 10 layers, and 0.50 for bottom 6 layers	0.133 and 0.200 respective of S_h	100 x 3.2 (smooth steel strip)	302	127,511

Table 1, Continued.

Case No.	Case Description and Date Built	Backfill ϕ	Backfill γ (kN/m³)	K_a	*Typical S_v (m)	S_h (m)	Reinforcement Coverage Ratio, R_c	Reinforcement Geometry (mm)	Reinforcement Area/Unit (mm²)	Global Wall Stiffness, S_r (kPa)
SS8	Millville, West Virginia Steel Strip Wall, Rectangular Section, 1983	44°	19.1	0.18	0.75 and 0.38	0.51 for top 3 layers, 0.38 for layer 4, 0.51 for layers 5 and 6, and 0.75 for bottom 4 layers	0.118 for top 2 layers, 0.158 for layer 4, 0.118 for layers 5 and 6, 0.053 for layers 7 and 8, and 0.080 for bottom 2 layers	60 x 5 for all layers except layers 7 and 8, where 40 x 5 was used (ribbed steel strip)	300 and 200, respectively	101,280
SS9	Millville, West Virginia Steel Strip Wall, Trapezoidal Section, 1983	44°	19.1	0.18	0.75 and 0.38	0.75 for top layer, 0.63 for layers 2 through 4, 0.51 for layers 5 and 6, 0.75 for layer 7, and 0.51 for bottom 3 layers	0.080, 0.095, 0.118, 0.080, and 0.118, respective of S_h	60 x 5 for all layers (ribbed steel strip)	300	95,395
SS10	Ngauranga Steel Strip Wall, 1985	50°	21.5	0.13	0.76	0.76 for top 12 layers, and 0.51 for bottom 5 layers	0.079 and 0.118 respective of S_h	60 x 5 (ribbed steel strip)	300	121,935
SS11	Algonquin Steel Strip Wall, 1988	40°	20.4	0.22	0.76	0.73	0.0694	50 x 4 (ribbed steel strip)	200	71,898
SS12	Gjovik (Norway) Steel Strip Wall, 1990	38°	19.0	0.24	0.76	0.76	0.053	40 x 5 (ribbed steel strip)	200	70,211
SS13	Bourron Marlotte Steel Strip Rectangular Test Wall, 1993	37°	16.8	0.25	0.76	0.76 for top 10 layers, 0.61 for 11th layer, and 0.51 for bottom 3 layers	0.079, 0.098, and 0.118 respective of S_h	60 x 5 (ribbed steel strip)	300	136,667

Table 1, Continued.

Case No.	Case Description and Date Built	Backfill ϕ	Backfill γ (kN/m^3)	K_a	*Typical S_v (m)	S_h (m)	Reinforcement Coverage Ratio, R_c	Reinforcement Geometry (mm)	Reinforcement Area/Unit (mm^2)	Global Wall Stiffness, S_r (kPa)
SS14	Bourron Marlotte Steel Strip Trapezoidal Test Wall, 1993	37°	16.8	0.25	0.76	0.76 for top 5 layers, 0.61 for 6th layer, and 0.51 for bottom 8 layers	0.079, 0.098, and 0.118 respective of S_h	60 x 5 (ribbed steel strip)	300	118,228
SS15	INDOT Minnow Creek Wall, 2001	38°	21.8	0.24	0.76	1.05 for top 8 layers, 0.76 for next 4 layers, 0.61 for next 3 layers, 0.51 for next 2 layers, 0.43 for next 2 layers, 0.38 for next 2 layers, and 0.34 for bottom layer	0.048, 0.066, 0.082, 0.098, 0.132, and 0.147 respective of S_h	50x4 (ribbed strip)	200	81,359

*See figures for details of any variations of S_v.

14

Table 2. Summary of wall geometry and material properties for steel bar mat reinforced walls.

Case No.	Case Description and Date Built	Backfill ϕ	Backfill γ (kN/m^3)	K_a	*Typical S_v (m)	S_h (m)	Reinforcement Coverage Ratio, R_c	Reinforcement Geometry (mm)	Reinforcement Area/Unit (mm^2)	Global Wall Stiffness, S_r (kPa)
BM1	Hayward Bar Mat Wall, Section 1, 1981	40.6^o	20.4	0.21	0.61	1.07	0.563	Five W11 bars spaced at 150 mm c-c	355	108,833
BM2	Hayward Bar Mat Wall, Section 2, 1981	40.6^o	20.4	0.21	0.61	1.07	0.563	Five W11 bars spaced at 150 mm c-c	355	108,073
BM3	Algonquin Bar Mat Wall (sand), 1988	40°	20.4	0.22	0.75	1.5	0.284	Four W11 bars spaced at 150 mm c-c	284	49,687
BM4	Algonquin Bar Mat Wall (silt), 1988	35°	20.4	0.27	0.75	1.5	0.284	Four W11 bars spaced at 150 mm c-c	284	49,687
BM5	Cloverdale Bar Mat Wall, 1988	40°	22.6	0.22	0.76	1.24	0.363 for top 5 layers, 0.605 for next 5 layers, 0.363 for next 5 layers, 0.605 for next 6 layers, and 0.847 for bottom 3 layers	Four W11 bars for top 5 layers, six W11 bars for next 5 layers, four W20 bars for next 5 layers, six W20 bars for next 6 layers, and eight W20 bars for bottom 3 layers, all spaced at 150 mm c-c	355 for top 5 layers, 426 for next 5 layers, 516 for next 5 layers, 774 for next 6 layers, 1,032 for bottom 3 layers	126,119

*See figures for details of any variations of S_v.

Table 3. Summary of wall geometry and material properties for welded wire reinforced walls.

Case No.	Case Description and Date Built	Backfill f	Backfill g (kN/m^3)	K_a	*Typical S_v (m)	S_h (m)	Reinforcement Coverage Ratio, R_c	Reinforcement Geometry (mm)	Reinforcement Area/Unit (mm^2)	Global Wall Stiffness, S_r (kPa)
WW1	Rainier Ave. Welded Wire Wall, 1985	43°	19.2	0.19	0.46	1.0	1.0	W4.5xW3.5 for top 13 layers, W7xW3.5 for next 7 layers, W9.5xW3.5 for next 11 layers, and W12xW5 for bottom 7 layers, with all longitudinal wires spaced at 150 mm c-c	193 mm^2/m for top 13 layers, 301 mm^2/m for next 7 layers, 409 mm^2/m for next 11 layers, and 516 mm^2/m for bottom 7 layers	146,535
WW2	Houston, Texas Welded Wire Wall, 1991	38°	18.6	0.24	0.76	1.91	0.64	W4.5xW7 for top 3 layers, W7xW7 for next 2 layers, W9.5xW7 for next 2 layers, W12xW7 for next 2 layers, and W12xW7 for bottom 5 layers, all mats use 9 longitudinal wires spaced at approx. 140 mm c-c	261 mm^2/mat for top 3 layers, 407 mm^2/mat for next 2 layers, 552 mm^2/mat for next 2 layers, 697 mm^2/mat for next 2 layers, and 813 mm^2/mat for bottom 5 layers	84,640

*See figures for details of any variations of S_v.

16
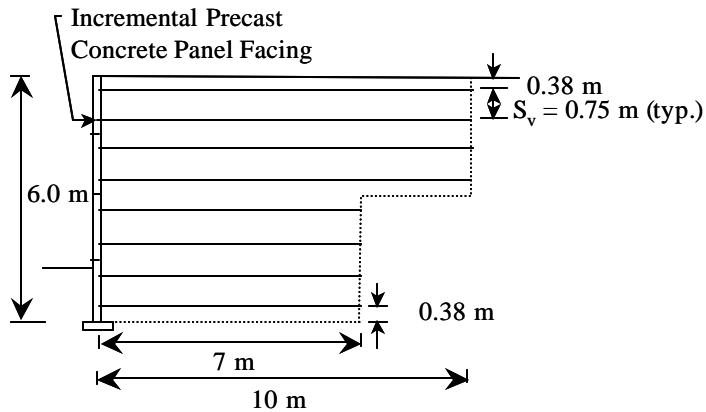
Figure 5. Lille, France, steel strip test wall (adapted from Bastick, 1984).

UCLA STEEL STRIP MSE TEST WALL, 1974

A full-scale test wall 6.1 m high and 34 m long was constructed at the UCLA Engineering Field Station in Saugus, California, in 1974 to investigate the static and dynamic behavior of steel strip reinforced Mechanically Stabilized Earth (MSE) walls (Richardson et al., 1977). Precast Reinforced Earth Company (RECO) concrete facing panels were used for the entire wall. RECO steel strips were used for the reinforcement. The overall geometry and wall details are shown in Figure 6. The wall backfill was described as a dusty sandy gravel obtained from a dry stream bed near the site, with d_{60} and d_{10} sizes of 1.0 mm and 0.15 mm, respectively. Soil shear strength was determined through laboratory triaxial testing, but only the resulting measured soil friction angle was provided. The unit weight of the soil was measured through density tests in-situ during wall construction after compaction. No water or special compaction procedure was used to compact the backfill, other than driving trucks and other hauling equipment over the fill, and placing the fill in 0.46-m lifts (actual lift thicknesses varied from 0.3 m to 0.75 m). Approximately 85 percent of Modified Proctor compaction was achieved. The foundation conditions beneath the wall were described as 0.3 to 1 m of sand underlain by sandstone. The tensile strength (F_u = 520 MPa) and modulus (200,000 MPa) of the steel were based on minimum specification requirements for the steel used.

Specifics of the instrumentation used to measure the strains and loads in the reinforcement were not provided. Only reinforcement loads, converted from strain gauge readings, were reported (Richardson et al, 1977).

17
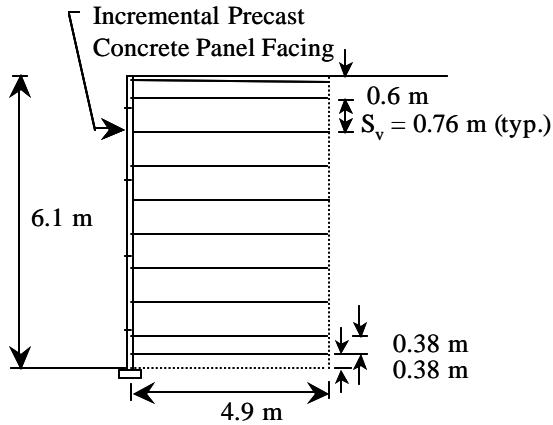
Figure 6. UCLA steel strip test wall (adapted from Richardson, et. al., 1977).

WATERWAYS EXPERIMENT STATION STEEL STRIP MSE TEST WALL, 1976

A full-scale test wall 3.66 m high was constructed in 1976 in a three-sided pit excavated into a bank of silty soil known as Vicksburg loess at the US Army Waterways Experiment Station (Al-Hussaini and Perry, 1978).   The wall section was 4.88 m long, and the width of the wall was 3.1 m.   The wall utilized Alcoa T11 high-strength aluminum panels, which were each 0.61 m wide, 3.66 m long, and 40.6 mm thick.   The panels connected together with a hinge-type connection.   The wall was reinforced with 24-gauge galvanized steel strips, and the wall geometry was as shown in Figure 7.   The backfill was a clean subangular to angular concrete sand with a d_{50} size of 0.48 mm and a C_u of 2.2.   Soil shear strength was determined through direct shear testing of 76-mm square specimens, though only a peak soil friction angle was provided for the results. The unit weight of the soil was measured in-situ during wall construction.   The soil was placed by hand in 0.31-m lifts and was not compacted.   Tensile strength (F_u = 430 MPa) was estimated on the basis of the reported F_y of 352 MPa from laboratory tests on the steel strip used.   The modulus of the steel (214,600 MPa) was also determined from laboratory tensile tests on the steel strip material used.

The wall was also surcharge loaded with lead weights in an attempt to take the wall to a point of collapse. A thin plastic membrane was placed on the top of the wall, with aluminum panels similar to those used for the facing elements placed on the wall top next, to more evenly distribute the surcharge load on the wall top. Lead weights (907 kg

18

each) were uniformly placed on the aluminum panels in a checkerboard fashion. The surcharge was increased in 24-kPa increments to a total load of 72 kPa over the entire wall top. After measurements were taken, the load was increased again. Collapse of the wall occurred while this last loading was in progress, with an estimated load at collapse of approximately 90.4 kPa. The collapse phase started as an audible sound of distress and significant bulging of the facing element located at the first and second row of reinforcing strips from the bottom. After this, collapse occurred rapidly, taking only 3 seconds to occur. Depending on the location within the wall, shear failure of either the connections to the face or of the reinforcing strips in the backfill occurred.

A vertical column of soil pressure cells developed by the Waterways Experiment Station was placed 0.3 m behind the face to monitor vertical soil pressure. Complete Wheatstone bridges consisting of four BLH strain gauges were attached in pairs (top and bottom of the reinforcement) at each measurement point to directly measure the load in the reinforcement. They were mounted top and bottom to account for any bending stresses in the reinforcement. Reinforcement strains, including their distribution along the reinforcement, were reported (Al-Hussaini and Perry, 1978).
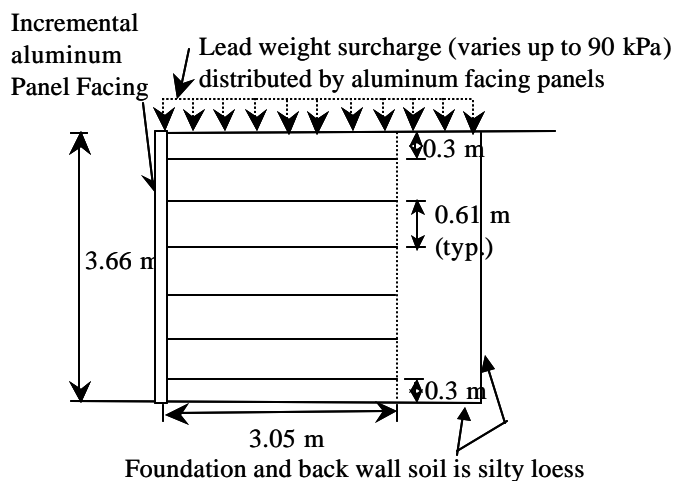
Figure 7. WES steel strip test wall (adapted from Al-Hussaini and Perry, 1978).

FREMERSDORF, GERMANY, STEEL STRIP MSE WALL, 1980

A RECO wall 7.3 m high was constructed in 1980 at Fremersdorf, Germany, along side the river Saar (Thamm, 1981). Precast Reinforced Earth Company (RECO) concrete

facing panels and steel reinforcing strips were used for the entire wall. The overall geometry and wall details are shown in Figure 8. The wall backfill was a peaty sand, with the exception of a free draining medium gravel zone near the face. Soil shear strength for the sand was determined through laboratory direct shear testing by using a 500-mm by 500-mm shear box, and only the resulting measured soil friction angle was provided. It is assumed that both the sand and the pea gravel had approximately the same soil friction angle. The unit weight of the soil was measured through density tests in-situ during wall construction after compaction. Compaction was accomplished with a 90-kN vibrating roller (frequency of 25 Hz), and 0.375-m soil lifts were used. The foundation soil beneath the wall consisted of 5 m of dense gravelly sand over sandstone. The tensile strength (F_u = 520 MPa) and modulus (200,000 MPa) of the steel were based on minimum specification requirements for the steel used.

Bonded resistance strain gauges were attached in pairs (top and bottom of the reinforcement) at each measurement point to account for any bending stresses in the reinforcement. Only reinforcement loads, converted from strain gauge readings, including their distribution along the reinforcement, were reported (Thamm, 1981). Earth pressure cells were also placed in a row approximately 0.7 m above the wall base to measure the vertical earth pressure distribution along the wall base.
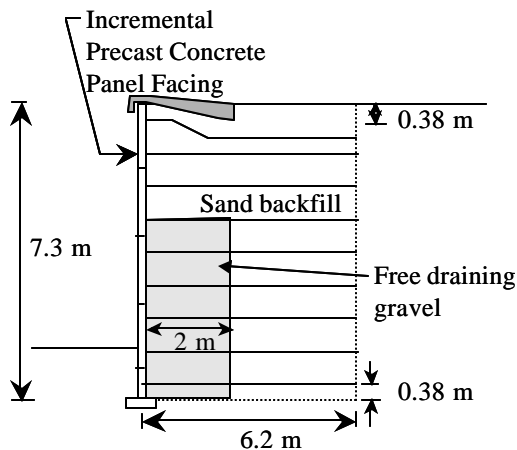

Figure 8. Fremersdorf steel strip MSE wall.

WALTHAM CROSS STEEL STRIP MSE WALL, 1981

A Reinforced Earth Company (RECO) wall was constructed to support the M25 motorway at Waltham Cross in Hertfordshire, UK (Murray and Farrar, 1990). Wall construction began and was for the most part completed in 1981. The wall was 8.2 m high. Precast RECO concrete facing panels and steel strips were used for the entire wall. The overall geometry and wall details are shown in Figure 9. The foundation soil was 1 m of dense gravelly sand fill underlain by 2 to 4 m of refuse subjected to dynamic compaction, which was underlain by 1 to 2 m of soft black clay. As the dynamic compaction did not improve the soil adequately to provide the needed bearing capacity beneath the higher sections of the wall, an 8-m-deep sheet pile wall was placed directly in front of the wall. This was tied by using 18-m-long tie rods cast in concrete to short piles, installed into firm foundation soil, which were located behind and beneath the back of the structure. Based on pressuremeter tests, the improved foundation soil had an average Young's modulus of 12 MPa and an undrained shear strength of 126 kPa. Settlement of the wall within the backfill area was not reported, but approximately 90 mm of vertical movement was observed in the footing that supported the facing.

The backfill sand was a well graded sand and gravel, with a maximum particle size of 40 mm and less than 5 percent fine sand. The shear strength of the backfill soil was determined through laboratory direct shear testing by using a large direct shear apparatus (300 mm by 300 mm by 175 mm deep). Only summary test results were reported. The unit weight of the soil was measured through density tests in-situ during wall construction after compaction. The tensile strength (F_u = 520 MPa) and modulus (200,000 MPa) of the steel were based on minimum specification requirements for the steel used.

Compaction of the backfill was carried out in accordance with Department of Transport specifications. A towed vibrating roller (Stothert and Pitt T182, weight 6.06 Mg, roll width 1371 mm) was used for the bulk of the fill. Within 2 m of the facing, a pedestrian operated Bomag 75S twin roll vibrating roller (weight 0.94 Mg, roll width 750 mm) was used.

Bonded electrical resistance strain gauges were attached to the top and bottom of the reinforcement at each measurement point to account for any bending stresses in the

21

reinforcement. Only reinforcement loads, converted from strain gauge readings, including their distribution along the reinforcement, were reported (Murray and Farrar, 1990). Vertical earth pressures were also measured by pneumatic pressure cells placed near the base of the wall. The earth pressure cells were calibrated, as well as compared to earth pressure cells placed behind the reinforced soil section.
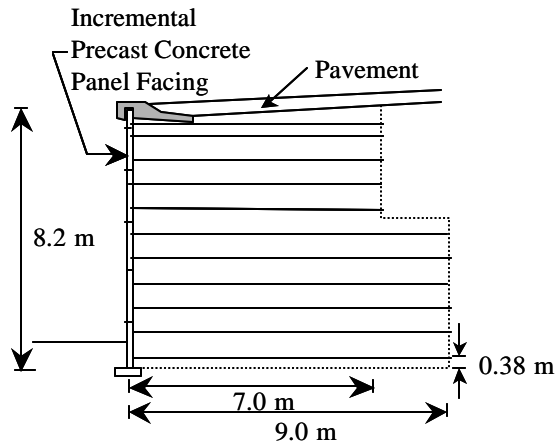
Figure 9. Waltham Cross steel strip MSE wall (adapted from Murray and Farrar, 1990).

GUILDFORD BYPASS STEEL STRIP MSE WALL, 1981

A steel strip reinforced, concrete panel-faced MSE wall 6 m high was constructed to support the A3 motorway as part of the A3/A322 interchange at Guildford (Hollinghurst and Murray, 1986). The walls were actually supported back-to-back to form the elevated roadway, but the face-to-face distance between the two walls was over 20 m, which is more than adequate to prevent one wall from affecting the other. Wall construction began and was for the most part completed in 1981. Small hexagonal precast facing panels were used. These had a dimension of 0.6 m diametrically across the flats and a maximum thickness of 0.1 m. Steel strips were used as the soil reinforcement. The overall geometry and wall details are shown in Figure 10. The foundation soil was weathered London clay. The backfill sand was a well graded sand and gravel, with a maximum particle size of 40 mm and less than 5 percent fine sand. The shear strength of the backfill soil was determined through laboratory direct shear testing by using a large direct shear apparatus (300mm by 300 mm by 150 mm deep). Only the peak soil friction angle was reported. The unit weight of the soil was measured through density tests in-

situ during wall construction after compaction. The foundation soil consisted of weathered London clay, which was moderately compressible. The tensile strength (F_u = 440 MPa) and modulus (200,000 MPa) of the steel were based on minimum specification requirements for the steel used.

Compaction of the backfill was not described in detail, but heavy compaction equipment was used for the bulk of the fill, and a light weight Wacker plate compactor was used within 0.5 m of the face.

Bonded electrical resistance strain gauges were attached to the top and bottom of the reinforcement at each measurement point to account for any bending stresses in the reinforcement. Two wall sections were instrumented. Only reinforcement loads, converted from calibrated strain gauge readings, including their distribution along the reinforcement, were reported (Murray and Hollinghurst, 1986). Pneumatic earth pressure cells were placed in a row at the ground elevation in front of the wall, as well as at higher depths within the wall. The cells were calibrated and compared to earth pressure cells placed behind the reinforced zone.
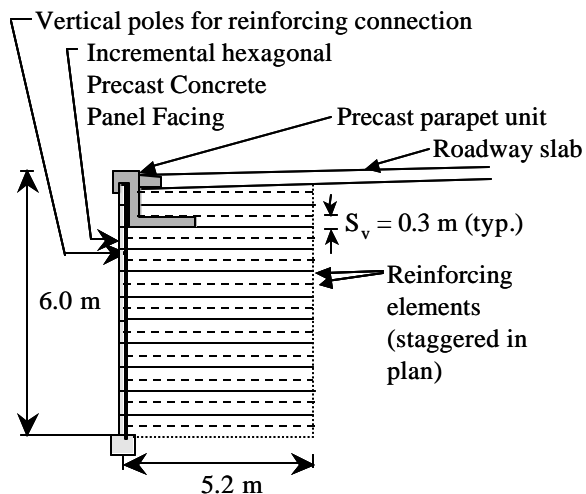
Figure 10. Guildford Bypass steel strip reinforced MSE wall (adapted from Murray and Hollinghurst, 1986).

ASAHIGAOKA, JAPAN, STEEL STRIP MSE WALL, 1982

A steel strip reinforced, concrete panel faced RECO wall 13.0 m high (including soil surcharge) was constructed in Asahigaoka, Japan, though the specifics of the application

were not reported (Terre Armee, 1984). Wall construction is estimated to be some time before 1982, given the date shown on a handwritten figure in the report for this structure (Bastick, 1984). RECO precast concrete facing panels, either 180 mm or 220 mm thick, and steel reinforcing strips placed in the backfill were used. The overall geometry and wall details are shown in Figure 11. Details of the foundation soil were not reported. Settlement of the wall was specifically not measured, which may be an indicator that settlements were not anticipated to be large. The backfill was granular, but with some cohesion. The measured backfill shear strength was reported (ϕ of 36°, with a cohesion of 18.6 kPa), but the details of the shear strength test were not reported. The unit weight of the soil was measured in-situ during wall construction, but details of the method used were not provided. Compaction method details were also not provided. The tensile strength (F_u = 440 MPa) and modulus (200,000 MPa) of the steel were based on minimum specification requirements for the steel used.

Bonded electrical resistance strain gauges were attached to the top and bottom of the reinforcement at each measurement point to account for any bending stresses in the reinforcement. Only reinforcement loads, converted from strain gauge readings, including their distribution along the reinforcement, were reported (Bastick, 1984).

Figure 11. Asahigaoka, Japan, steel strip MSE wall (adopted from Bastick, 1984).

MILLVILLE, WEST VIRGINIA, STEEL STRIP MSE WALL, 1983

A steel strip reinforced, concrete panel-faced RECO test wall 6.0 m high was constructed in Millville, West Virginia, as a test wall to investigate the effect of narrow wall base widths (Bastick, 1984). Wall construction was in 1983. RECO precast concrete facing panels and steel reinforcing strips placed in the backfill were used. Two wall sections were constructed, one with a constant strip length, and one with a variable strength length. The overall geometry and wall details are shown in Figure 12 (a and b) for both sections. Details of the foundation soil were not reported. The backfill was granular, but with some cohesion. The measured backfill shear strength was reported, but the details of the shear strength test were not reported. The unit weight of the soil was measured in-situ during wall construction, but details of the method used were not provided. Compaction method details were also not provided. The tensile strength (F_u = 520 MPa) and modulus (200,000 MPa) of the steel were based on minimum specification requirements for the steel used.

(a) Rectangular section   (b) Trapezoidal section
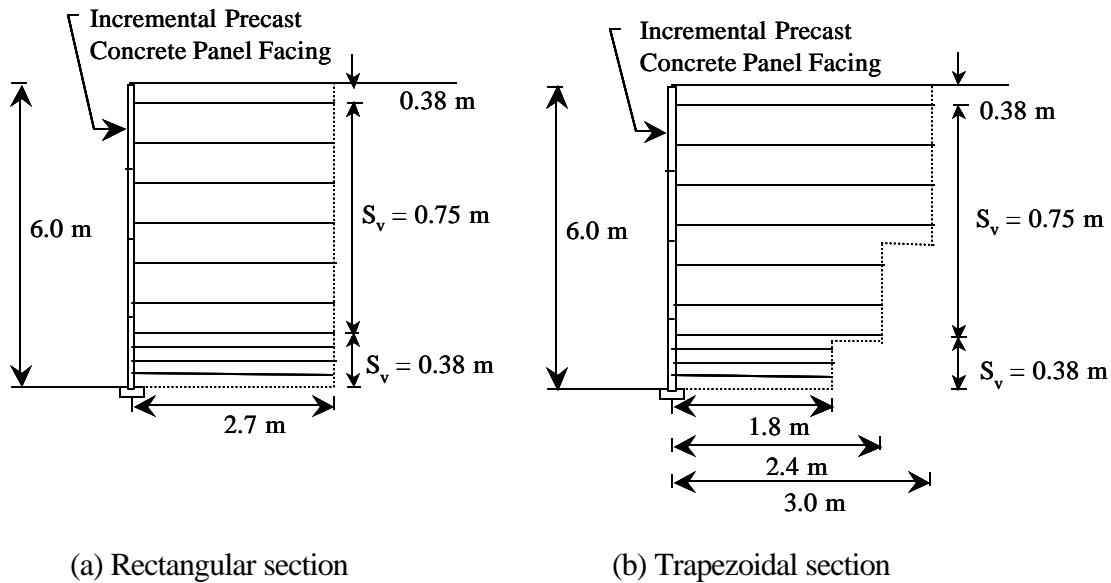
Figure 12. Millville, West Virginia, steel strip MSE walls (adopted from Bastick, 1984).

Bonded electrical resistance strain gauges were attached to the top and bottom of the reinforcement at each measurement point to account for any bending stresses in the reinforcement. However, because of wiring and other problems, reliable strain readings could not be obtained. Soil stress cells were placed at the bottom of the wall to measure

vertical soil stress. Since these vertical soil stress data are useful for evaluating one of the key assumptions used in one of the reinforcement stress prediction methods (i.e., the Coherent Gravity Method), this case history is included despite the problems with the strain gauges.

NGAURANGA, NEW ZEALAND, STEEL STRIP MSE WALL, 1985

A steel strip reinforced, concrete panel-faced RECO wall 12.6 m high was constructed to support a bridge abutment and approach fill as part of the Ngauranga Interchange near Wellington City (Boyd, 1993). Wall construction is assumed to be some time before 1985, given the reference cited in Boyd (1993). Standard RECO precast concrete facing panels and steel reinforcing strips placed in the backfill were used. The overall geometry and wall details are shown in Figure 13. Details of the foundation soil were not reported, but it was apparently moderately compressible, given the 200 mm of settlement observed below the wall. The backfill was a well graded granular greywacke, with a maximum particle size of 180 mm, a d_{50} of over 40 mm, and less than 1 percent silt. Measured shear strength of the backfill soil was not specifically reported, but on the basis of the results of pullout tests on the backfill soil with ribbed steel strips, the peak soil friction angle is estimated to be in excess of 50 degrees. The unit weight of the soil was measured in-situ through density tests during wall construction after compaction. Foundation conditions beneath the wall were not specifically reported, though the soil was apparently moderately compressible, as approximately 200 mm of settlement were measured. The tensile strength (F_u = 520 MPa) and modulus (200,000 MPa) of the steel were based on minimum specification requirements for the steel used.

Boyd (1993) reported that compaction of the backfill was carried out by a four-tonne vibratory roller and 12-tonne smooth wheeled rollers. Within 2 m of the wall face, a one-tonne static roller was used for compaction, and a small plate compactor was used near the facing panels.

Details of the instrumentation used were not provided. Only reinforcement loads, converted from strain gauge readings, including their distribution along the reinforcement, were reported (Boyd, 1993). They were as high as 47.8 kN/m.
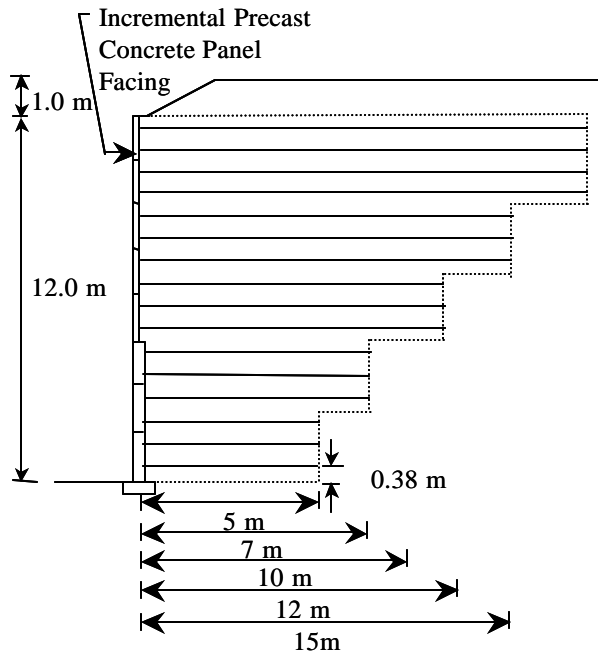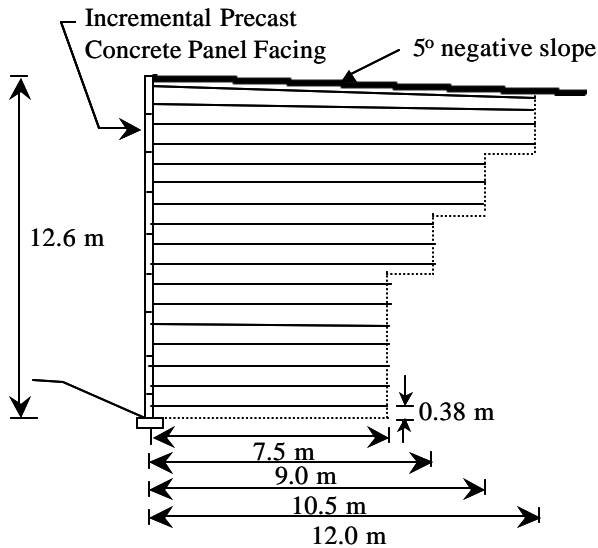
Figure 13. Ngauranga, New Zealand, steel strip MSE wall (adapted from Boyd, 1993).

ALGONQUIN STEEL STRIP AND BAR MAT CONCRETE PANEL WALLS, 1988

A series of full-scale test walls 6 m high were constructed in a gravel pit in Algonquin, Illinois, as part of a Federal Highway Administration investigation of the behavior of MSE walls (Christopher, 1993). Seven wall sections, each 10 m long, were constructed. Five of the walls utilized the same precast concrete facing panels. One of these sections (Wall 1) used Reinforced Earth Company (RECO) steel strips (see Figure 14). Wall 3 used VSL steel bar mats with transverse W11 bars spaced at 0.6 m center to center (see Figure 14). Two of the walls (walls 4 and 5) were the same as Wall 3, but a cobble backfill and a low plasticity silt, respectively, were used as backfill rather than the gravelly sand backfill used for the other walls (see Figure 14). The remaining sections were other types of steel reinforced and geosynthetic reinforced MSE systems, which afforded an opportunity to compare geosynthetic reinforced systems with steel reinforced systems. The gravelly sand backfill used was a well graded gravelly sand with a maximum particle size of 50 mm and a d_{50} size of 4 mm. The silt backfill was a low plasticity silt obtained from a washed-screens sluice pond that was part of a gravel operation at the site, and 90 percent passed the 0.074 mm sieve. Soil shear strength was determined through triaxial testing in both cases. A peak soil friction angle was provided

27

for the sand, and both a peak soil friction angle and a cohesion (2.4 kPa) was reported for the silt backfill. The unit weight of the soil was measured in-situ with a nuclear densometer during wall construction after compaction. Foundation conditions beneath the wall consisted of 5 m of dense gravelly sand underlain by very dense sandy silt. The tensile strength (F_u = 520 MPa) and modulus (200,000 MPa) of the steel were based on minimum ASTM specification requirements for the steel used.

Construction of the walls began in June 1987 and was completed in early 1988. A majority of the wall backfill was compacted with a Wacker model W74 "walk behind" vibrating drum type compactor that delivered a centrifugal force of 17.8 kN (Christopher, 1993). A smaller vibratory plate type compactor with a 0.9 kN impact at 5900 cycles/min. was used near the wall face and around the inclinometer casings. The backfill soil was compacted to 95 percent of Standard Proctor (ASTM D 698). This was typically obtained with four to five passes of the compactor by using a lift thickness of approximately 200 mm.

Bonded resistance strain gauges were attached in pairs (top and bottom of the reinforcement) at each measurement point to account for any bending stresses in the reinforcement. Strains, including their distribution along the reinforcement were as high as 0.09 percent (Christopher, 1993) . Note that there were some strain readings, in particular for Wall 1, that were higher than 0.09 percent, but they were also erratic. Christopher (1999) considered those particular readings, specifically the maximum readings in layers 2 and 3 in Wall 1, to be unreliable (see Christopher, 1993). Some erratic readings were also observed in some of the reinforcement layers for walls 3 and 5, and overall patterns of strain along the reinforcement were used to determine the maximum reinforcement load in those layers. In addition, the uppermost instrumented reinforcement layer in Wall 5, which had a pure silt backfill, were observed to be affected by frost heave (Christopher, 1999).

Three earth pressure cells were placed at the base of Walls 3 and 5 to measure vertical earth pressure.
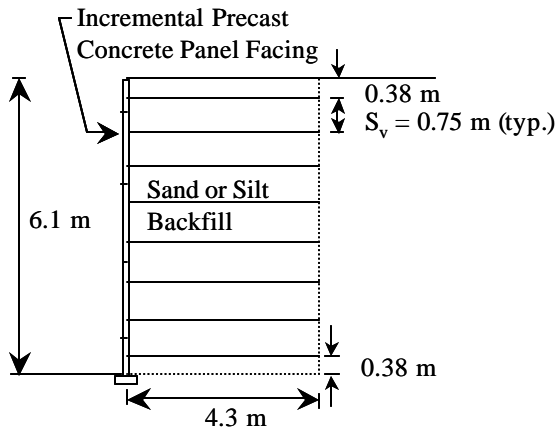
Figure 14.   Algonquin steel strip and bar mat MSE wall (adapted from Christopher, 1993).

GJOVIK, NORWAY, STEEL STRIP MSE WALL, 1990

A steel strip reinforced, concrete panel-faced RECO wall 12.0 m high was constructed to support the Rv 4 roadway near Gjovik, Norway (Vaslestad, 1993).   Wall construction was some time around 1990, but the specific date of construction was not reported.   Standard RECO precast concrete facing panels and steel reinforcing strips placed in the backfill were used.   The overall geometry and wall details are shown in Figure 15.   Details of the foundation soil were not available.   The backfill was granular in nature, but details were not available.   The measured shear strength of the soil was provided, but the specific test method used to obtain the shear strength was not available. The unit weight of the soil was measured in-situ through density tests during wall construction after compaction.   The backfill was compacted to 97 percent of Standard proctor (ASTM D 698) by using full-sized vibratory rollers (Vaslestad, 1996).   The tensile strength (F_u = 520 MPa) and modulus (200,000 MPa) of the steel were based on minimum specification requirements for the steel used.

Details of the instrumentation were not provided.   Only reinforcement loads, converted from strain gauge readings, including their distribution along the reinforcement, were reported (Vaslestad, 1993).

Figure 15. Gjovik, Norway, steel strip MSE wall (adapted from Vaslestad, 1993).

BOURRON MARLOTTE STEEL STRIP MSE TEST WALLS, 1993

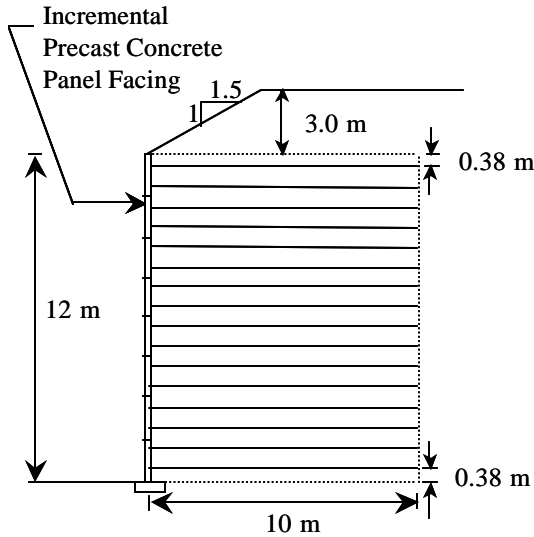Full-scale test walls 10.5 m high were constructed in a sand quarry near Bourron Marlotte in the Fontainbleau Forest to investigate the behavior of slender steel strip reinforced, MSE walls (Bastick et al., 1993). The actual year of the wall construction was not reported. Two wall sections, each 5.4 m long, but with a 3.9-m isolation section between them and with 14.7-m-long isolation sections at each end of the wall, were constructed. Precast Reinforced Earth Company (RECO) concrete facing panels were used for the entire wall. RECO steel strips were used for the reinforcement. The overall geometry and wall details are shown in Figure 16 (a and b). Fontainbleau sand was used as wall backfill and as replacement material for the foundation soil below the wall to provide more consistent foundation soil characteristics. The sand was uniformly graded with a d_{50} size of approximately 0.27 mm, with virtually no silt sized particles. Soil shear strength was determined through laboratory testing, but the type of test conducted was not reported, and only the resulting measured soil friction angle was provided. The unit weight of the soil was measured through density tests in-situ during wall construction after compaction. Details of the compaction method was not reported, but it was described as light but uniform compaction to a lower standard than would typically be used for real full-scale structures. The tensile strength (F_u = 520 MPa) and modulus (200,000 MPa) of the steel were considered to be relatively constant, but variations in

30

strip thickness and width were possible. Tensile tests were conducted on sections of the instrumented strips to calibrate the gauges, so that the measured strain to load could be correctly interpreted.

Bonded resistance strain gauges were attached in pairs (top and bottom of the reinforcement) at each measurement point to account for any bending stresses in the reinforcement. Only reinforcement loads, converted from calibrated strain gauge readings, including their distribution along the reinforcement, were reported (Bastick etal, 1993). Glotzl total pressure cells were placed along the wall base and behind the wall to measure vertical earth pressure.

(a) Rectangular section   (b) Trapezoidal section
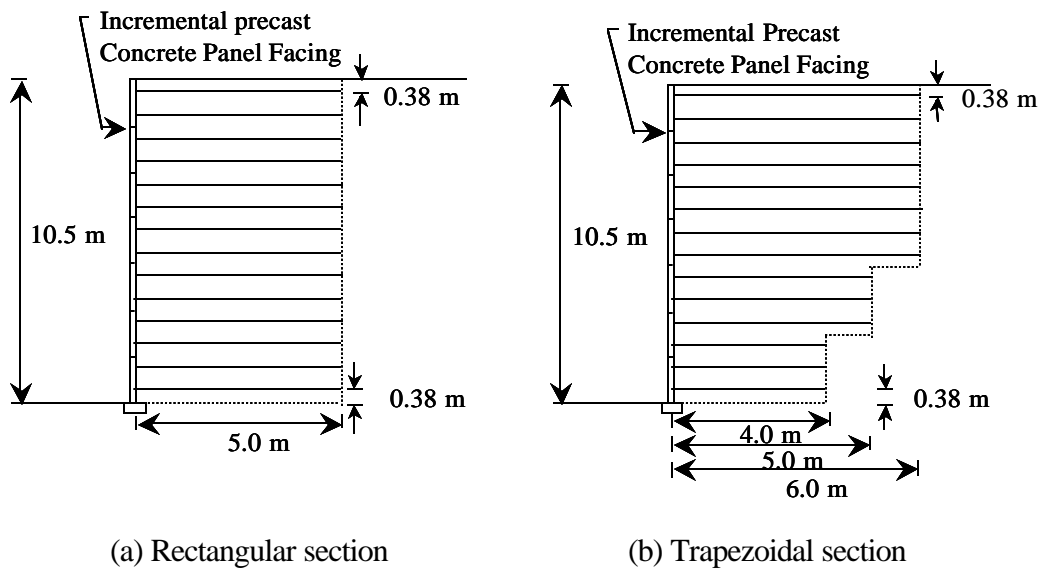
Figure 16. Bourron Marlotte steel strip MSE test walls (adapted from Bastick et al., 1993).

INDOT MINNOW CREEK STEEL STRIP MSE WALL, 1999

A RECO wall 16.9 m high was constructed in 1999 near Logansport, Indiana, on US-24 to support a bridge approach fill at Minnow Creek (Runser et al., in press). Precast Reinforced Earth Company (RECO) concrete facing panels and steel reinforcing strips were used for the entire wall. The overall geometry and wall details are shown in Figure 17. The wall backfill was a poorly graded sand with gravel. Soil shear strength for the sand was determined through six 150-mm-diameter consolidated drained triaxial tests in the laboratory, and only the resulting measured soil friction angle was provided. The friction angle of the retained soil (reported as 35.3^{o} on average) was determined in

the same manner as the backfill soil, and six triaxial tests were also performed. The unit weight of the soil was measured through density tests in-situ during wall construction after compaction. Details of the compaction method were not reported, but since this was a production wall for a state department of transportation, it can be assumed that the backfill soil was well compacted with full-scale rollers in accordance with AASHTO specifications (AASHTO, 1998). A description of the foundation soil was not provided, but the bridge was pile supported, and concern about inadequate bearing capacity resulted in the bottom five reinforcement layers being lengthened. This implies that the foundation soils were relatively soft or loose. The ultimate tensile strength of the strips was determined from laboratory tests on three strips (average F_u of 143 kN), and the modulus (200,000 MPa) of the steel was based on minimum specification requirements for the steel used.

Bonded resistance strain gauges were attached in pairs (top and bottom of the reinforcement) at each measurement point to account for any bending stresses in the reinforcement. Only reinforcement loads, converted from strain gauge readings, including their distribution along the reinforcement, were reported. Earth pressure cells were also placed in a row at the wall base to measure the vertical earth pressure distribution along the wall base, as well as at several levels above the wall base.

HAYWARD BAR MAT MSE WALL, 1981

MSE retaining walls up to 6.1 m high were constructed to support an embankment at grade separation at Hayward, California, in 1981 (Neely, 1993). Precast Retained Earth (VSL) 1.2-m-high hexagonal concrete facing panels were used for the entire wall (Neely and Gandy, 1995). Steel bar mats with transverse W11 bars spaced at 0.61 m center to center were used for the backfill reinforcement. The overall geometry and wall details are shown in Figure 18 (a and b) for the two instrumented wall sections. The backfill soil was a well graded gravelly sand, though specific gradational details were not reported. Soil shear strength was determined through laboratory testing, but the type of test conducted was not reported, and only the resulting measured soil friction angle was provided. The unit weight of the soil was measured through density tests *in-situ* during wall construction after compaction. Details of the compaction method was not reported,
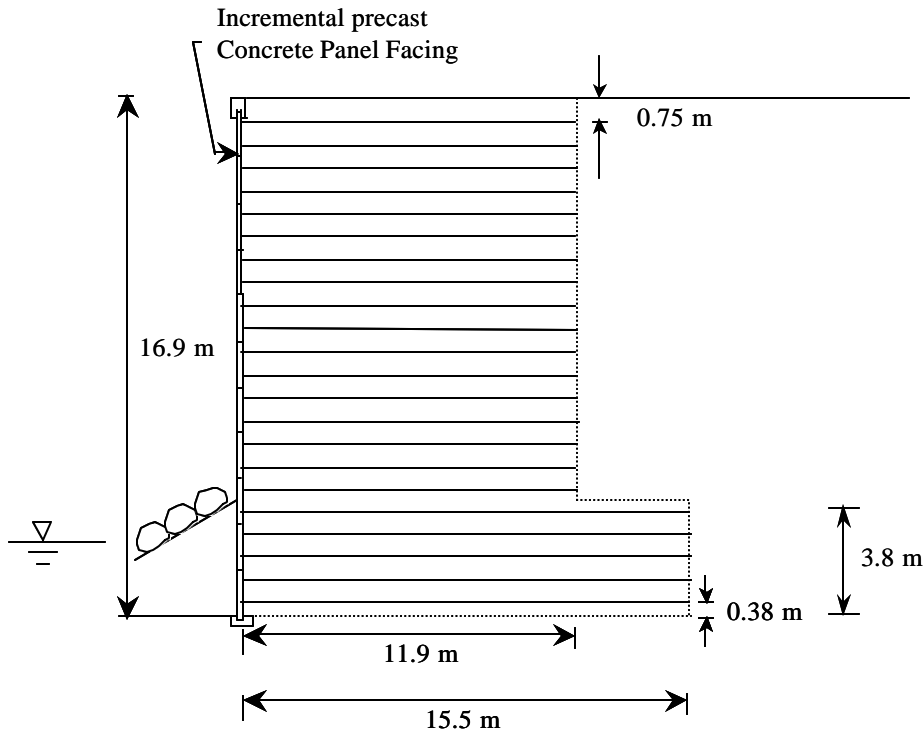
Figure 17. INDOT Minnow Creek steel strip MSE wall (adapted from Runser et al., in press).

though it was described as being done to specification (typical of a full-scale production wall). Foundation conditions beneath the wall were not reported. However, Al-Yassin (1983) did report that approximately 0.6 m of settlement was measured for the fill behind the wall, indicating that soft soil was present below the wall. The tensile strength (F_u = 520 MPa) and modulus (200,000 MPa) of the steel were based on minimum specification requirements for the steel used.

Bonded resistance strain gauges were attached to the reinforcement, but no other instrumentation details were given. Only reinforcement loads, converted from strain gauge readings, including their distribution along the reinforcement, were reported (Neely, 1993; Al-Yassin, 1983).

(a) Section 1   (b) Section 2
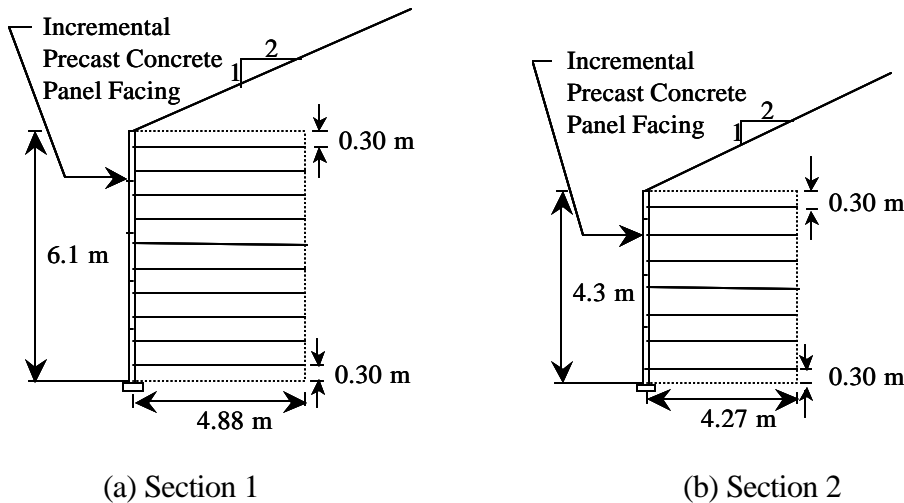
Figure 18. Hayward bar mat walls (adapted from Neely, 1993).

CLOVERDALE, CALIFORNIA, BAR MAT MSE WALL, 1988

MSE retaining walls up to 18.2 m high were constructed to support the realignment of Highway 101 near Cloverdale, California, in 1988 to avoid an existing slide (Jackura, 1988). Precast Retained Earth (VSL) 1.5-m-high hexagonal concrete facing panels were used for the entire wall. Steel bar mats with transverse W11 bars spaced at 0.3 to 0.6 m center to center were used for the backfill reinforcement.   The overall geometry and wall details are shown in Figure 19 for the highest instrumented wall section. The backfill soil was obtained from within the project limits and was clayey, sandy gravel. The maximum particle size was 150 mm, the d_{50} size was on the order of 5 mm, and 11 to 17 percent passed the 0.075 mm sieve.   The plasticity index was approximately 10 or less.   Soil shear strength was determined through laboratory testing by using a 150-mm-diameter triaxial testing device, but only the resulting measured soil friction angle and cohesion were provided. The measured cohesion was relatively high (a ϕ of 32° and a C of 48 kPa) and likely did not represent fully drained, long-term soil strength for the backfill.   The true drained triaxial ϕ for the backfill was thought to be approximately 40° (Jackura, 1996).   The unit weight of the soil was measured through nuclear density tests in-situ during wall construction after compaction.   Compaction was described as done to specification using full-size vibratory rollers for the main part of the backfill (typical of a full-scale production wall).   Within 0.9 m of the face, to prevent distortion of the facing panels, a wedge of pea gravel was placed in each lift with minimal compaction.

34

Foundation conditions beneath the wall consisted of weathered to fresh sandstone and mudstone. The tensile strength (F_u = 520 MPa) and modulus (200,000 MPa) of the steel were based on minimum specification requirements for the steel used.

Bonded electrical resistance strain gauges were attached to the top and bottom of the reinforcement at each measurement point to account for any bending stresses in the reinforcement. Note that the reinforcement loads continued to increase with time over the first year of measurement (Jackura, 1988), indicating some time-dependent behavior of the backfill, a likely consequence of using a relatively cohesive backfill.
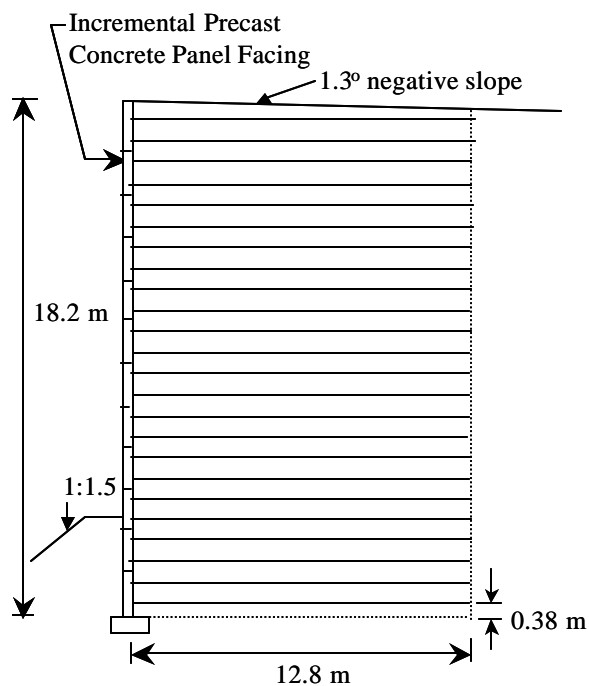
Figure 19. Cloverdale, California, bar mat wall (adapted from Jackura, 1988).

RAINIER AVENUE WELDED WIRE WALL, 1985

MSE welded wire retaining walls up to 16.8 m high were constructed to support a preload embankment at grade separation on Interstate 90 in Seattle, Washington, in 1985 (Anderson et al., 1987). Welded wire mats, with transverse wire spacing of 230 mm that formed both the facing and the backfill reinforcement, were used for the entire wall. The overall geometry and wall details are shown in Figure 20. The backfill soil was a clean, uniformly graded, gravelly sand, with a d_{50} of 0.7 mm. Two percent of the material

passed the 0.075 mm sieve. Soil shear strength was not directly determined for the specific backfill used, although the source of the backfill was the same as that used for a geosynthetic wall constructed in a later phase of this project where the backfill shear strength, both triaxial and plane strain, was measured (Allen et al., 1992). Given the similarities of the backfill soils used for both phases of this project, a triaxial soil friction angle of approximately 43° was estimated for the welded wire wall backfill. The unit weight of the soil was measured through nuclear density tests in-situ during wall construction after compaction. Compaction was conducted with a large vibratory roller, except that within 1 m of the face lighter weight compactors were used. Foundation conditions beneath the wall consisted of 6 m of medium dense gravelly sand underlain by 15 m of soft to stiff lacustrine clay. The tensile strength (F_u = 550 MPa) and modulus (200,000 MPa) of the steel were based on minimum specification requirements for the steel used.

Bonded electrical resistance strain gauges were attached to the top and bottom of the reinforcement at each measurement point to account for any bending stresses in the reinforcement. Only reinforcement loads, converted from strain gauge readings, including their distribution along the reinforcement, were reported (Anderson et al., 1987).
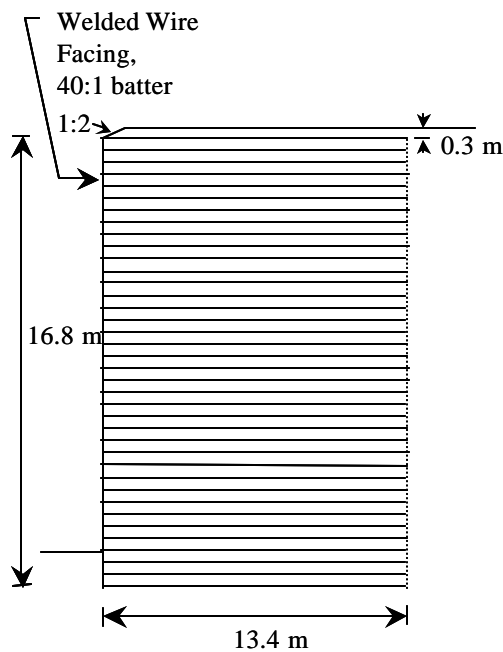

Figure 20. Rainier Avenue welded wire wall (adapted from Anderson, 1987).

HOUSTON, TEXAS, WELDED WIRE WALL, 1991

MSE welded wire retaining walls up to 10.1 m high were constructed to support State Highway 225 in Houston, Texas (Sampaco, 1995). The overall geometry and wall details are shown in Figure 21. Precast concrete panels were approximately 3.8 m long, 0.75 m high, and 130 mm thick. Welded wire mats attached to the facing elements, with transverse wires spaced at 0.6 m center to center, were used to reinforce the backfill. The walls were constructed back to back to support the elevated ramps. The back-to-back walls were for the most part identical. At the instrumented section shown in Figure 24, the reinforcement mats overlapped one another by up to 0.6 m, but they were staggered in a way that prevented the mats from touching. The backfill soil was a nonplastic, poorly graded sand, with a d_{50} of 0.15 mm. Eleven to 14 percent of the material passed the 0.075-mm sieve. Soil shear strength was determined from partially drained triaxial tests on the backfill. The unit weight of the soil was measured through nuclear density tests in-situ during wall construction after compaction. Compaction was conducted with a large vibratory roller, except that within 1 m of the face lighter weight, walk-behind plate compactors were used. The target compaction level was 95 percent of standard proctor (ASTM D 698). The foundation soil consisted of at least 10 m of stiff silty clay. The eensile strength (F_u = 550 MPa) and modulus (200,000 MPa) of the steel were based on minimum specification requirements for the steel used.

Bonded electrical resistance strain gauges were attached to the top and bottom of the reinforcement at each measurement point to account for any bending stresses in the reinforcement. Only reinforcement loads, converted from strain gauge readings, including their distribution along the reinforcement, were reported (Sampaco, 1995).

Note that because of the back-to-back configuration, this wall represents a unique condition regarding potential stress levels in welded wire reinforced structures. This is because reinforcement stress levels have the potential to be reduced relative to single, stand-alone walls (Elias and Christopher, 1997). Because of this, the Texas welded wire wall was not included in the database used to develop and evaluate the Simplified Method. The data from this wall are presented separately, however, to show the effect of placing walls back –to back.
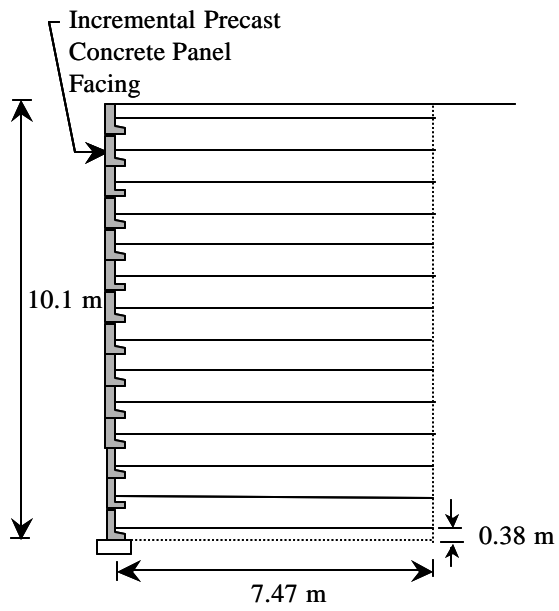
Figure 21. Houston, Texas, welded wire wall (adapted from Sampaco, 1995).

FINDINGS

SUMMARY OF MEASURED RESULTS

Tables 4 through 6 provide a tabulated summary of the measured reinforcement loads and strains for each of the case histories described in the previous section. Measured strains were not available for all of the case histories, such as when only the resulting loads were reported. However, in all cases, with the exception of the WES steel strip test walls (Al-Hussaini and Perry, 1978), a modulus of 200,000 MPA was used to convert strains to load. The measured loads for example case histories are plotted as a function of depth below the wall top (the wall top defined as the ground surface elevation immediately behind the wall face) in Appendix A, Figures A-1 through A-27.

Table 4. Summary of measured reinforcement loads and strains for steel strip reinforced walls.

Case Description	Height, H (m)	Surcharge Thickness, S (m)	Depth of Layer Below Wall Top, Z (m)	Reinforcement Stiffness (kN/m)	*Measured Peak Reinforcement Strain (%)	Peak Reinforcement Load, T_{max} (kN/m)
SS1	6.0	0.0	1.9	48000		6.74
	6.0	0.0	2.6	48000		10.0
	6.0	0.0	3.4	48000		9.82
	6.0	0.0	4.1	48000		7.19
	6.0	0.0	4.9	48000		11.9
	6.0	0.0	5.6	48000		7.53
SS2	6.1	0.0	0.6	63200		3.84
	6.1	0.0	1.9	63200		7.40
	6.1	0.0	3.4	63200		20.8
	6.1	0.0	5.0	63200		21.9
	6.1	0.0	5.5	63200		6.85
SS3	3.66	0.0	0.9	18000	0.0207	3.72
	3.66	0.0	2.1	18000	0.0429	7.71
	3.66	0.0	3.4	18000	0.0383	6.89
SS3, with 24 kPa Surcharge	3.66	1.3	0.9	18000	0.047	8.45
	3.66	1.3	2.1	18000	0.0641	11.5
	3.66	1.3	3.4	18000	0.0701	12.6
SS3, with 48 kPa Surcharge	3.66	2.6	0.9	18000	0.0679	12.2
	3.66	2.6	2.1	18000	0.0804	14.5
	3.66	2.6	3.4	18000	0.0981	17.6
SS3, with 72 kPa Surcharge	3.66	3.9	0.9	18000	0.084	15.1
	3.66	3.9	2.1	18000	0.0914	16.4
	3.66	3.9	3.4	18000	0.116	20.9
SS4	7.3	0.0	2.7	79000		12.2
	7.3	0.0	3.4	79000		12.9
	7.3	0.0	4.3	79000		16.1
	7.3	0.0	5.1	79000		14.9
	7.3	0.0	5.9	79000		16.7
	7.3	0.0	6.6	79000		19.1
SS5	8.2	0.0	2.0	52700		19.5
	8.2	0.0	3.4	52700		18.8
	8.2	0.0	4.9	78500		36.0
	8.2	0.0	6.4	105000		27.0
	8.2	0.0	7.1	129000		46.5
SS6, Section A	6.0	0.0	1.2	83400		6.50
	6.0	0.0	2.4	83400		8.35
	6.0	0.0	3.0	83400		9.54
	6.0	0.0	4.2	83400		9.32

*If reported in the literature.

Table 4, continued.

Case Description	Height, H (m)	Surcharge Thickness, S (m)	Depth of Layer Below Wall Top, Z (m)	Reinforcement Stiffness (kN/m)	*Measured Peak Reinforcement Strain (%)	Peak Reinforcement Load, T_{max} (kN/m)
SS6, Section B	6.0	0.0	1.2	83400		8.46
	6.0	0.0	2.4	83400		9.54
	6.0	0.0	3.0	83400		9.97
	6.0	0.0	4.2	83400		8.78
	6.0	0.0	4.9	83400		13.7
SS7	12.0	1.0	1.1	80500		11.0
	12.0	1.0	4.1	80500		25.6
	12.0	1.0	6.4	80500		40.2
	12.0	1.0	8.6	120800		47.1
	12.0	1.0	10.1	120800		50.7
	12.0	1.0	10.9	120800		42.5
	12.0	1.0	11.6	120800		42.5
SS10	12.6	0.0	0.6	79000		12.0
	12.6	0.0	3.2	79000		22.1
	12.6	0.0	6.2	79000		25.8
	12.6	0.0	9.3	118000		36.8
	12.6	0.0	12.3	118000		47.8
SS11	6.1	0	1.2	54800	0.029	15.9
	6.1	0	2.7	54800	0.0316	17.3
	6.1	0	5	54800	0.04	21.9
	6.1	0	5.7	54800	0.045	24.7
SS12	12.0	0.0	3.4	52700		20.5
	12.0	0.0	6.5	52700		26.5
	12.0	0.0	11.0	52700		20.2
	12.0	3.0	3.4	52700		29.8
	12.0	3.0	6.5	52700		30.9
	12.0	3.0	11.0	52700		28.7
SS13	10.5	0.0	2.7	79000		15.8
	10.5	0.0	5.0	118000		24.0
	10.5	0.0	7.2	118000		36.0
	10.5	0.0	9.7	118000		46.0
SS14	10.5	0.0	2.7	79000		17.8
	10.5	0.0	5.0	79000		26.9
	10.5	0.0	7.2	79000		33.7
	10.5	0.0	9.7	118000		45.9
SS15	17.0	0.0	3.0	38095		21.3
	17.0	0.0	6.0	38095		26.4
	17.0	0.0	9.0	52632		48.8
	17.0	0.0	12.0	78431		57.6
	17.0	0.0	15.0	105263		61.1

*If reported in the literature.

Table 5. Summary of measured reinforcement loads and strains for bar mat reinforced walls.

Case Description	Height, H (m)	Surcharge Thickness, S (m)	Depth of Layer Below Wall Top, Z (m)	Reinforcement Stiffness (kN/m)	*Measured Peak Reinforcement Strain (%)	Peak Reinforcement Load, T_{max} (kN/m)
BM1	6.1	0	0.9	66400		3.7
	6.1	0	2.1	66400		17.6
	6.1	0	3.4	66400		15.3
	6.1	0	4.6	66400		18.9
	6.1	0	5.8	66400		31.1
	6.1	1.22	0.9	66400		15.6
	6.1	1.22	2.1	66400		17.8
	6.1	1.22	3.4	66400		13.6
	6.1	1.22	4.6	66400		23.9
	6.1	1.22	5.8	66400		36.2
BM2	4.3	0.0	0.91	66400		1.67
	4.3	0.0	2.13	66400		8.14
	4.3	0.0	3.35	66400		10.3
	4.3	1.07	0.91	66400		12.1
	4.3	1.07	2.13	66400		12.0
	4.3	1.07	3.35	66400		17.6
BM3	6.1	0	1.2	37900	0.018	6.82
	6.1	0	2.7	37900	0.025	9.47
	6.1	0	4.2	37900	0.0262	9.93
	6.1	0	5	37900	0.039	14.8
	6.1	0	5.7	37900	0.0279	10.6
BM4	6.1	0	2.7	37900	0.06	22.7
	6.1	0	4.2	37900	0.055	20.8
	6.1	0	5	37900	0.0648	24.6
	6.1	0	5.7	37900	0.0631	23.9
BM5	18.2	0.0	1.9	57300		30.6
	18.2	0.0	5.0	68700		31.2
	18.2	0.0	8.0	83300		33.2
	18.2	0.0	13.3	125000		58.6
	18.2	0.0	16.4	166000		50.4

*If reported in the literature.

Table 6. Summary of measured reinforcement loads and strains for welded wire reinforced walls.

Case Description	Height, H (m)	Surcharge Thickness, S (m)	Depth of Layer Below Wall Top, Z (m)	Reinforcement Stiffness (kN/m)	*Measured Peak Reinforcement Strain (%)	Peak Reinforcement Load, T_{max} (kN/m)
WW1	16.8	0.3	2.8	38600	0.0386	14.9
	16.8	0.3	5.5	60200	0.0396	23.9
	16.8	0.3	7.9	60200	0.0455	27.4
	16.8	0.3	10.1	81800	0.0453	37.1
	16.8	0.3	12.4	81800	0.0501	41.0
	16.8	0.3	13.8	103000	0.0364	37.6
	16.8	0.3	15.1	103000	0.0293	30.3
WW2	10.1	0.0	0.3	27300		0.60
	10.1	0.0	1.2	42600		6.30
	10.1	0.0	2.7	57800		16.3
	10.1	0.0	4.3	73000		18.2
	10.1	0.0	5.0	73000		13.5
	10.1	0.0	6.7	85200		24.8
	10.1	0.0	8.1	85200		17.8
	10.1	0.0	8.8	85200		8.50

*If reported in the literature.

COMPARISON OF MEASURED RESULTS TO PREDICTION METHODS

To investigate the accuracy and shortcomings of the various reinforcement load prediction methods, reinforcement load and other measurements can be compared to predictions. Conclusions can then be developed regarding the freedom and limitations of these methods.

Note that for the comparisons that follow, reinforcement load measurements that were known to be influenced by unusual conditions and that also appeared to be well out of line with the pattern observed from the case history data were eliminated from the data set used for the comparisons. The data points eliminated included the following:

- Wall SS5, the bottom reinforcement layer measurement, because of excess settlement resulting from nonuniform soft ground conditions.

- Wall BM1, the bottom reinforcement layer measurement, because of excess large differential settlement from the front to the back of the wall.

- Wall BM4, the top reinforcement layer measurement, because of the influence of frost heave on the reinforcement stress.

43

- Wall WW2, the entire wall, as the back-to-back configuration for this wall could potentially reduce the stresses in individual reinforcement layers. (The data for this wall are provided in Figure A-27, which shows that the wall reinforcement stresses are indeed lower than would be expected.)

However, these data points are shown in the plots provided in Appendix A. By studying these plots, the effect of influences such as significant differential settlement, frost heave, and special configurations such as back-to-back walls can be observed.

The prediction methods considered include the Coherent Gravity, the FHWA Structure Stiffness, and the Simplified methods, all of which are used for steel reinforced MSE wall systems. The Tieback Wedge Method is typically only used for geosynthetic reinforced systems and for all practical purposes is identical to the Simplified Method for geosynthetics. Therefore, the Tieback Wedge Method will not be discussed further here, since the focus of this paper is steel reinforced systems.

All of these methods have inherent assumptions, but they have also been adjusted to predict empirical measurements obtained from full-scale and reduced scale walls. The assumptions that all these methods have in common are as follows:

- The soil reinforcement stress is indexed through lateral earth pressure coefficients to the peak soil shear strength.
- Limited equilibrium conditions are assumed in that the soil shearing resistance is fully mobilized. However, reinforcement stresses may be adjusted from this for working stress conditions based on empirical reinforcement stress data.
- The soil reinforcement is treated as a tieback in that the reinforcement stress is equal to the lateral soil stress over the tributary area of the reinforcement. A lateral earth pressure coefficient that varies with depth below the wall top is used to convert vertical stress to lateral soil stress. Each reinforcement must maintain horizontal equilibrium with the applied lateral soil stresses. The use of the peak friction angle and K_a or K_o in these methods, combined with calculation of the reinforcement stress using this horizontal equilibrium, implies that the reinforcement stress is directly related to the soil state of stress.

44

- Granular soil conditions are assumed. The presence of soil cohesion cannot be taken directly into account using these methods.
- Wall facing type and rigidity, as well as toe restraint, are assumed to have no effect on the resulting soil reinforcement stresses (or at least, they are not directly taken into account).

The various methods also use assumptions and empirical adjustments that are not common to all the methods. The assumptions and empirical adjustments not common to all the methods are as follows:

- For the Coherent Gravity Method, the reinforced backfill zone is assumed internally and externally to behave as a rigid body capable of transmitting overturning stresses, thereby increasing the vertical stress acting at each reinforcement level. This is adapted from the work by Meyerhof (1953) for pressures beneath rigid concrete footings. This in turn increases the lateral stress the reinforcement must carry, as the lateral stress is assumed to be directly proportional to the vertical stress through a lateral earth pressure coefficient. The Simplified and FHWA Structure Stiffness methods assume that only gravity forces (no overturning) contribute to the vertical soil stress.
- The Coherent Gravity Method assumes that the lateral earth pressure coefficients K_o and K_a can be used directly to translate vertical stress to lateral stress for calculating reinforcement stresses and that the reinforcement type, density, and stiffness have no influence on the lateral stress carried by the reinforcement. On the other hand, the FHWA Structure Stiffness and Simplified methods empirically adjust K_a for the various reinforcement types and/or stiffnesses. The FHWA Structure Stiffness Method adjusts the lateral earth pressure coefficient for both the reinforcement type and global stiffness of the reinforcement in the wall, whereas the Simplified Method only adjusts the lateral earth pressure coefficient for the reinforcement type.
- All of the methods assume that the lateral earth pressure coefficient is at maximum near the top of the reinforced soil mass and decreases with depth below that point. However, whereas the Coherent Gravity Method assumes that this decrease begins

where the theoretical failure surface intersects the soil surface, the FHWA Structure Stiffness and Simplified methods assume that this decrease begins where the ground surface intersects the back of the structural wall face (see Figure 3). This is only an issue where sloping soil surcharges are present.

To evaluate the differences and commonalities of these methods discussed above, comparisons were made and evaluated in terms of the soil reinforcement type, the backfill soil shear strength, the effect of soil surcharge, the degree of compaction, and the effect of overturning stresses on the vertical stresses in the wall. From these comparisons, general conclusions were drawn as to the limitations and usability of the various methods.

Comparison of the Prediction Methods to Measured Behavior--General Observations

Figures A-1 through A-27 in Appendix A show the predicted reinforcement loads as a function of depth below the wall top. These were determined with the various prediction methods described herein, allowing direct comparison to the measured reinforcement loads. The measured triaxial or direct shear soil friction angle was used for these predictions rather than an estimated plane strain soil friction angle or a constant volume friction angle, as current design specifications (AASHTO, 1999) refer to direct shear or triaxial shear strength for use with these methods. Though there is a considerable amount of scatter in the measured results relative to the predicted reinforcement loads, the following general trends can be observed:

- All of the methods provide predictions that are close, except when a significant soil surcharge is present. In that case, the Coherent Gravity Method consistently provides lower predicted loads than the other two methods in the upper half of the wall, but more closely agrees with the other two methods in the lower half of the wall.
- If the measured reinforcement loads are significantly different than the predicted loads, all methods tend to err on the same side relative to the measured loads.

46

- In general, reinforcement stresses increase as a function of depth below the wall top, but whether that increase is linear as assumed in design, especially near the base of the wall, is not clear from the measurements.

Effect of Soil Reinforcement Type

Table 7 and figures 22 through 27 provide an overall view of how well each method predicts reinforcement stresses for steel strip and bar mat reinforcement, for all granular backfills. Since only one well defined case history was available for welded wire MSE walls, the welded wire wall was grouped with the bar mat walls because of their similar reinforcement structure. Table 7 summarizes a statistical analysis of the ratio of the predicted to measured loads for each method for each wall reinforcement type. A normal distribution was assumed. This information suggests that the Simplified Method provides the best prediction, on average, of the reinforcement loads for steel strip reinforced walls, while the Coherent Gravity and FHWA Structure Stiffness methods tend to underestimate the reinforcement loads, on average. Though the FHWA Structure Stiffness Method appears to under-predict the reinforcement loads for steel strip reinforced walls, it also has a lower coefficient of variation, indicating a slightly tighter distribution of the data.

The Coherent Gravity Method tends to predict the lowest reinforcement loads of the three methods for bar mat and welded wire reinforced walls, with the FHWA Structure Stiffness Method providing the most conservative prediction, and the Simplified Method being in between the two. Note that the scatter in the data for the bar mat walls is a little greater for the Coherent Gravity Method than for the other two methods. Furthermore, a visual comparison of Figure 25 to figures 26 and 27 reveals that the majority of the data points for the Coherent Gravity Method are below the 1:1 correspondence line, indicating that the Coherent Gravity Method tends to under-predict reinforcement stresses for bar mat and welded wire systems. Overall, the Simplified Method and the FHWA Structure Stiffness Method produce a prediction that is slightly conservative, whereas the Coherent Gravity Method produces a prediction that is slightly nonconservative.

Table 7. Summary of the average and coefficient of variation for the ratio of the predicted to measured reinforcement loads, assuming a normal distribution, for each prediction method for all granular backfill soils.

| MSE Wall Reinforcement Type (# of Walls) | Ratio: Predicted/Measured Reinforcement Load | | | | | |
| | Coherent Gravity Method | | FHWA Structure Stiffness Method | | Simplified Method | |
	Average	COV	Average	COV	Average	COV
Steel Strip (14)	0.88	49.2%	0.87	43.6%	0.96	50.2%
Steel Bar Mat Only (5)	1.02	45.7%	1.54	41.7%	1.34	42.6%
Steel Bar Mat and welded wire (6)	0.93	49.3%	1.40	45.9%	1.20	48.2%
All Walls Combined (20)	0.90	49.5%	1.05	51.7%	1.04	50.7%
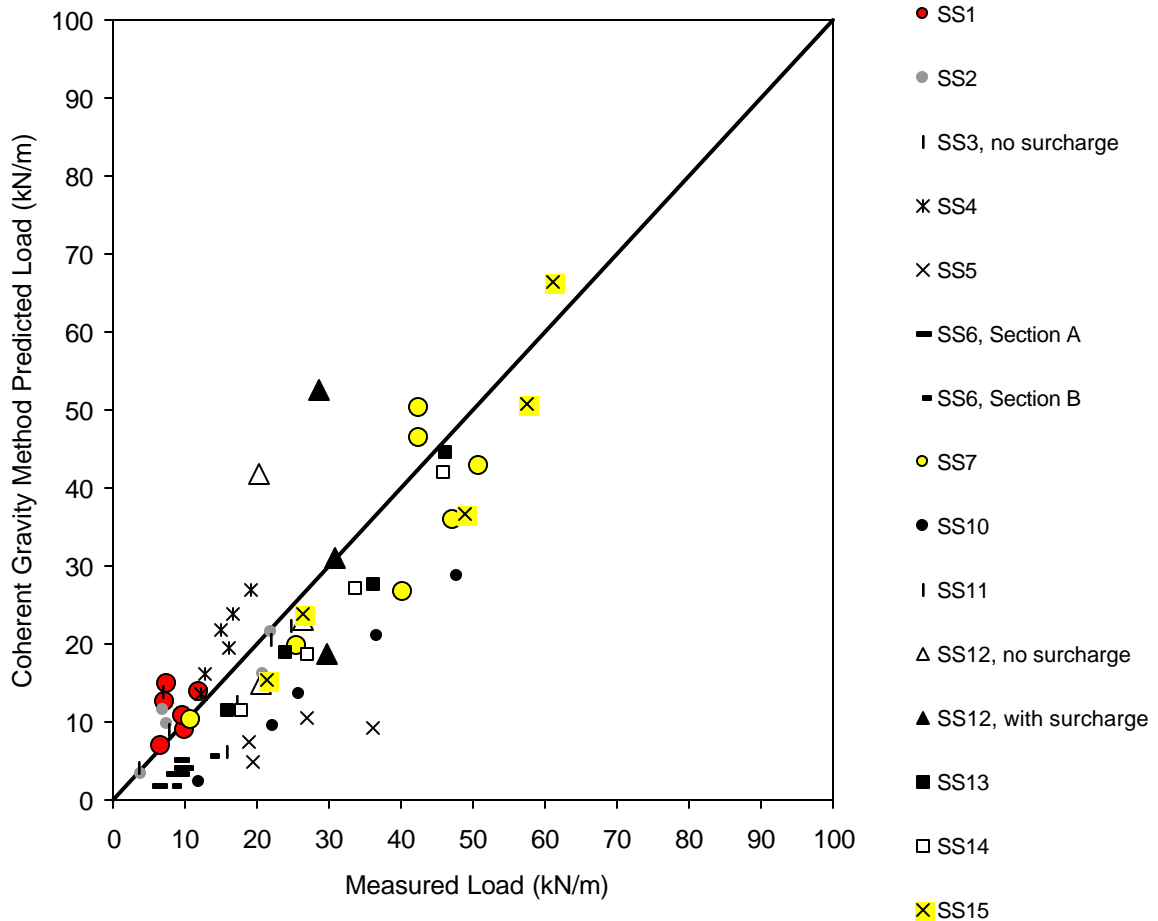
Figure 22. Coherent Gravity Method predicted load versus measured reinforcement peak load for steel strip reinforced MSE walls.
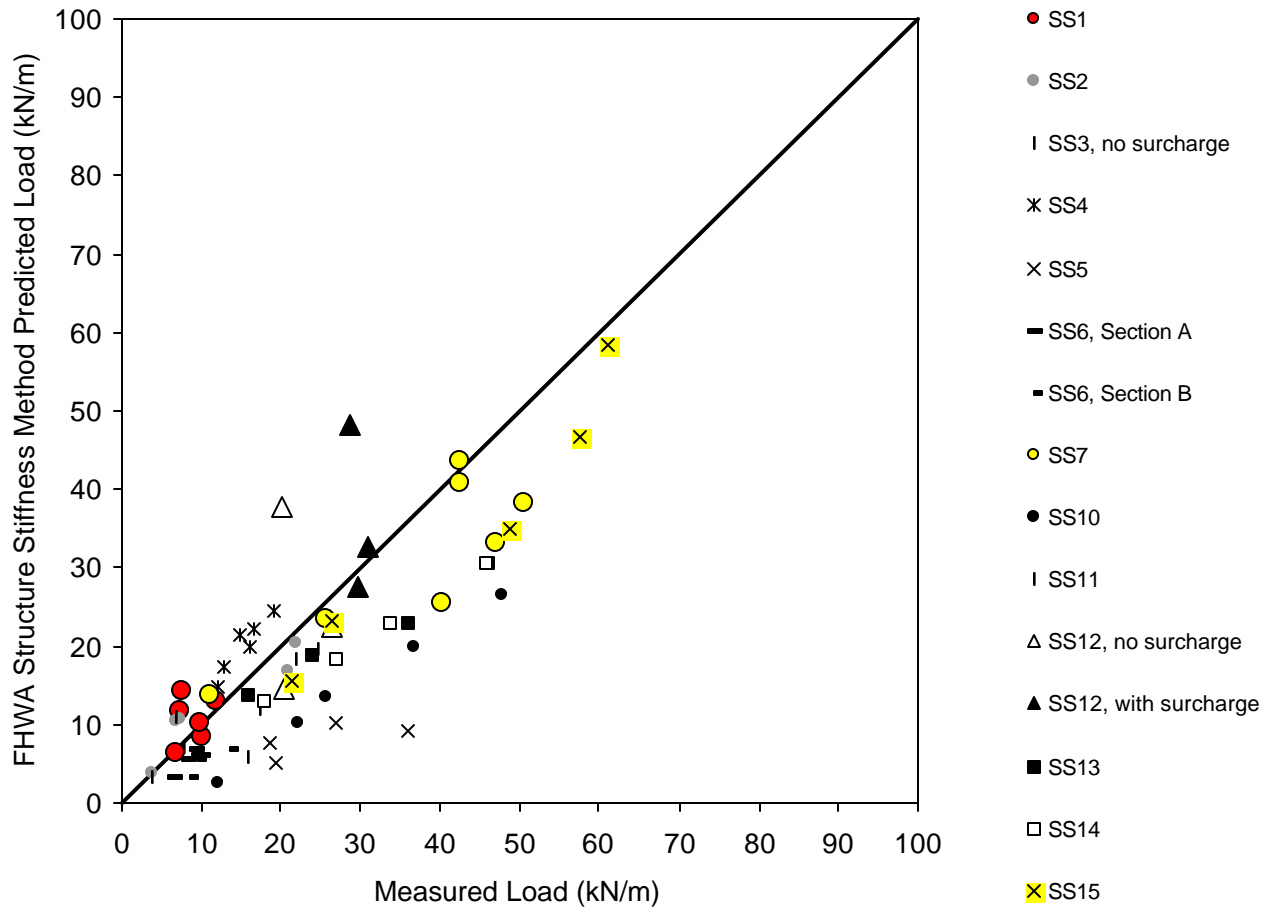
Figure 23. FHWA Structure Stiffness Method predicted load versus measured reinforcement peak load for steel strip reinforced MSE walls.
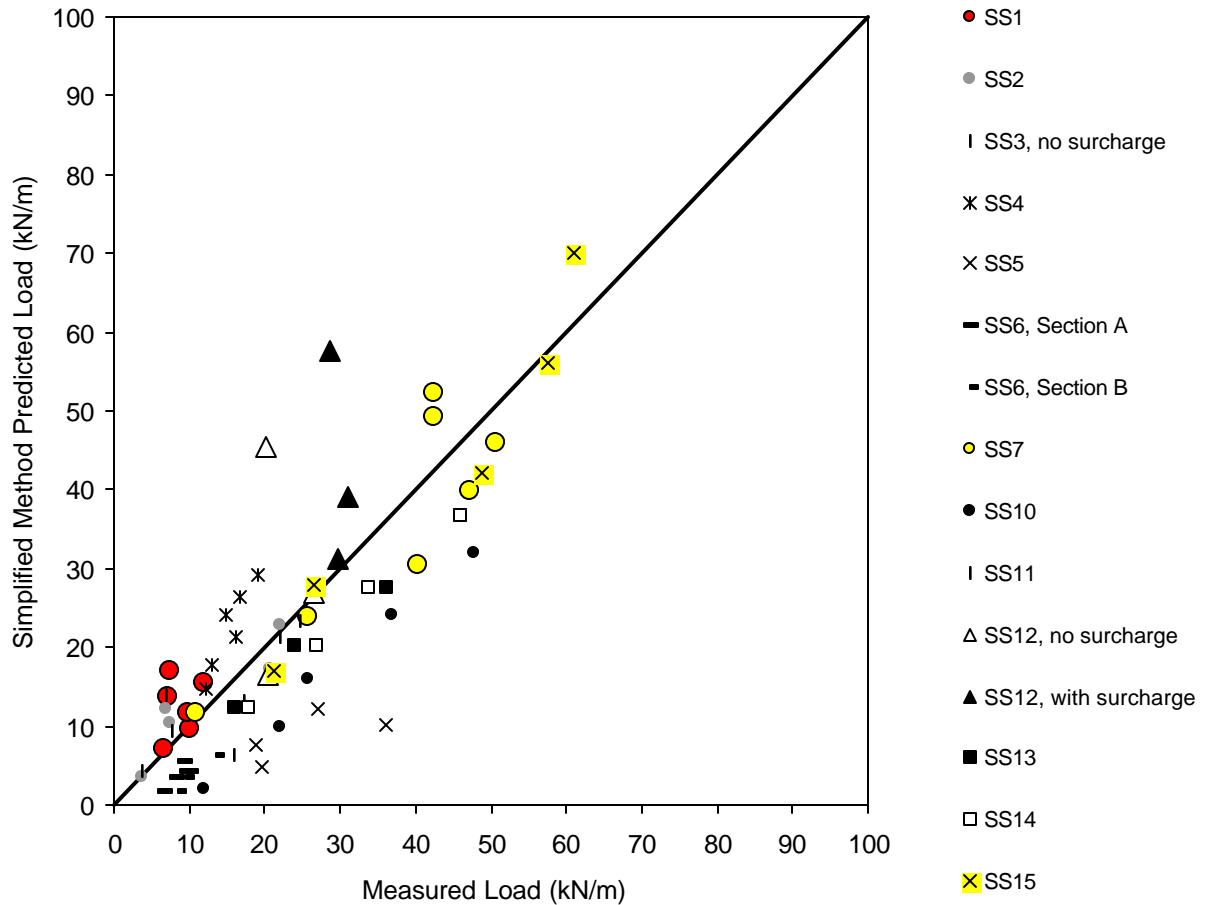
Figure 24. Simplified Method predicted load versus measured reinforcement peak load for steel strip reinforced MSE walls.
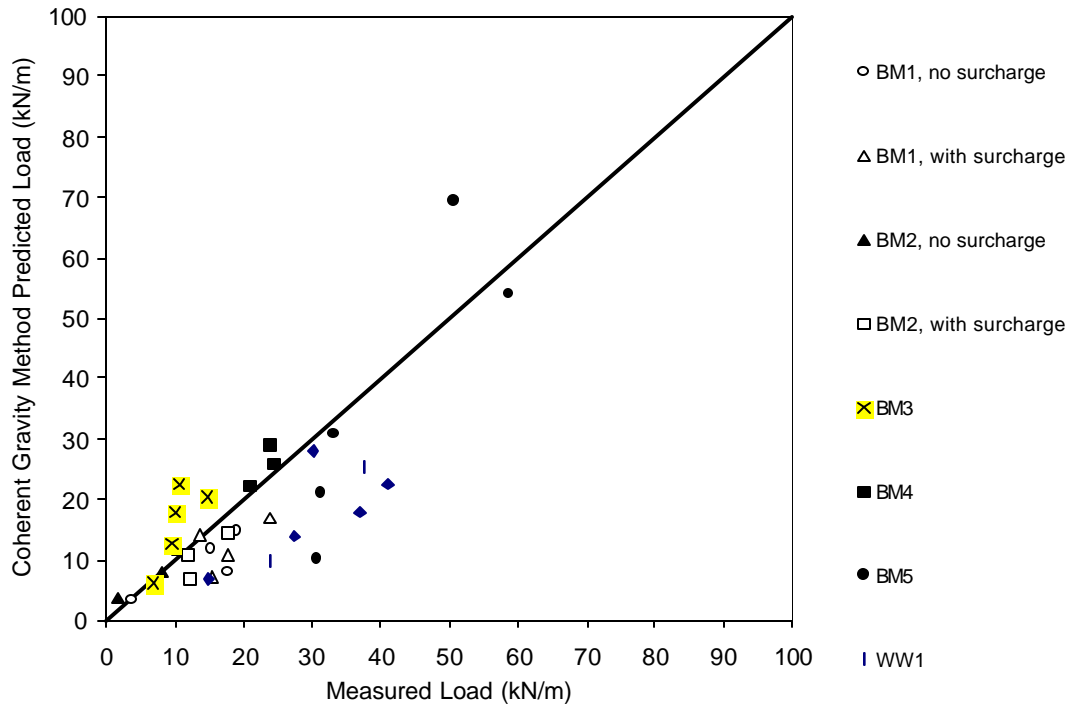
Figure 25. Coherent Gravity Method predicted load versus measured reinforcement peak load for bar mat and welded wire reinforced MSE walls.
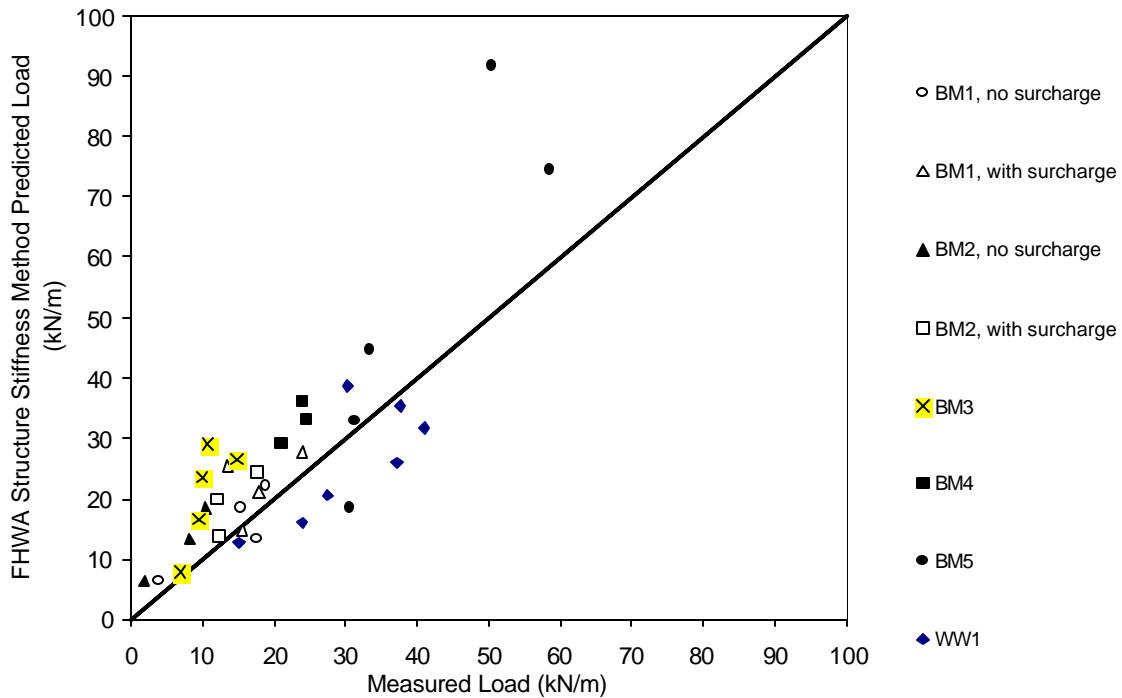
Figure 26. FHWA Structure Stiffness Method predicted load versus measured reinforcement peak load for bar mat and welded wire reinforced MSE walls.
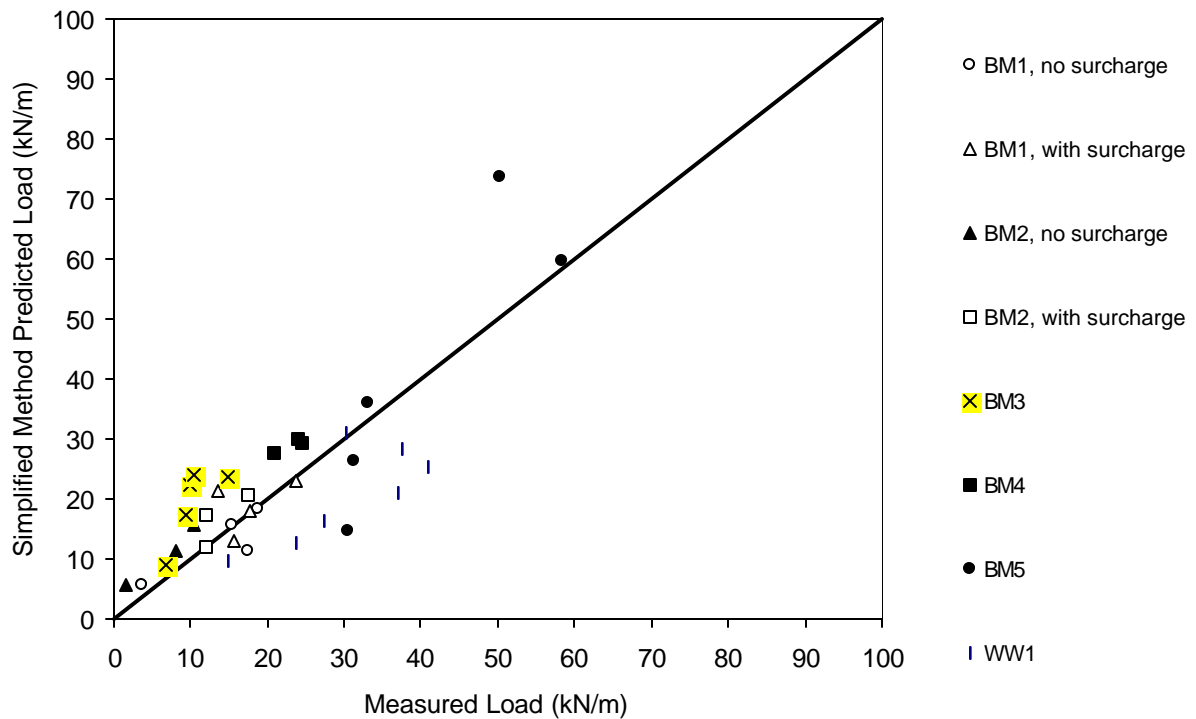
Figure 27. Simplified Method predicted load versus measured reinforcement peak load for bar mat and welded wire reinforced MSE walls.

For all the methods, the reinforcement stresses in the welded wire-faced welded wire wall (WW1) were significantly under-predicted (figures 31 to 33). The reinforcement stresses in both welded wire wall WW1 and the back-to-back welded wire wall (WW2, which had a precast concrete panel facing) are shown in figures A-26 and A-27 in Appendix A. Figure A-27 shows, in contrast to WW1 in Figure A-26, that the reinforcement stresses in WW2 tended to be over-predicted by two of the three methods. These two case histories may be demonstrating the effect of facing rigidity on reinforcement stresses and the effect of the back-to-back configuration, though some of the difference may be due to differences in the soil shear strength for the two wall cases (see discussion in next section). This facing rigidity effect has been observed by others, at least for geosynthetic reinforced systems (Bathurst et al., 2000). Given that there could be several significant reasons beyond the scope of this paper for the difference in the ability of these calculation methods to predict the reinforcement stresses in WW2 , further evaluation of this wall is not provided.

Effect of Backfill Soil Shear Strength

Table 8 is similar to Table 7, but it shows a comparison between the average ratio of predicted to measured reinforcement loads and coefficients of variation for walls with backfill soil friction angles of 40° or less and those with backfill soil friction angles of over 40°. The friction angles referred to here are from triaxial or direct shear testing. The data sets for the steel strip entry in this table for the Simplified Method are shown in figures 28 and 29. Additional data for the bar mat and welded wire walls above and below a soil friction angle of 40° is provided in figures 30 and 31. What becomes immediately obvious is that all of the methods tend to significantly under-predict the reinforcement loads when the soil backfill shear strength exceeds 40°. Average ratios of predicted to measured reinforcement loads for steel strip walls range from 0.63 to 0.69 for all three methods, and all three methods exhibit rather poor predictions in terms of data scatter, with the coefficient of variation being approximately twice that of the dataset for soil friction angles of 40° or less. When the backfill shear strength is 40° or less, all of the methods produce a reasonably accurate prediction, if not slightly conservative. Of the three methods, the Simplified Method produced the most conservative prediction, though the differences among all three methods are really quite small for soil friction angles at or below 40°.

Table 8. Effect of wall backfill soil friction angle on the bias and data scatter regarding MSE wall reinforcement load prediction.

MSE Wall Reinforcement Type (# of Walls)	Backfill Soil Friction Angle	Ratio: Predicted/Measured Reinforcement Load					
		Coherent Gravity Method		FHWA Structure Stiffness Method		Simplified Method	
		Average	COV	Average	COV	Average	COV
Steel Strip (9)	$\leq 40^o$	1.02	36.0%	0.97	33.5%	1.10	35.3%
Steel Strip (5)	$> 40^o$	0.63	72.9%	0.69	59.4%	0.69	76.0%
All walls (12)	$\leq 40^o$	1.05	37.3%	1.11	41.4%	1.17	37.0%
All walls (9)	$> 40^o$	0.70	61.8%	0.97	64.7%	0.88	67.6%

For steel reinforced MSE wall systems at working stress conditions, it is unlikely that enough strain can occur in the soil to fully mobilize the soil shear strength, particularly since for most granular soils, 2 to 5 percent strain is required to reach the peak shear stress for the soil, and steel reinforcement will only strain on the order of a

few tenths of a percent strain. The steel reinforcement prevents the necessary soil strain from developing. Inability to fully mobilize soil shear strength at working stress conditions in steel reinforced MSE walls has long been recognized (Mitchell and Villet, 1987). Furthermore, the use of the peak friction angle and K_a or K_o in these methods implies that the reinforcement stress is directly related to the soil state of stress. This may not be the case.

How do these observations affect the validity of the assumption that the peak soil friction angle can be used for design, since all currently available methods use this assumption? It must be recognized that the soil parameter that best characterizes the soil response at working stress conditions is the soil modulus. At working stress conditions, the amount of stress carried by the reinforcement will depend on the stiffness of the reinforcement relative to the soil stiffness, if the soil shear strength is not fully mobilized. The stiffer the reinforcement relative to the soil modulus, the more load the reinforcement will attract. However, accurately estimating the soil modulus is not a simple task, and at this point it has generally been reserved as part of a research activity, for example, to perform finite element modeling of MSE walls. For this reason, a semi-empirical approach using measurements from full-scale walls has been taken to modify the limit equilibrium approach to more accurately reflect working stress conditions. This approach uses soil parameters such as the peak soil friction angle that are readily available to designers. Because the active or at-rest earth pressure coefficient is being used to index the lateral soil stress carried by the reinforcement to the soil properties, the key issue is how similar the soil response characterization based on the lateral earth pressure coefficient is to the variation of the soil modulus for the range of soils typically encountered.

The results plotted in figures 28 through 31 and summarized in Table 8 suggest that as long as the soil friction angle is approximately 40° or less, the use of the peak soil friction angle in lieu of the soil modulus is sufficiently accurate for practical estimation of reinforcement loads for all three methods. This also means that these methods should not be used with a design peak soil friction angle of higher than 40°, or reinforcement load under-prediction could result. This is a limitation of all three methods that must be recognized for steel reinforced MSE walls.
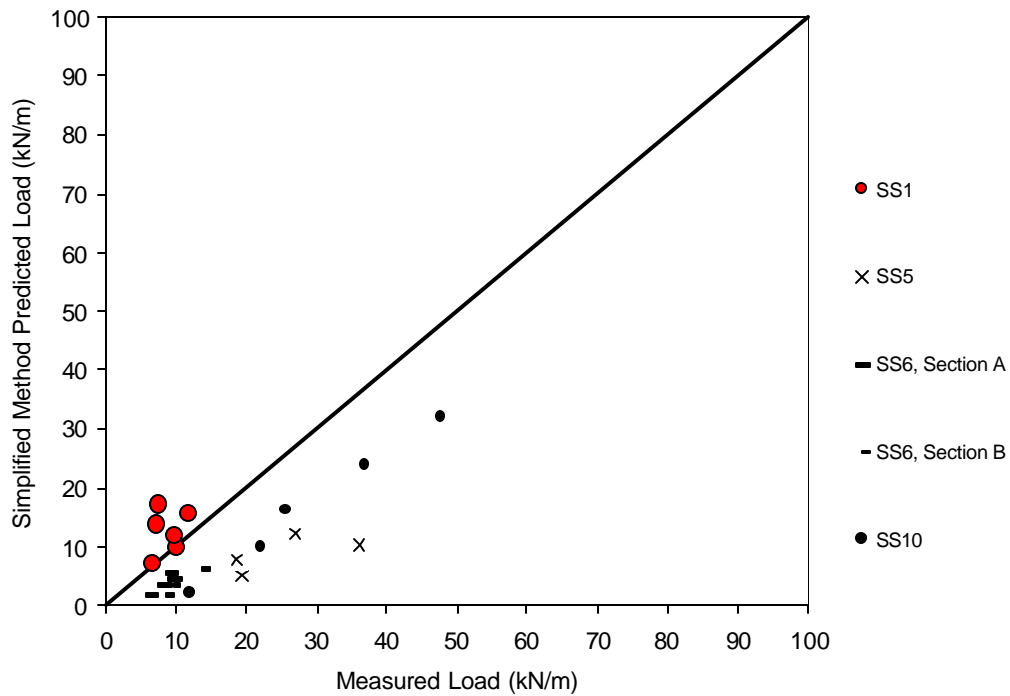
Figure 28.   Simplified Method predicted load versus measured reinforcement peak load for steel strip reinforced MSE walls, with phi greater than 40°.
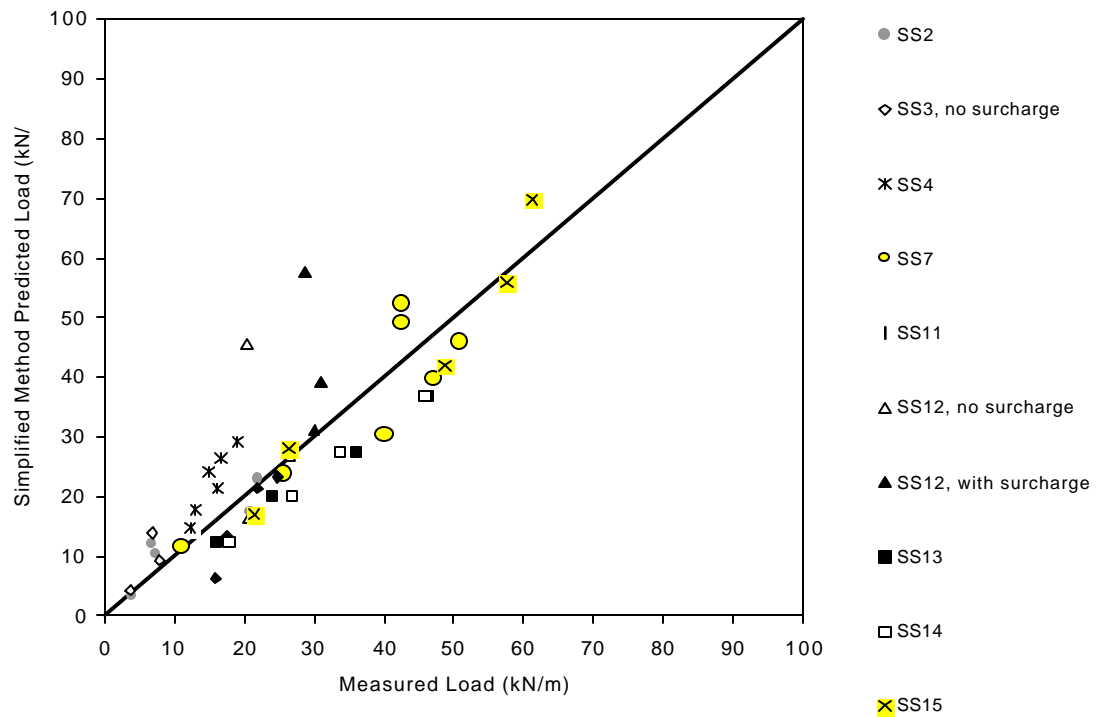

Figure 29.   Simplified Method predicted load versus measured reinforcement peak load for steel strip reinforced MSE walls, with phi of 40° or less.
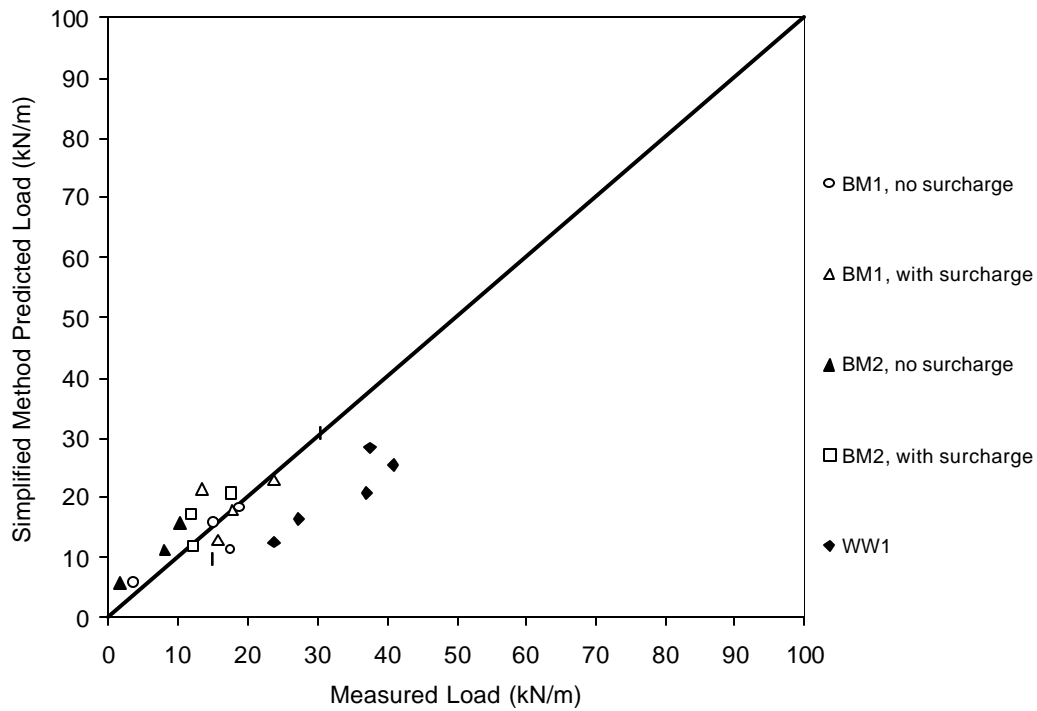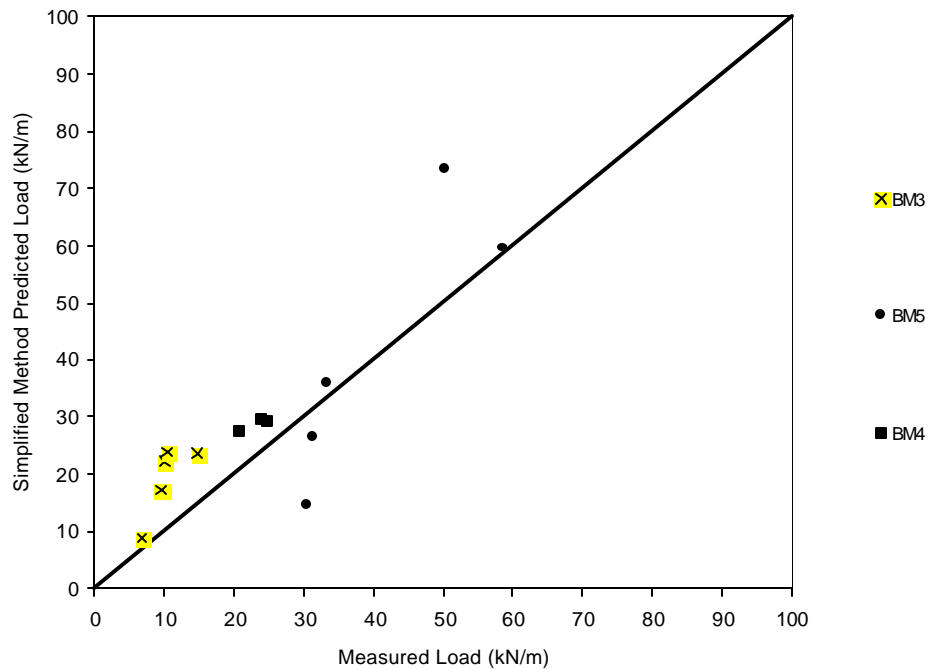
Figure 30.   Simplified Method predicted load versus measured reinforcement peak load for steel bar mat and welded wire reinforced MSE walls, with phi greater than 40$^{\mathrm{o}}$.

Figure 31.   Simplified Method predicted load versus measured reinforcement peak load for steel bar mat and welded wire reinforced MSE walls, with phi of 40$^{\mathrm{o}}$ or less.

Effect of Soil Surcharge above the Wall

Regarding the effectiveness of these methods to predict reinforcement loads when significant soil surcharges are present, all three methods show a significant drop in the ratio of the predicted to measured reinforcement load, as shown in Table 9. All three methods exhibit a similar amount of drop in the predicted to measured reinforcement load when a soil surcharge is applied. However, only the Coherent Gravity Method drops enough to provide a nonconservative prediction of reinforcement load. Figures A-14, A-20, and A-22 show that the soil surcharge causes the greatest increase in reinforcement stress in the upper half of the walls. Though the presence of the surcharge should increase the overturning stress, thereby increasing the vertical and lateral stress acting within the wall mass in the Coherent Gravity Method, the $K_o - K_a$ curve for determining the lateral stress coefficient begins where the failure surface intersects the sloping soil surcharge rather than at the wall face. This causes the lateral stress coefficient to be lower relative the lateral stress coefficient calculated from the other methods, which likely contributes to the tendency of the Coherent Gravity Method to under-predict the reinforcement loads relative to the other methods when a significant soil surcharge is present.

Table 9. Comparison of soil surcharge effects on the bias and data scatter regarding MSE wall reinforcement load prediction.

MSE Wall Reinforcement Type (# of Walls)	Soil Sur-charge Present?	Ratio: Predicted/Measured Reinforcement Load					
		Coherent Gravity Method		FHWA Structure Stiffness Method		Simplified Method	
		Average	COV	Average	COV	Average	COV
All walls (3)	No	1.10	53.1%	1.55	58.2%	1.44	55.4%
All walls (3)	Yes	0.86	45.8%	1.30	25.2%	1.23	40.8%

Effect of Compaction Stresses

Table 10 and figures 32 and 33 allow a comparison of walls that were compacted "lightly" to walls that were compacted in accordance with typical construction practice. For this analysis, "light" compaction is defined as compaction with light weight compactors or spreading equipment only, and no attempt is made to achieve typical target backfill densities (e.g., 95 percent of Standard or Modified Proctor). This is typically the

case for test walls. Typical construction practice (termed "heavy" compaction in the figures and table) for wall backfill compaction is defined as compaction with moderate to large vibratory rollers, except light weight compactors near the wall face, where typical target backfill densities to meet contract requirements are achieved. Only the steel strip wall data provided enough wall cases with and without heavy compaction. Therefore, this comparison is limited to steel strip reinforced walls. Furthermore, since all of the walls that were constructed with light compaction had backfill soil shear strengths of 40° or less, the light compaction wall case histories are only compared to case history walls that were constructed with conventional compaction and had backfill shear strengths of 40° or less. Though it could be argued that heavy compaction could result in backfill shear strengths well in excess of 40°, the potential underestimate in reinforcement loads that could result from inadequate consideration of compaction effects would overshadowed by the soil shear strength effects mentioned previously. Therefore, to keep the comparison as pure as possible, only steel strip MSE wall case histories with soil shear strengths of 40° or less are considered.

Table 10. Comparison of compaction effects on the bias and data scatter regarding MSE wall reinforcement load prediction (steel strip reinforced walls, backfill phi of 40° or less).

MSE Wall Reinforcement Type (# of Walls)	Degree of Backfill Compac-tion	Ratio: Predicted/Measured Reinforcement Load					
		Coherent Gravity Method		FHWA Structure Stiffness Method		Simplified Method	
		Average	COV	Average	COV	Average	COV
Steel Strip (4)	Light	1.01	37.0%	0.93	34.2%	1.04	37.6%
Steel Strip (6)	Heavy	1.07	36.4%	1.04	34.3%	1.19	35.5%

The scatter in the available data in Table 10 and figures 32 and 33 show that the overall effect of compaction on the prediction accuracy of all three methods is small. . All three methods are slightly less conservative on average for lightly compacted backfills relative to heavily compacted backfills. Previous research has shown that compaction of soil on the reinforcement tends to cause compaction stresses to develop within the reinforcement (Ehrlich and Mitchell, 1994). This not only affects the stress level in the reinforcement, but it also may affect the soil modulus and the soil friction

angle.   None of the methods mentioned in this paper directly accounts for compaction effects from a theoretical standpoint, but each does attempt to take them into account generally through the empirically derived lateral stress coefficient K_r.

The empirical adjustments to the lateral stress coefficient attempt to address this theoretical deficiency, apparently allowing the prediction methods to not be significantly affected by the degree of compaction, even though, theoretically, the degree of compaction should have a significant effect on the reinforcement stresses.   It appears that all three methods adequately account for the effect of compaction stresses on the soil reinforcement loads, and none of the methods has a clear advantage over the other methods on this issue.
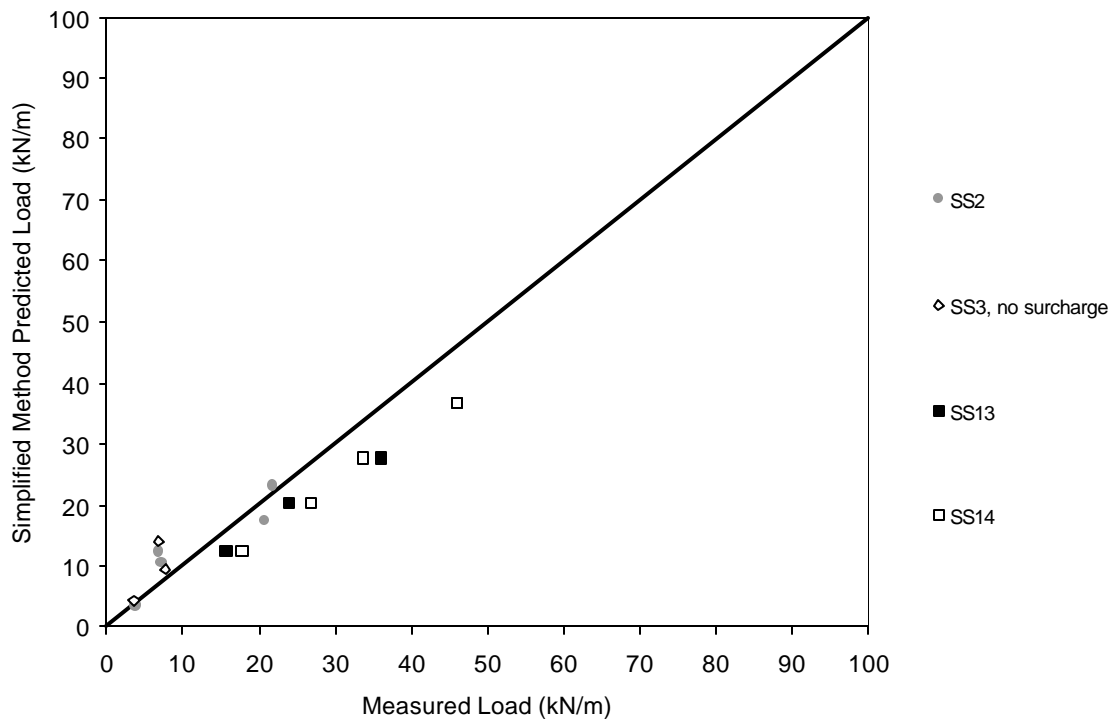
Figure 32.   Simplified Method predicted load versus measured reinforcement peak load for steel strip reinforced MSE walls, with phi of 40° or less and light compaction.
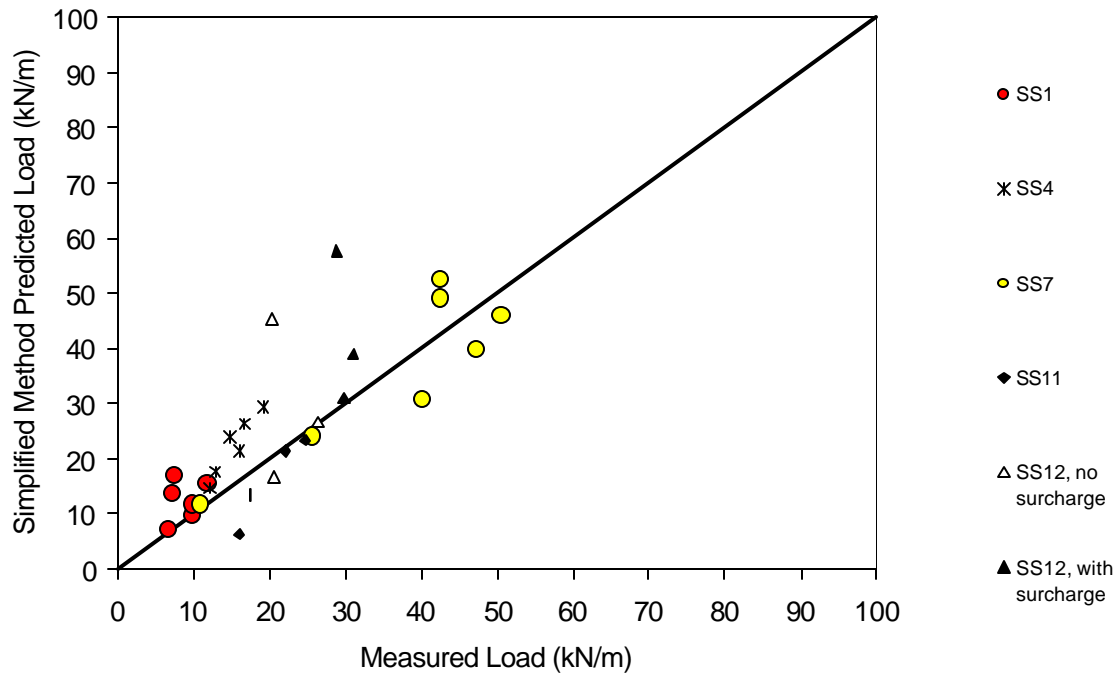
Figure 33.   Simplified Method predicted load versus measured reinforcement peak load for steel strip reinforced MSE walls, with phi of 40° or less and heavy compaction.

Effect of Overturning Stresses on Vertical Stresses within the Wall

Is the reinforced soil mass rigid enough to transmit overturning forces caused by externally applied forces to the interior of the reinforced soil mass , thereby increasing the vertical stress acting at any level within the wall mass?   The Coherent Gravity Method makes the assumption that it is rigid enough, whereas the other two methods do not.   If this assumption is valid, it should be possible to observe vertical stresses that are consistently greater than what would result from gravity forces alone (i.e., γZ).   For most walls designed and built to date, this overturning stress assumption has only a minor effect on vertical stresses (on the order of a 10 to 20 percent difference).   The difference can be more significant for walls with very steep sloping soil surcharges, very narrow base width walls, or very poor backfill soils behind the reinforced soil zone.   However, the latter two of these cases are rarely seen in practice and would be a violation of the other provisions in the AASHTO design specifications (AASHTO, 1996).   This assessment, of course, assumes that this theoretical assumption is valid.   Furthermore, if narrow base width is an issue that affects vertical stress at the base of MSE walls, then it

60

would follow that lengthening the wall reinforcement at the base would decrease the vertical stresses at the wall base. Regarding the soil surcharge issue, however, the increase in vertical stress due to overturning effects is more than compensated for by the reduction in the lateral earth pressure coefficient in the Coherent Gravity Method. This is because K_o decreases relative to the intersection of the failure surface with the soil surcharge surface, rather than being referenced to the top of the wall at the face as is true of the other two methods (see Figure 3).

Figures 34 through 38 show the measured vertical stresses obtained from several of the wall case histories as measured at the base of the wall. Stresses from steel reinforced walls and geosynthetic reinforced walls are shown. Figures 34 (steel) and 36 (geosynthetic) are normalized to vertical stresses on the basis of gravity forces alone (i.e., the FHWA Structure Stiffness Method and the Simplified Method), whereas Figure 35 (steel) is normalized to vertical stresses that include the increases caused by overturning effects (i.e., the Coherent Gravity Method). The stresses measured beneath the steel reinforced walls include walls with a narrow base width but do not include walls with significant soil surcharges above them because of the lack of availability of such cases for steel MSE walls. To evaluate stresses beneath walls with significant soil surcharges, only geosynthetic wall case histories were available.

The scatter in the vertical stress data is significant. This is typical of soil stress measurements, as such measurements are highly dependent on how the stress cells are installed, how well the modulus of the stress cell versus that of the surrounding soil is maintained, and the adequacy of the calibration. The typical variance on such measurements is on the order of 20 percent. However, even with this possible variance, some trends can be observed.

Though there is apparently a zone behind the wall where the stresses at the base of the wall are higher than would be predicted from gravity forces alone, accounting for the overturning moment (as is done in the Coherent Gravity Method) does not eliminate that problem (compare figures 34 and 35 for steel reinforced walls). Furthermore, if the wall mass should be treated internally as a rigid body, then walls with a very narrow base width should be more affected by the overturning moment than walls with a more conventional base width. The Bourron Marlotte steel strip MSE walls are a good

example of this (see Figure 16 for a typical cross-section). As shown in figures 34 and 35, accounting for the overturning moment appears to over-predict the vertical stresses beneath the wall. Therefore, the overturning assumption appears to be too conservative, particularly for the Bourron Marlotte walls and more generally for the other steel MSE wall data shown in the figures.

The vertical stress data from the geosynthetic wall case histories also demonstrate that overturning stress may not contribute significantly to vertical stress within the wall. The details of these geosynthetic wall cases are not reported here, but they may be found in their respective references (Berg et al., 1986; Bathurst et al., 1993(a); Bathurst et al., 1993(b), Allen et al., 1992). Some of these geosynthetic wall cases for which vertical stress data are provided do have significant soil surcharges on them, and therefore, should have larger overturning stresses on them than walls without significant soil surcharges on them (at least theoretically, if the Meyerhof (1953) approach is valid for MSE walls).. Figure 36 shows that for the geosynthetic walls, vertical stresses are in general less than or equal to gravity forces without overturning effects. In general, the geosynthetic wall cases do not consistently exhibit as much of a peak in the vertical stresses behind the wall face as do the steel reinforced MSE wall cases. This may be the result of the difference in the flexibility of steel reinforced versus geosynthetic reinforced wall systems.

Furthermore, figures 37 and 38 show plots of the peak vertical stresses in each wall as a function of the ratio of the theoretical (calculated) vertical stress with overturning effect to the vertical stress without overturning effect. If overturning stresses influence the vertical stress within the wall mass (based on the Meyerhof (1953) rigid body assumption), there should be a general trend of increasing normalized peak vertical stress with an increase in the ratio of the calculated vertical stress with overturning effects to the vertical stress without overturning effects. As shown in figures 37 and 38, no such trend can be observed for either the steel reinforced walls or the geosynthetic reinforced walls.

Given all this, overturning stresses apparently do not contribute to vertical stress as much as originally assumed, if at all. This does not mean, however, that the properties of the soil behind the reinforced soil zone have no effect on the vertical and lateral stresses within the reinforced soil mass. Instead, it is more likely that some overturning stresses

are being transmitted into the reinforced soil zone, depending on the reinforcement and soil stiffness, but not to the degree assumed by the Coherent Gravity Method. It must be recognized that the original work performed by Meyerhof (1953) was on a rigid metal plate model footing. His work showed that because the soil is not nearly as stiff as the footing, the soil is not capable of carrying high peak forces at the toe of the footing. Instead, the overturning stresses beneath the footing will redistribute themselves in accordance with the soil's ability to carry those stresses. It is from this finding that the equivalent rectangular bearing stress distribution was born, the issue being the soil's rigidity beneath a rigid foundation element. For MSE walls, the equivalent "footing" is not rigid at all, so perfect transmission of overturning stresses would definitely not be expected.

What then is the cause of the higher stresses that appear to occur in a narrow zone just behind the back of the wall face? Christopher (1993) concluded that at least in some cases this increase in vertical stresses is due to downdrag forces on the back of the wall facing. If this is the case, it is possible that the wrong theoretical assumption is being used to account for the phenomenon of increased stresses. Given that one method assumes full overturning effects while the other two methods assume no overturning effects, yet all the methods have a similar level of accuracy, this issue does not appear to be terribly critical to producing estimates of reinforcement stress with adequate accuracy.
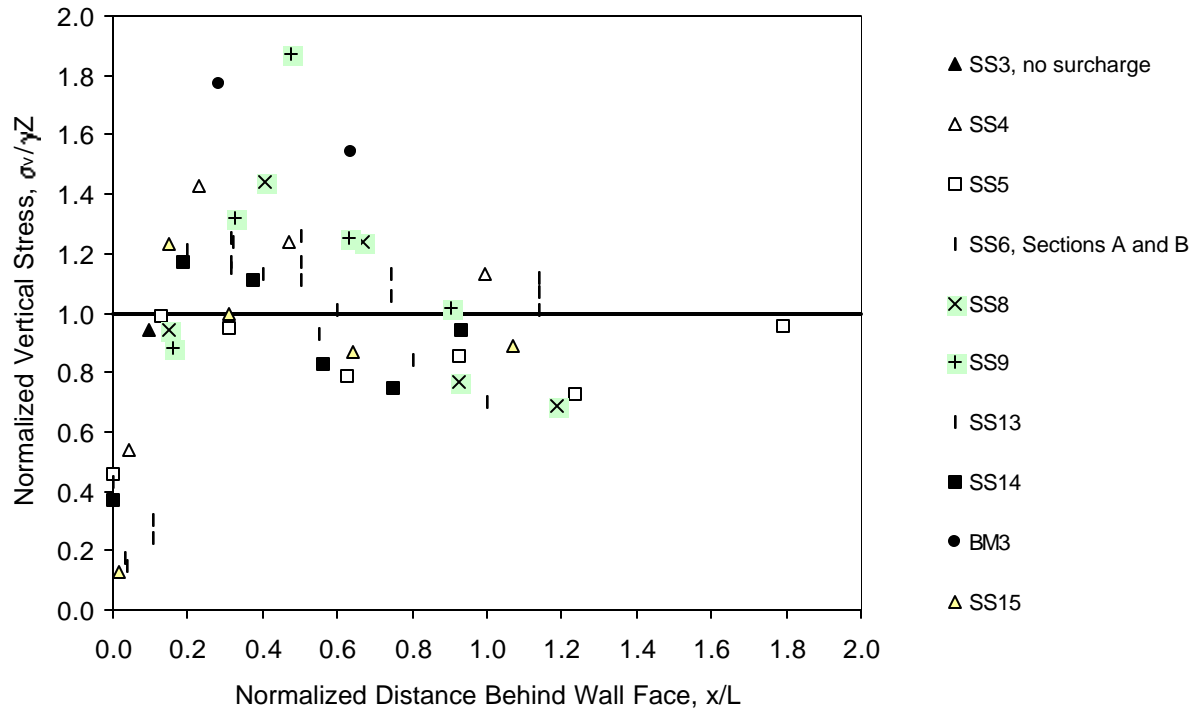
Figure 34.   Vertical stress measured at the wall base for steel reinforced MSE walls, normalized with the theoretical vertical stress without overturning effect.
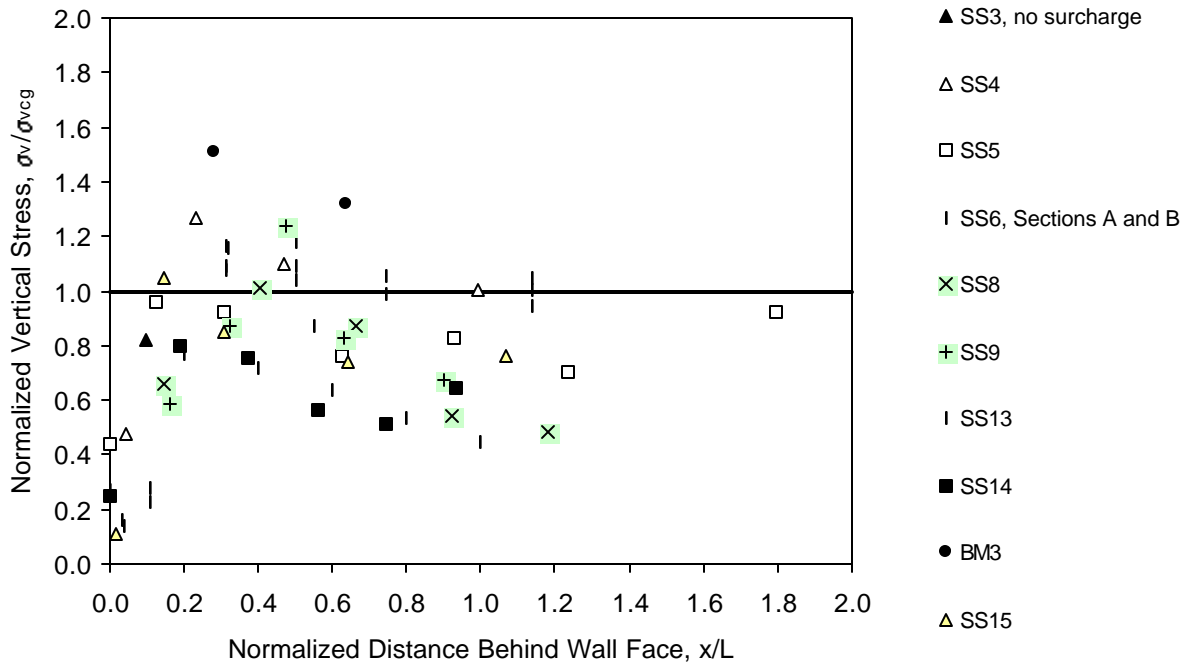
Figure 35.   Vertical stress measured at the wall base for steel reinforced MSE walls, normalized with the theoretical vertical stress with overturning effect.
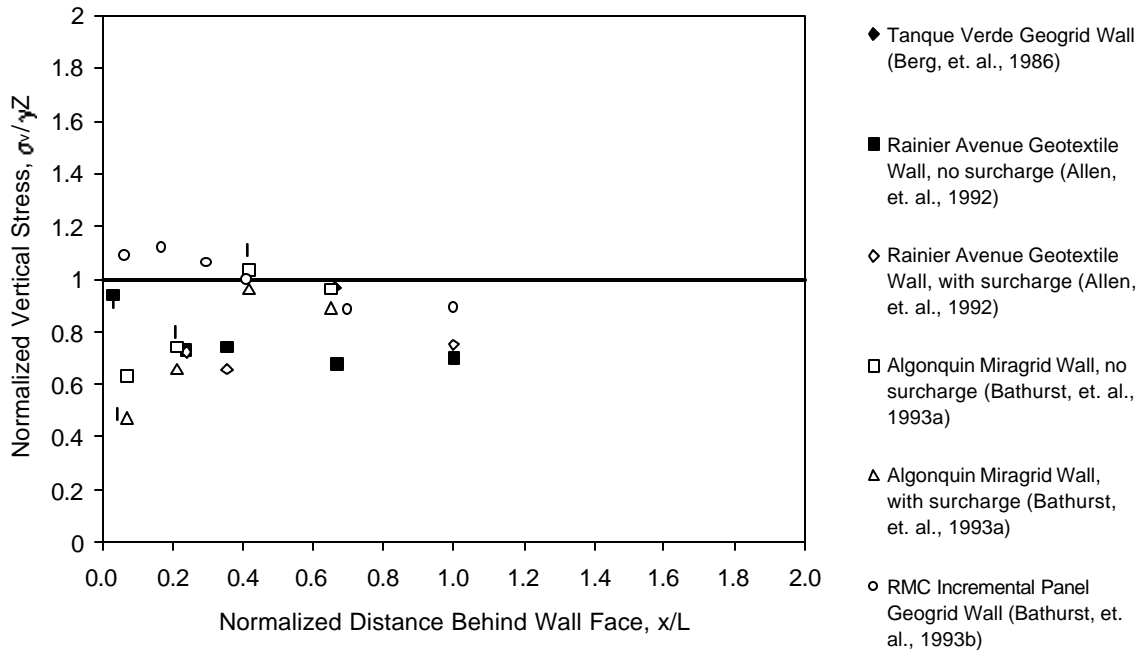
Figure 36. Vertical stress measured at the wall base for geosynthetic reinforced MSE walls, normalized with the theoretical vertical stress without overturning effect.
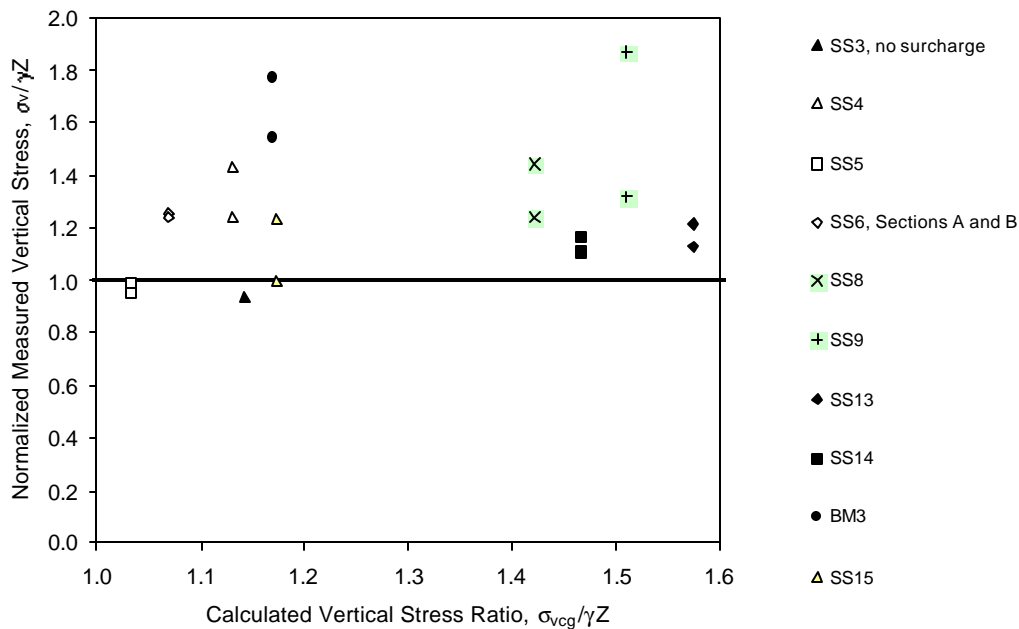
Figure 37. Maximum (2 highest values) vertical stress measured at the wall base for steel reinforced MSE walls, normalized with the theoretical vertical stress without overturning effect, versus the calculated vertical stress ratio (calculated Coherent Gravity vertical stress/γZ).
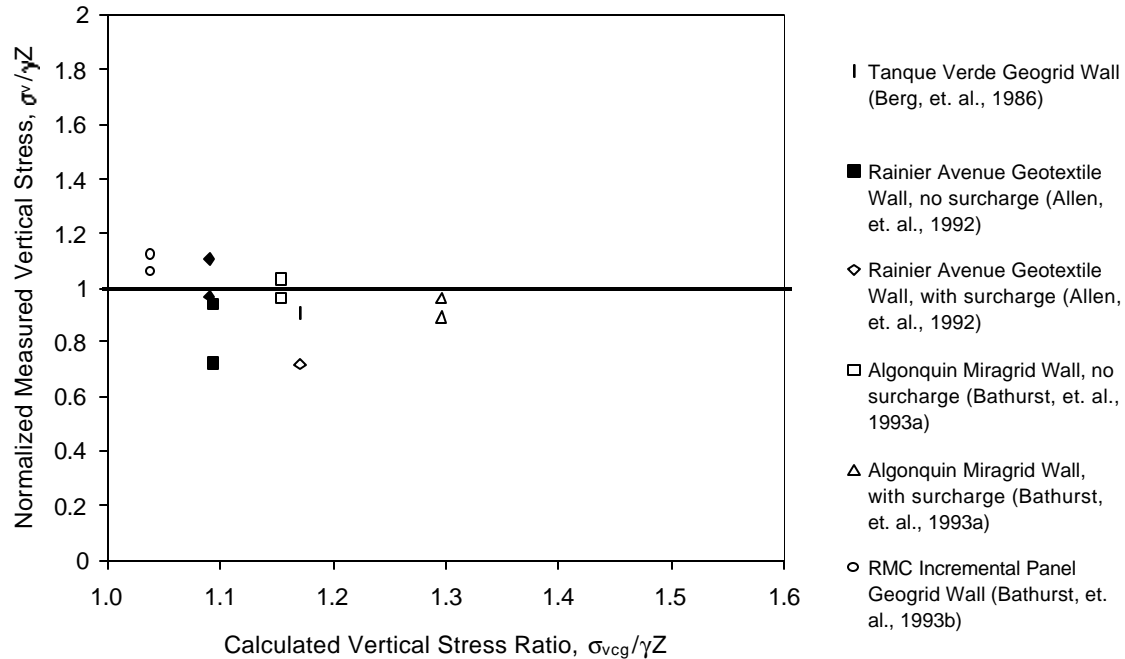
Figure 38. Maximum (2 highest values) vertical stress measured at the wall base for geosynthetic reinforced MSE walls, normalized with the theoretical vertical stress without overturning effect, versus the calculated vertical stress ratio (calculated Coherent Gravity vertical stress/γZ).

BASIS FOR AND FINAL DEVELOPMENT OF THE SIMPLIFIED METHOD

As discussed previously, the development of the Simplified Method began as an attempt to combine the best features of the Coherent Gravity and FHWA Structure Stiffness methods into a unified but simple method to predict reinforcement stresses in MSE walls. To accomplish this, an evaluation of the various theoretical assumptions, as well as of the overall predictive accuracy of the two methods relative to the proposed Simplified Method and the measured results from a number of full-scale MSE wall case histories, was conducted as described in the previous section. On the basis of that evaluation, the following can be concluded:

- In general, the accuracy of the Simplified Method's predictions is similar to that of the other two methods (see Table 7 and figures 22 through 27).

- The application of the Meyerhof (1953) rigid body assumption to the calculation of vertical stress within the reinforced soil mass appears to be conservative, and the justification to use this assumption from a theoretical viewpoint is

66

questionable, since the reinforced soil mass is very flexible. The validity of this assumption has been evaluated relative to measured vertical stresses beneath MSE walls for walls with very narrow base widths, walls with high soil surcharges, relatively tall walls, and more typical wall geometries. This assumption has also been evaluated in terms of its effect on the measured stresses in the reinforcement. In light of both evaluations, removing this overturning stress assumption from the calculation method does not appear to compromise the predictive accuracy of the Simplified Method.

- Though the effect of the reinforcement type and stiffness on the reinforcement loads is more fully taken into account using the FHWA Structure Stiffness Method, the simplification of by a single K_r/K_a curve for each reinforcement type appears to provide prediction accuracy that is similar to that of the other methods. Figures 39 through 42 show the measured reinforcement data, presented as K_r/K_a ratios, relative to the Simplified Method K_r/K_a curves. For steel strip reinforcement, especially when only the data for a backfill phi of approximately 40° or less are considered, the Simplified Method K_r/K_a curve appears to provide a sufficiently accurate match to the data (see figures 39 and 40). For bar mat and welded wire walls, the paucity of data and the scatter in the data make an assessment of the accuracy of the Simplified Method K_r/K_a curve more difficult, but this data limitation applies to the other prediction methods as well. Because of the paucity of data, some conservatism in locating the K_r/K_a curve for the Simplified Method was thought to be warranted. Hence, the bar mat and welded wire reinforcement types were grouped together regarding the K_r/K_a curve for the Simplified Method, which is consistent with the approach used by the FHWA Structure Stiffness Method, and were set higher than the K_r/K_a curve for steel strip reinforcements because of the observed trend of generally higher reinforcement stresses for bar mat and welded wire reinforced walls. Though it could possibly be argued that for bar mat walls the K_r/K_a curve could be set a little lower near the wall top, to 2.0 rather than 2.5, the paucity and scatter of the data influenced the authors and the AASHTO TWG involved with the development of this method to set the K_r/K_a curve to be the same as for

welded wire walls. As more full-scale measurements on bar mat and welded wire walls, combined with good backfill soil property data, become available, it is certainly possible that the K_r/K_a curve for these two reinforcement types will need to be lowered.

- The database of full-scale MSE wall reinforcement load measurements used for the Simplified Method is larger and more current than that used for the other two methods. Though it is a relatively new method, it is at least as well justified empirically as the other two methods, and the simplifications proposed do not appear to compromise the Simplified Method's accuracy. The database of full-scale walls includes walls with and without significant soil surcharges, narrow and wide base-width walls, walls with trapezoidal cross-sections, tall walls up to 18 m high, walls with a wide range of reinforcement coverage ratios, and walls with a variety of soil shear strengths. Therefore, the Simplified Method is valid empirically for walls that fit within these parameters. This does not mean that the Simplified Method cannot be extrapolated to walls that do not fit within these parameters (e.g., walls taller than 18 m). But extrapolation to walls that are beyond the range of walls that are part of the empirical basis for this and the other two methods should be done with caution, and more refined analyses may be needed.

- It is recommended that walls designed with the Simplified Method, as well as the other methods evaluated in the paper, use a design soil friction angle of not greater than 40° for steel reinforced MSE walls, even if the measured soil friction angle is greater than 40°.

- Only one case history did not have an incremental concrete panel facing. Therefore, the accuracy of this method, as well as the other methods with flexible facings, is not well known, and some judgment may be needed to apply the Simplified and other methods to walls with flexible facings.
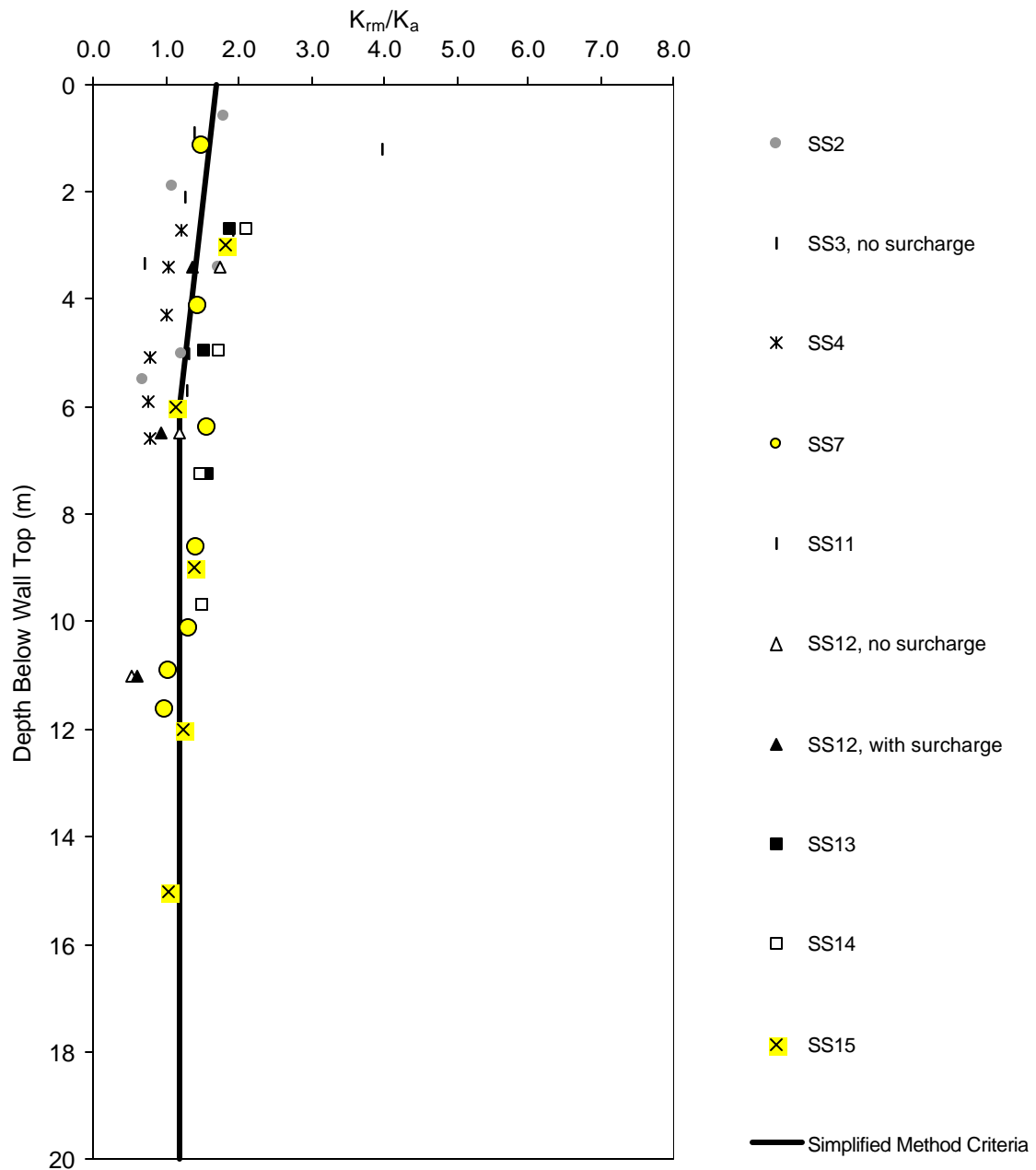
Figure 39. Measured K_r/K_a ratios for steel strip walls in comparison to the Simplified Method design criteria, for a backfill phi of 40° or less.
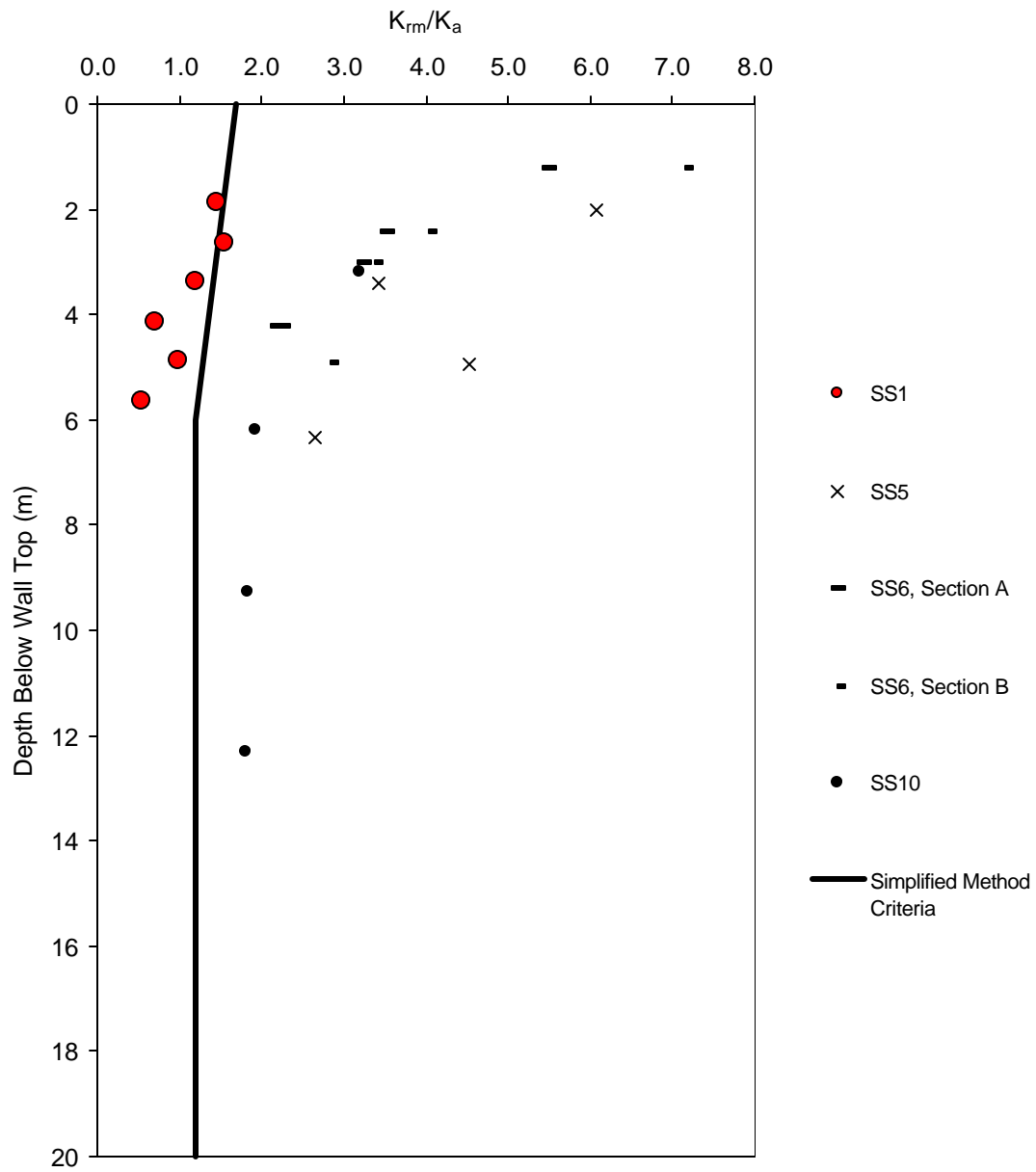
Figure 40.   Measured K_r/K_a ratios for steel strip walls in comparison to the Simplified Method design criteria, for a backfill phi of greater than 40°.
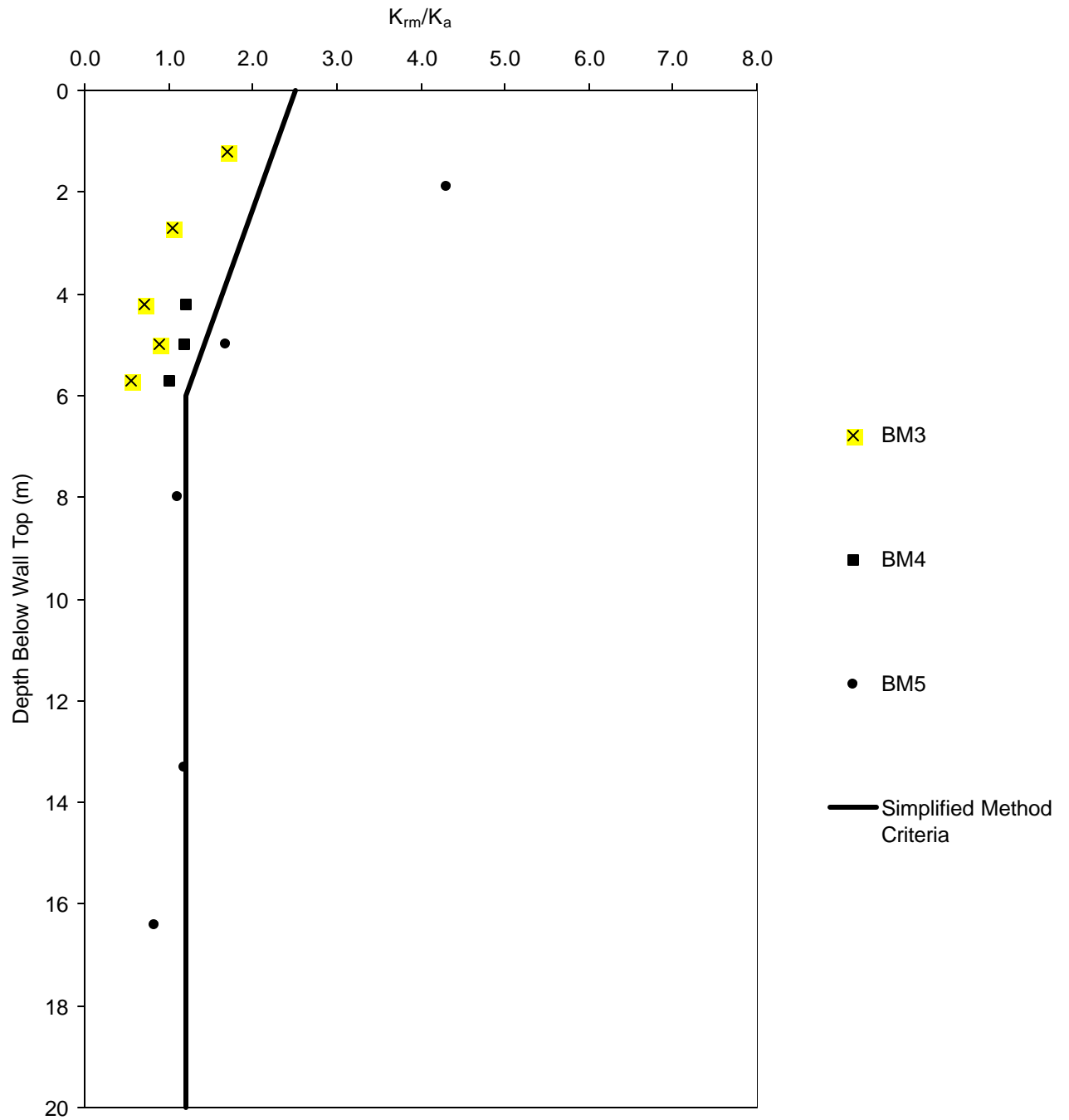
Figure 41. Measured K_r/K_a ratios for bar mat and welded wire walls in comparison to the Simplified Method design criteria, for a backfill phi of $40°$ or less.
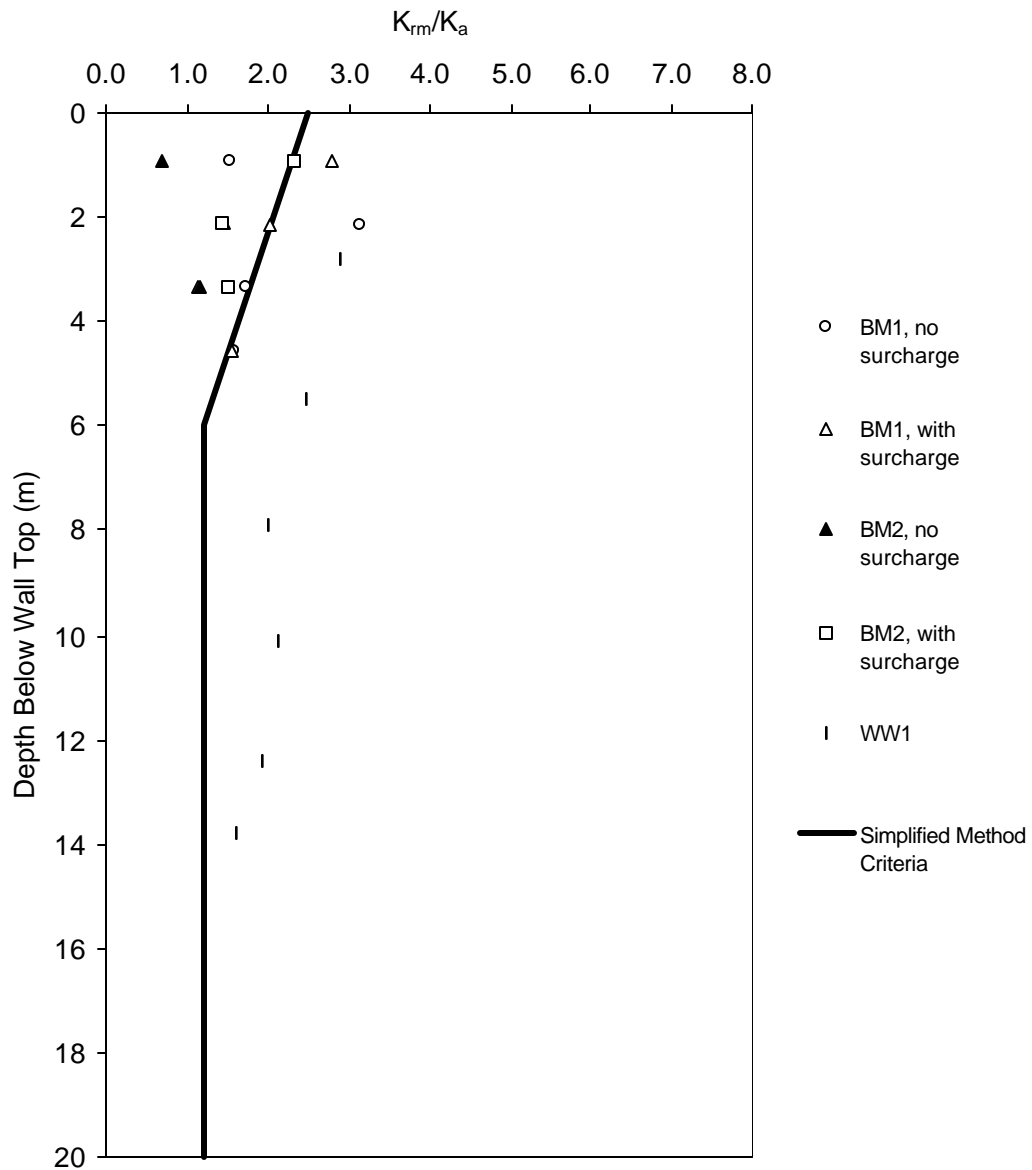
Figure 42. Measured K_r/K_a ratios for bar mat and welded wire walls in comparison to the Simplified Method design criteria, for a backfill phi of greater than 40°.

CONCLUSIONS

All of the methods (i.e., the Coherent Gravity, Simplified, and FHWA Structure Stiffness methods) that have been included in design codes to date have, for the most part, the same theoretical deficiencies, and empirical adjustments were made to each of the methods to account for those deficiencies. Extrapolating these empirically adjusted methods to wall design situations that are significantly beyond the cases for which they have been evaluated must be done with caution. This paper provides details of the case histories and data used to provide empirical support for each of these methods. At this point, at least until a more theoretically sound yet practical method becomes available and accepted, the most important test for a method such as the Simplified Method is how well it predicts the stress levels in the reinforcement relative to full-scale MSE wall empirical data. On the basis of the comparison of the prediction methods to the measured data presented and discussed previously, the Simplified Method appears to meet that test. This is not to say that the other methods mentioned in this paper are invalid or should not be used. As has been demonstrated, all of these methods tend to produce similar reinforcement load level predictions. However, the Simplified Method should be considered an update of the other methods, and it is the simplest and easiest to use of the methods investigated in this paper.

For future development and improvement of design methods used to determine MSE wall reinforcement loads, the following areas should be addressed:

- Develop a better yet practical method of characterizing the soil properties needed to predict reinforcement loads under working stress conditions, especially for high strength backfill soils with a peak phi of over 40°.
- Limit equilibrium concepts are currently mixed with empirical adjustments to predict working loads. As design codes move toward Load and Resistance Factor Design (LRFD), this combined limit state approach will no longer be usable. The design approach needs to be purified so that working stress concepts are used for the working stress design, and limit equilibrium concepts are used for ultimate limit state design.

- The effect of wall toe restraint and facing stiffness needs to be determined and directly accounted for in the wall reinforcement design.

- The effect of backfill compaction on the working stress soil behavior and the resulting reinforcement loads must be better addressed.

- More instrumented bar mat walls and welded wire walls are needed, as are walls with flexible facings to provide a better empirical basis for these types of walls.

ACKNOWLEDGMENTS

REFERENCES

AASHTO, 1996, *Standard Specifications for Highway Bridges, with 1999 Interims*, American Association of State Highway and Transportation Officials, Sixteenth Edition, Washington, D.C., USA, 686 p.

Adib, M. E., 1988, Internal Lateral Earth Pressure in Earth Walls, Doctoral Thesis Submitted to the University of California, Berkeley, California, 376 pp.

Al-Hussaini, M., and Perry, E. B., 1978, "Field Experiment of Reinforced Earth Wall," Symposium on Earth Reinforcement, Pittsburgh, ASCE, pp. 127-156.

Allen, T. M., Christopher, B.R., and Holtz, R.D., 1992, "Performance of a 12.6 m High Geotextile Wall in Seattle, Washington", *Geosynthetic Reinforced Soil Retaining Walls*, J. T. H. Wu (editor), Balkema, Rotterdam, pp. 81-100.

Al-Yassin, Z. A., 1983, VSL Retained Earth – Hayward Test Results, Internal Report to the VSL Corporation.

Anderson, L. R., Sharp, K. D., Harding, O. T., 1987, "Performance of a 50-Foot High Welded Wire Wall," Soil Improvement – a Ten Year Update, J. P. Welsh, ed., Geotechnical Special Publication No. 12, ASCE, pp. 280-308.

Bastick, M., 1984, Reinforced Earth Walls with Short Strips, Terre Armee Internal Report R-35.

Bastick, M., Schlosser, F., Segrestin, P., Amar, S., and Canepa, Y., 1993, "Experimental Reinforced Earth Structure of Bourron Marlotte: Slender Wall and Abutment Test," Renforcement Des Sols: Experimentations en Vraie Grandeur des Annees 80, Paris, pp. 201-228.

Bathurst, R. J., Simac, M. R., Christopher, B. R., and Bonczkiewicz, C., 1993(a), *A Database of Results from a Geosynthetic Reinforced Modular Block Soil Retaining Wall*, Renforcement Des Sols: Experimentations en Vraie Grandeur des Annees 80, Paris, pp. 341-365.

Bathurst, R. J., Jarrett, P.M., and Benjamin, D. J., 1993(b), "A Database of Results from an Incrementally Constructed Geogrid-Reinforced Soil Wall Test," Renforcement Des Sols: Experimentations en Vraie Grandeur des Annees 80, Paris, pp. 401-430.

Bathurst, R. J., Walters, D., Vlachopoulos, N., Burgess, P., and Allen, T. M., 2000, "Full Scale Testing of Geosynthetic Reinforced Walls," ASCE Geo Denver 2000, Denver, Colorado, pp.   .

Bell, J. R., Stilley, A. N., and Vandre, B., 1975, "Fabric Retained Earth Walls," Proceedings of the Thirteenth Annual Engineering Geology and Soils Engineering Symposium, University of Idaho, Moscow, Idaho, pp. 271-287.

Bell, J. R., Barrett, R. K., and Ruckman, A. C., 1983, "Geotextile Earth-Reinforced Retaining Wall tests: Glenwood Canyon, Colorado," Transportation Research Record 916, Washington, DC, pp. 59-69.

Berg, R.R., Bonaparte, R., Anderson, R. P., and Chouery, V.E., 1986, "Design, Construction, and Performance of Two Geogrid Reinforced Soil Retaining Walls," Proceedings of the Third International Conference on Geotextiles, Vienna, pp. 401-406.

Berg, R. R., Allen, T. M., and Bell, J. R., 1998, "Design Procedures for Reinforced Soil Walls - A Historical Perspective," *Proceedings of the Sixth International Conference on Geosynthetics,* Atlanta, GA, Vol. 2, pp. 491-496.

Boyd, M. S., 1993, "Behavior of a Reinforced Earth Wall at Ngauranga, New Zealand," Renforcement Des Sols: Experimentations en Vraie Grandeur des Annees 80, Paris, pp. 229-257.

Christopher, B. R., 1993, *Deformation Response and Wall Stiffness in Relation to Reinforced Soil Wall Design,* Ph.D. Dissertation, Purdue University, 352 pp.

Christopher, B. R., 1999, Personal Communication.

Christopher, B R., Gill, S. A., Giroud, J.-P., Juran, I., Mitchell, J. K., Schlosser, F., and Dunnicliff, J., 1990, Reinforced Soil Structures, Vol. 1 Design and Construction Guidelines, FHWA Report FHWA-RD-89-043, 285 pp.

Ehrlich, M., and Mitchell, J. K., 1994, "Working Stress Design Method for Reinforced Earth Soil Walls," ASCE Journal of Geotechnical Engineering, Vol. 120, No. 4, pp. 625-645.

Elias, V., and Christopher, B.R., 1997, Mechanically Stabilized Earth Walls and Reinforced Soil Slopes Design and Construction Guidelines, Federal Highway Administration, No. FHWA-SA-96-071.

Hollinghurst, E., and Murray, R. T., 1986, "Reinforced Earth Retaining Wall at A3/A322 Interchange: Design, Construction, and Cost," Proceedings Institution of Civil Engineers, Part 1, No. 80, pp. 1327-1341.

Jackura, K. A., 1988, Performance of a 62-Foot High Soil Reinforced Wall in California's North Coast Range, CALTRANS, Division of New Technology and Research, Internal Report.

Jackura, K. A., 1996, Personal Communication.

Juran, I., and Schlosser, F., 1978, "Theoretical Analysis of Failure in Reinforced Earth Structures," Proceedings, ASCE Symposium on Earth Reinforcement, Pittsburgh, pp. 528-555.

Lee, K. L., Adams, B. D., and Vagneron, J. J., 1973, "Reinforced Earth Retaining Walls," Journal, Soil Mechanics Division, ASCE, Vol. 99, No. SM10, pp. 745-764.

Meyerhof, G. G., 1953, "The Bearing Capacity of Foundations Under Eccentric and Inclined Loads," Proceedings of the Third International Conference of Soil Mechanics and Foundation Engineering, Vol. 1, pp. 225-244.

Mitchell, J. K., and Villet, W. C.B., 1987, Reinforcement of Earth Slopes and Embankments, NCHRP Report 290, Transportation Research Board, Washington, DC., 323 pp.

Murray, R. T., and Farrar, D. M., 1990, "Reinforced Earth Wall on the M25 Motorway at Waltham Cross," Proceedings Institution of Civil Engineers, Part 1, No. 88, pp. 261-282.

Murray, R. T., and Hollinghurst, E., 1986, "Reinforced Earth Retaining Wall at A3/A322 Interchange: Instrumentation, Site Observation, and Performance," Proceedings Institution of Civil Engineers, Part 1, No. 80, pp. 1343-1362.

Neely, W. J., 1993, "Field Performance of a Retained Earth Wall," Renforcement Des Sols: Experimentations en Vraie Grandeur des Annees 80, Paris, pp. 171-200.

Neely, W. J., Gandy, G., 1995, "Internal K-Values for Retained Earth Walls," Panamerican Conference on Soil Mechanics and Foundation Engineering, Guadalajara, Mexico, Vol. 2, pp. 895-906.

Netlon Limited, 1983, Guidelines for the Design and Construction of Reinforced Soil Retaining Walls Using Tensar Geogrids, Blackburn, England, 39 pp.

Richardson, G. N., Feger, D., Fong, A., and Lee, K. L., 1977, "Seismic Testing of Reinforced Earth Walls," Journal of the Geotechnical Engineering Division, ASCE, GT1, pp. 1-17.

Runser, D. J., Fox, P. J., and Bourdeau, P. L. (in press), "Field Performance of a 17 m Reinforced Soil Retaining Wall," *Geosynthetics International*, Vol. ___, No. ___, pp. ___.

Sampaco, C. L., 1995, Behavior of Welded Wire Mesh Reinforced Soil Walls from Field Evaluation and Finite Element Simulation, PhD Dissertation, Utah State University, Logan, UT.

Schlosser, F., 1978, "History, Current Development, and Future Developments of Reinforced Earth," Symposium on Soil Reinforcing and Stabilizing Techniques, sponsored by New South Wales Institute of Technology and the university of Sidney, Austrailia.

Schlosser, F., and Segrestin, P., 1979, "Dimensionnement des Ouvrages en Terre Armee par la Methode de l'Equilibre Local," International Conference on Soil Reinforcement: Reinforced Earth and Other Techniques, Paris, Vol. 1, pp. 157-162.

Steward, J., Williamson, R., and Mohney, J., 1977, Guidelines for the Use of Fabrics in Construction and Maintenance of Low-Volume Roads, Report No. FHWA-TS-78-205.

Thamm, B. R., 1981, "Messungen an einer Stutzkonstruktion aus ''Bewehrte Erde' unter dynamischer Belastung", Bundesanstalt fur Strassenwesen, Koln.

Vaslestad, J., 1993, Stal-og Bentongelementer I Losmassetunneler – Stottekonstruksjoner I Armert Jord, PubliKasjon Nr. 69, Statens Vegvesen, Veglaboratoriet, Oslo, pp. 42-47.

Vaslestad, J., 1996, Personal Communication

.

APPENDIX A

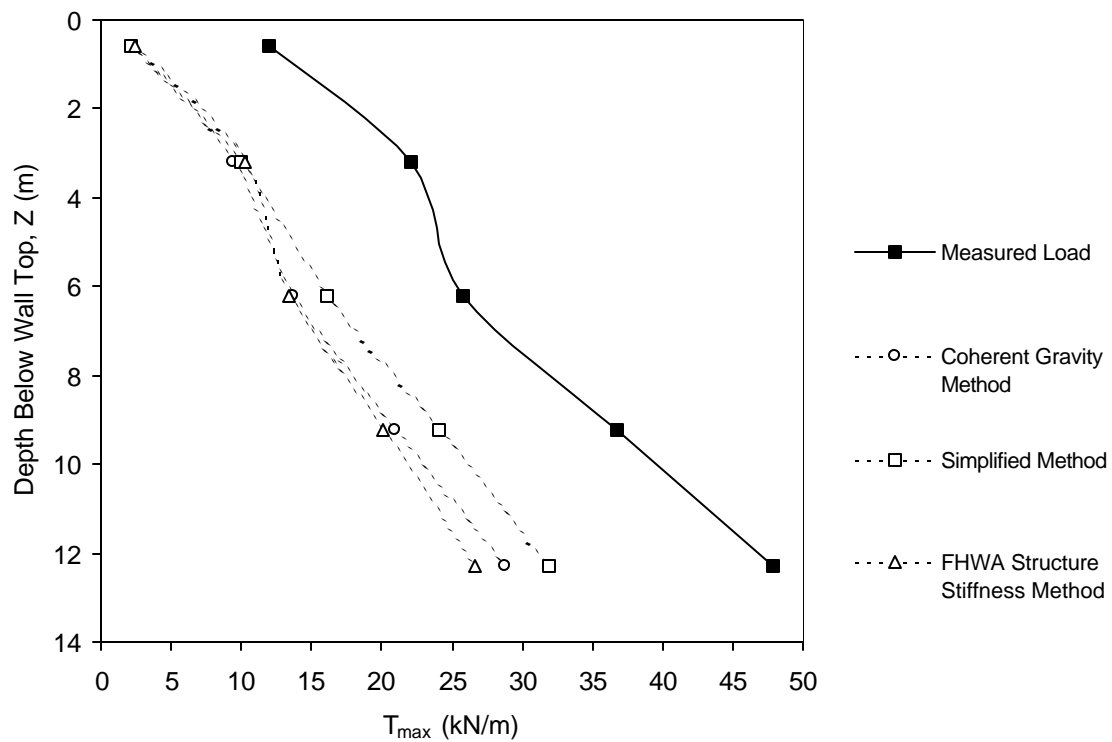**MEASURED REINFORCEMENT STRESS LEVELS IN STEEL
REINFORCED MSE WALLS**
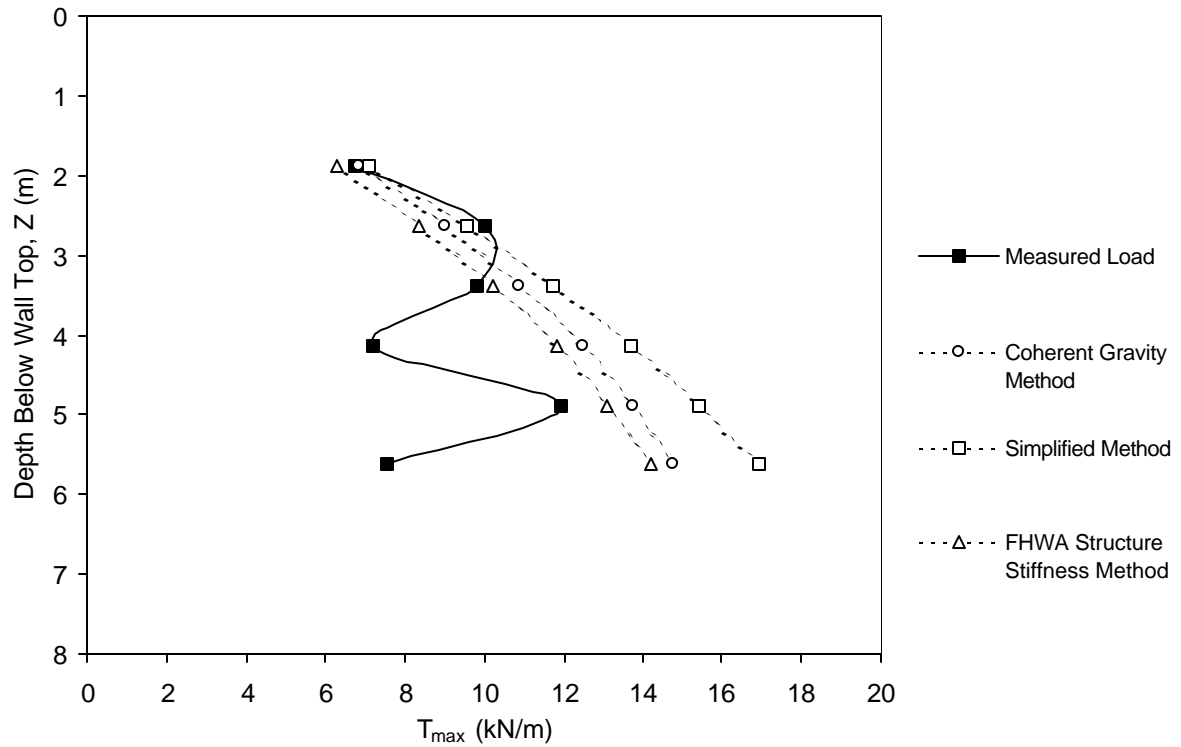
Figure A-1. Predicted and measured reinforcement peak loads for Lille, France, steel strip reinforced wall (SS1).
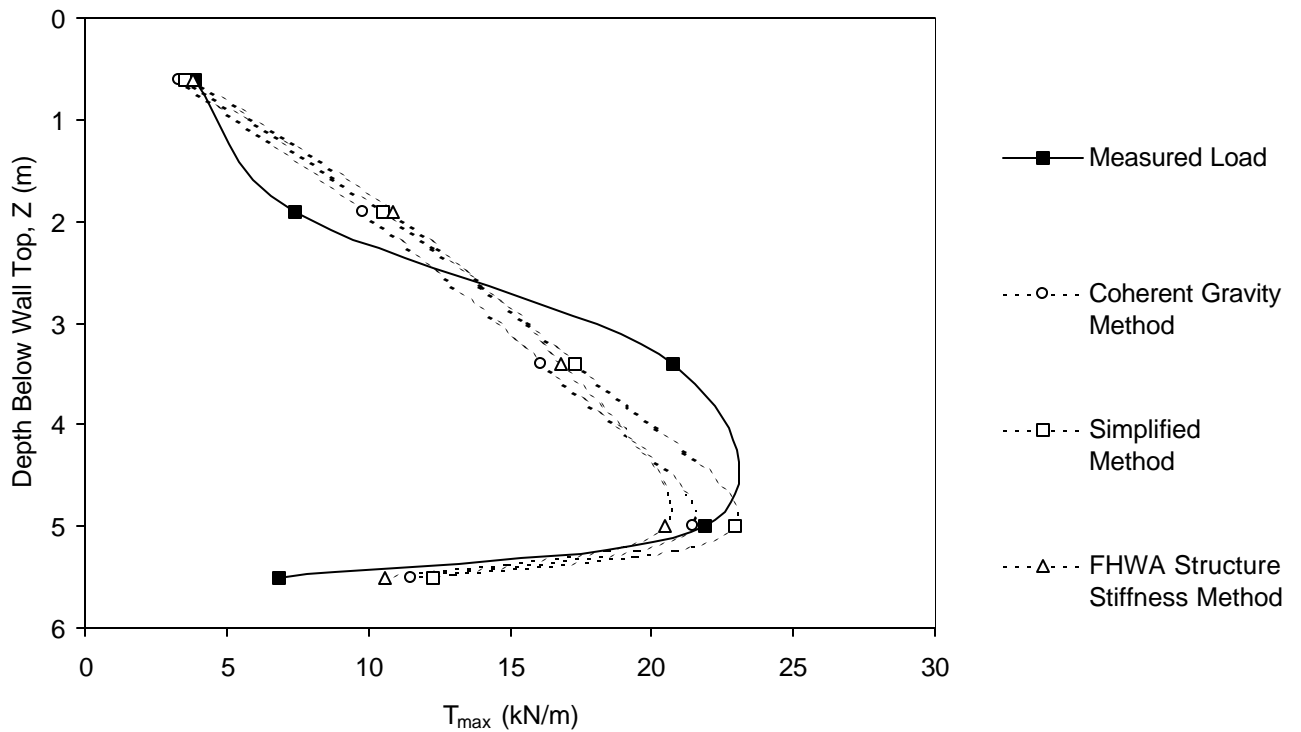
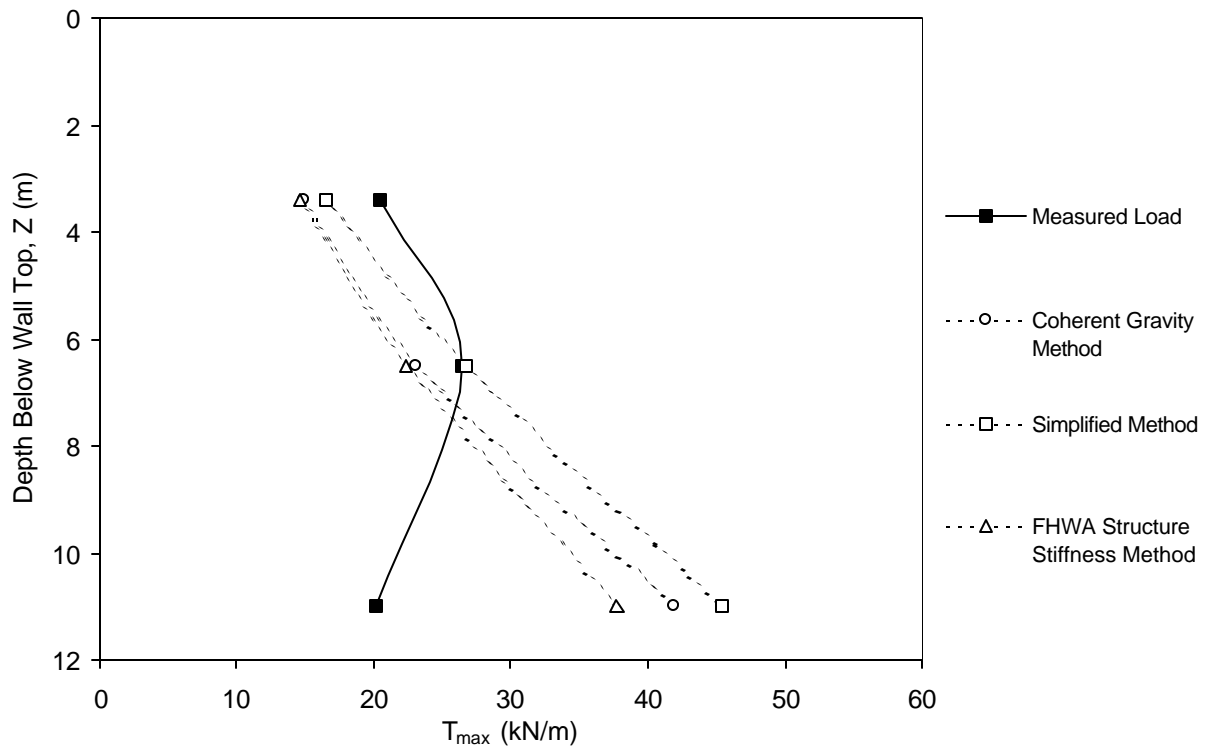Figure A-2. Predicted and measured reinforcement peak loads for UCLA steel strip reinforced test wall (SS2).
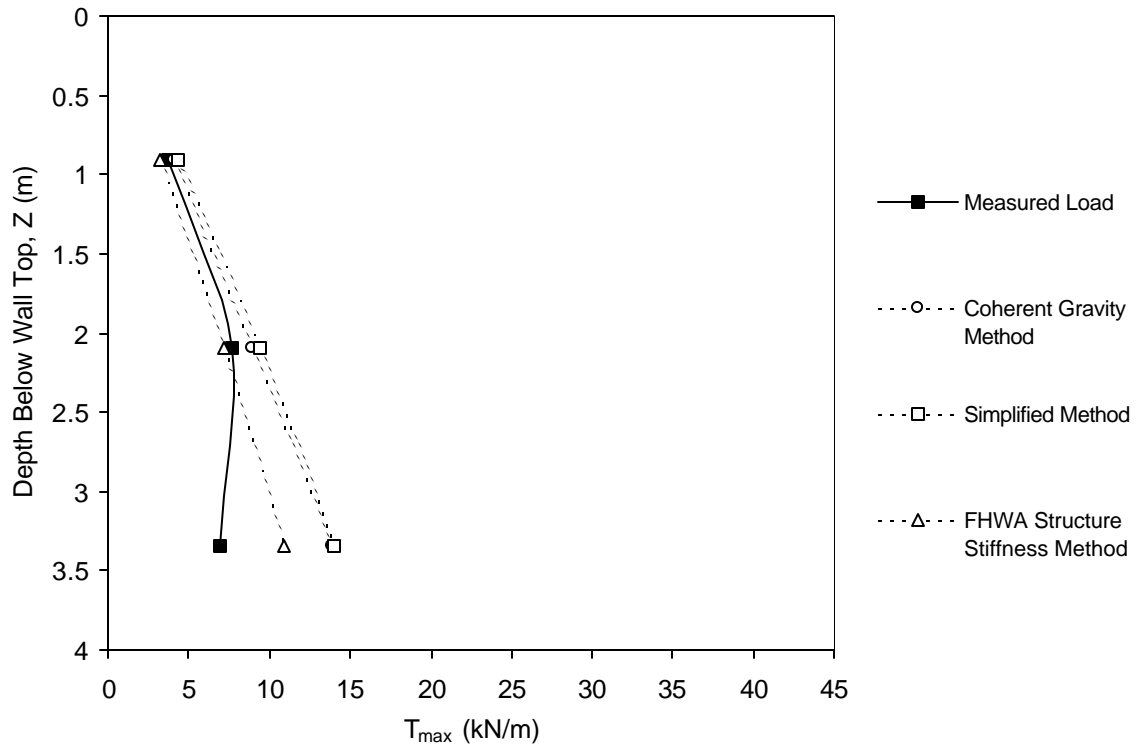
Figure A-3. Predicted and measured reinforcement peak loads for WES steel strip reinforced test wall, with no surcharge (SS3).
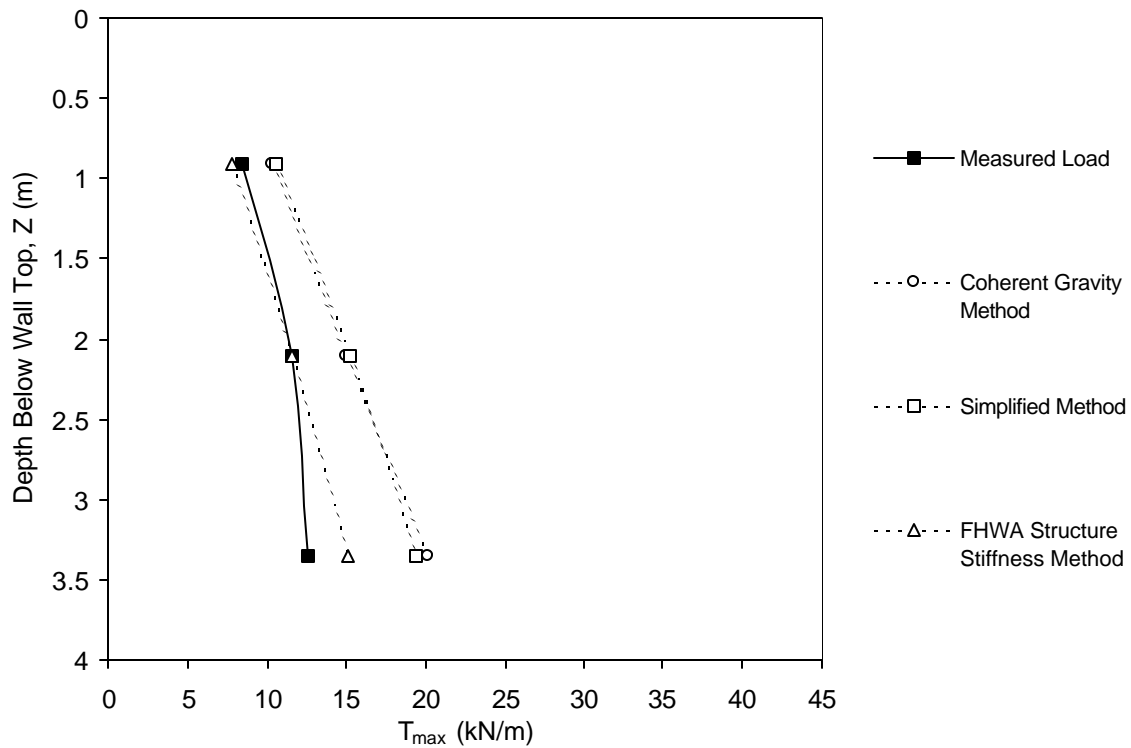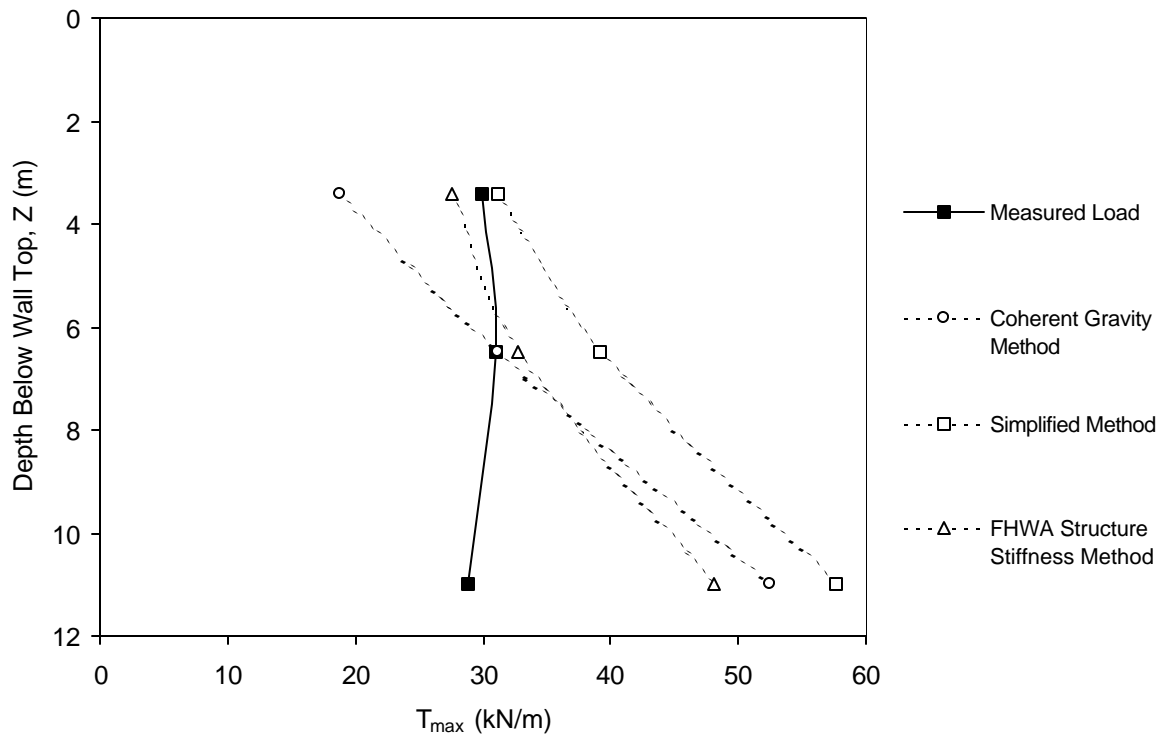

Figure A-4. Predicted and measured reinforcement peak loads for WES steel strip reinforced test wall, with 24 kPa surcharge (SS3).
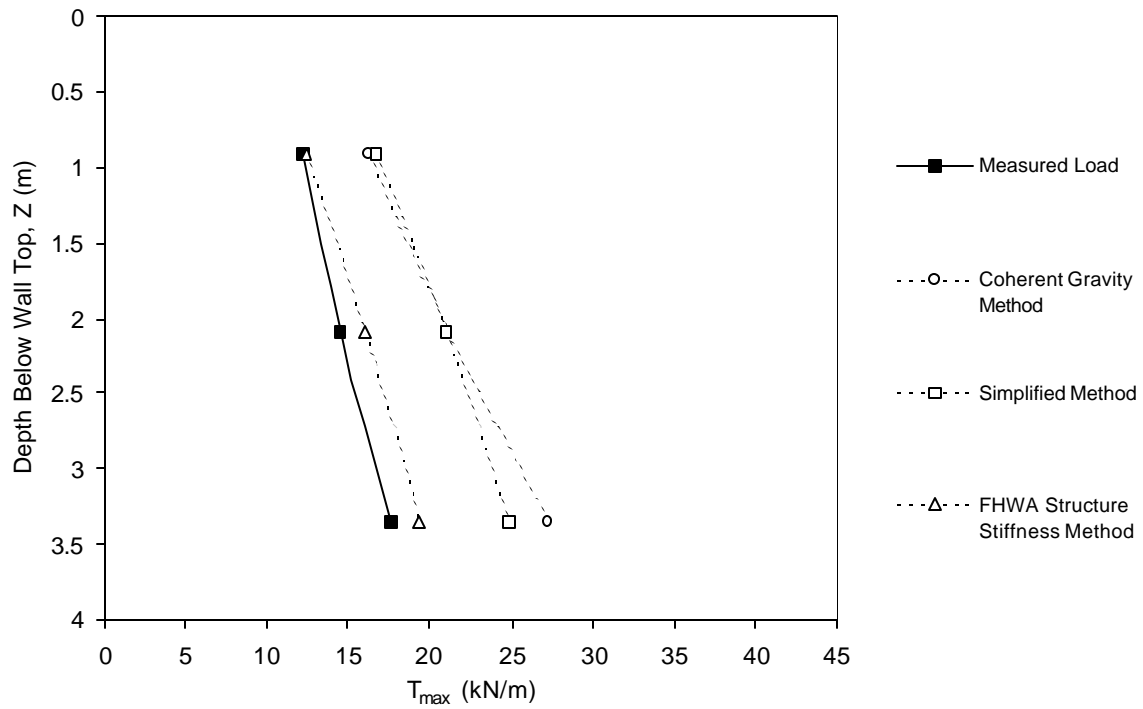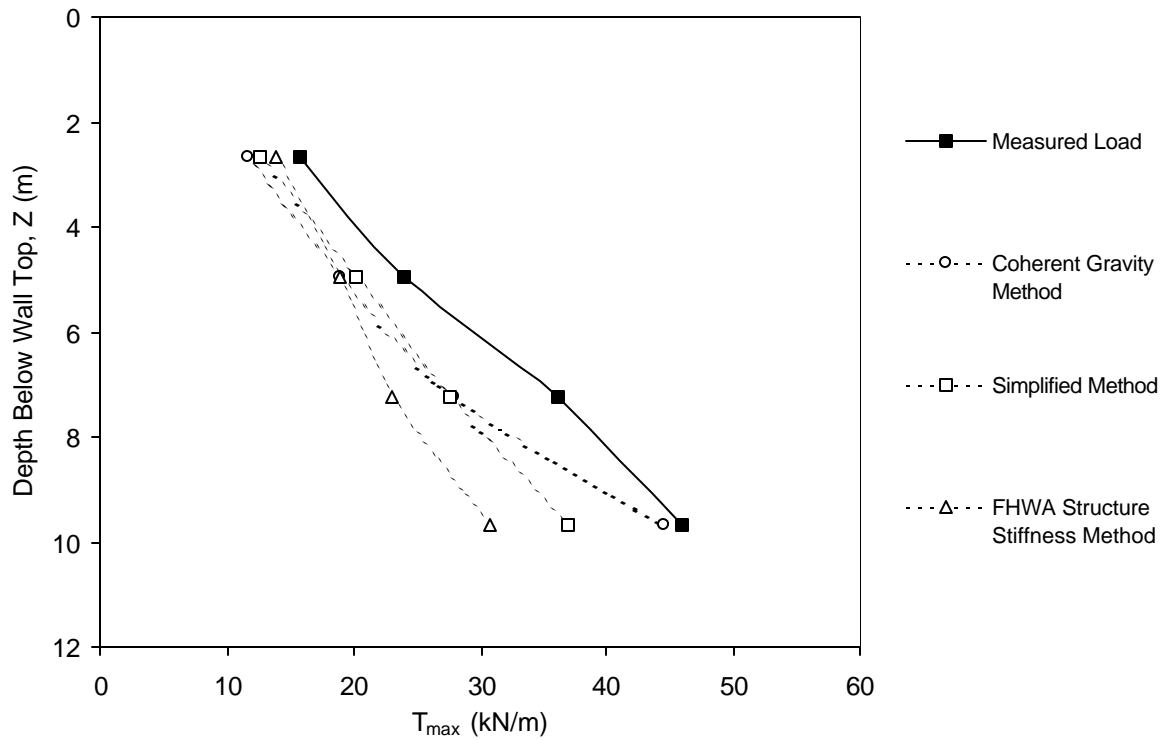
Figure A-5.   Predicted and measured reinforcement peak loads for WES steel strip reinforced test wall, with 48 kPa surcharge (SS3).
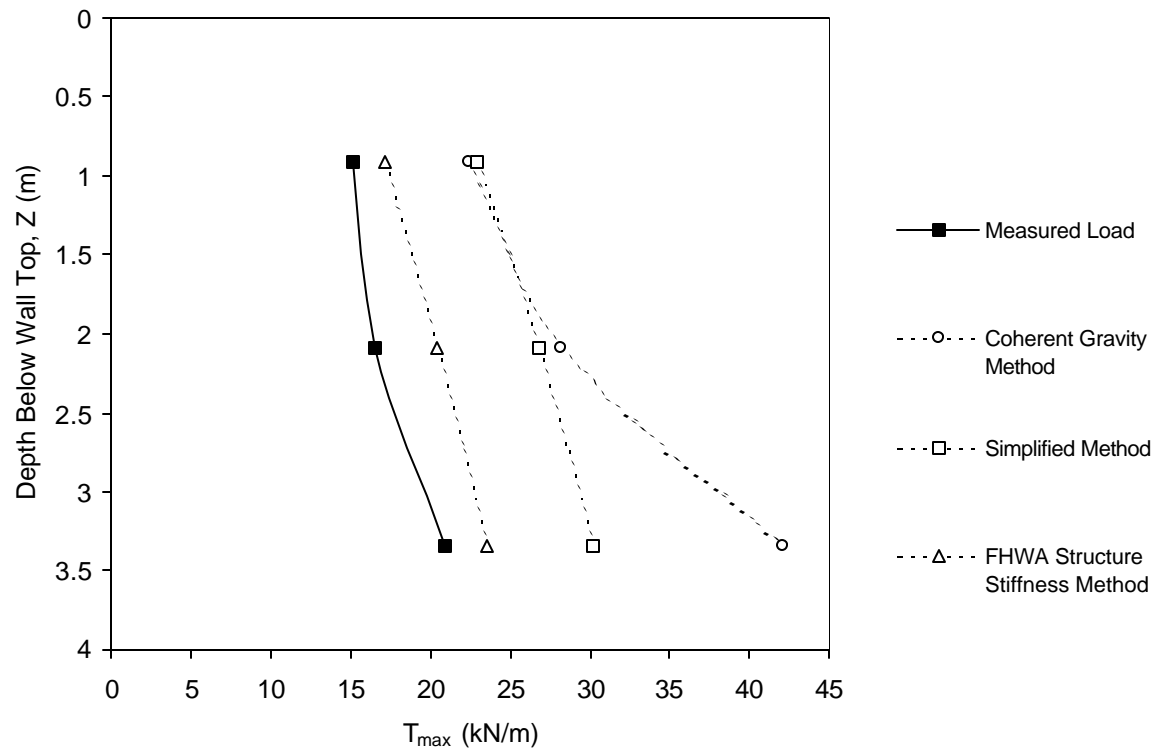
Figure A-6.   Predicted and measured reinforcement peak loads for WES steel strip reinforced test wall, with 72 kPa surcharge (SS3).

A-5
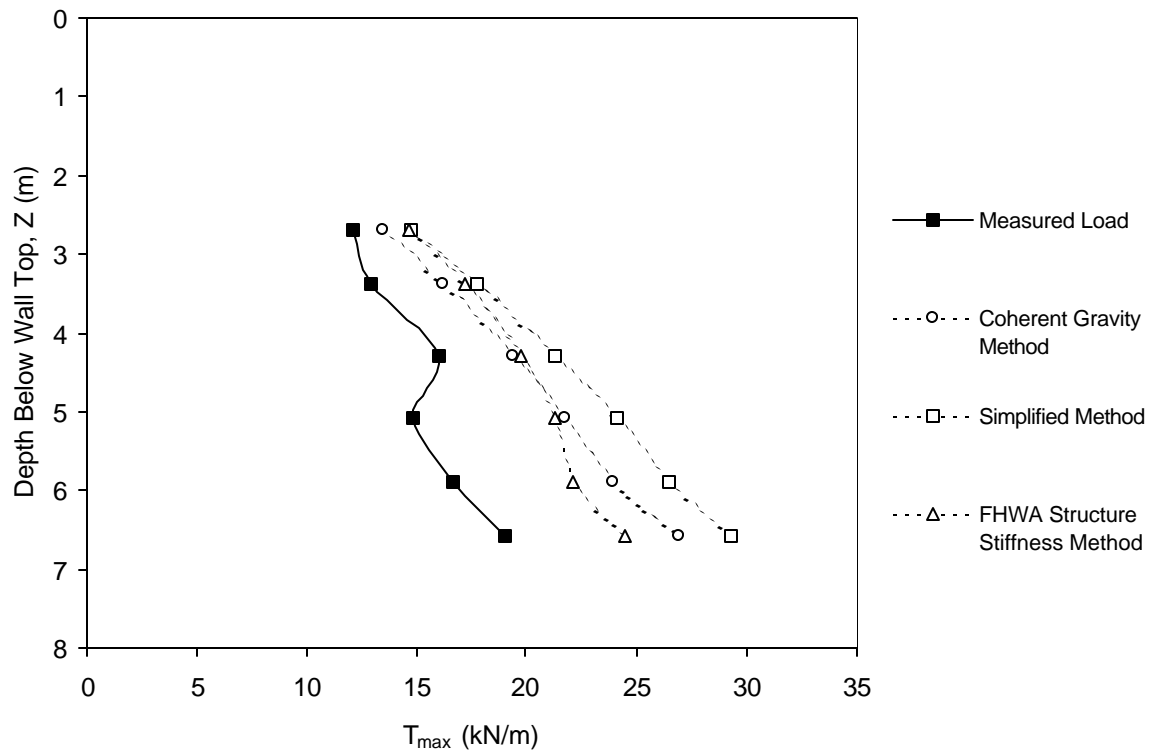
Figure A-7.   Predicted and measured reinforcement peak loads for Fremersdorf, Germany, steel strip reinforced wall (SS4).
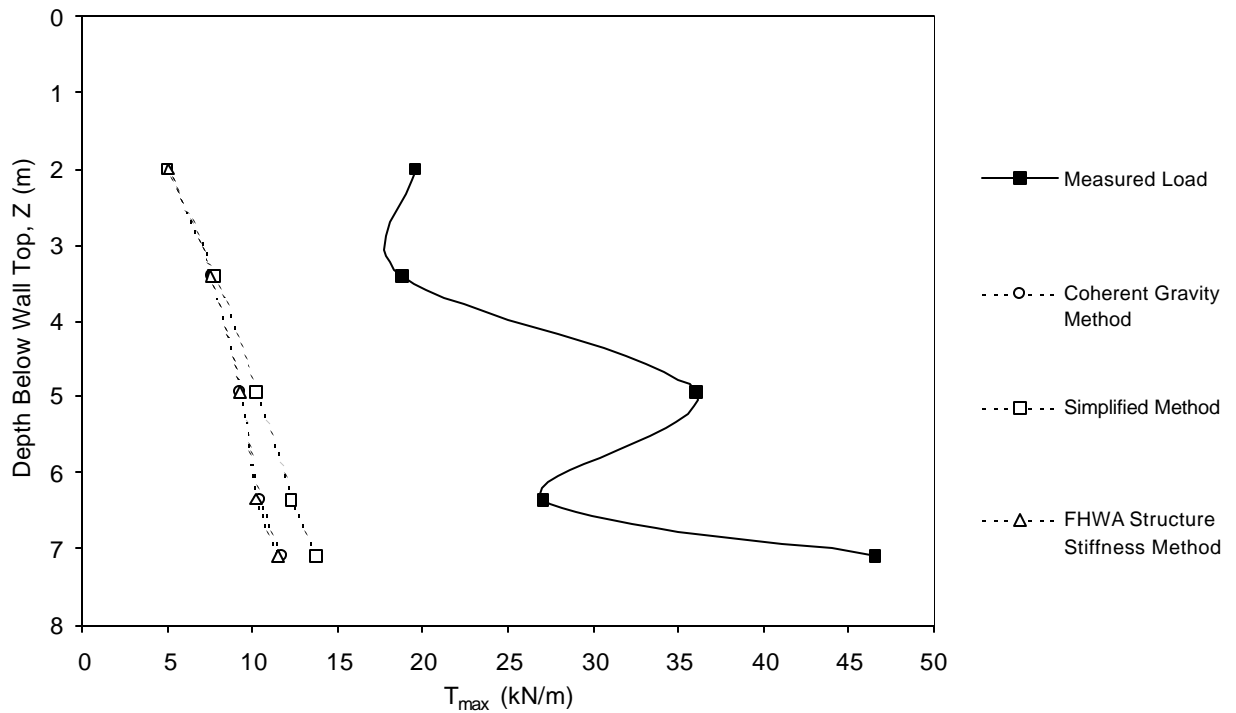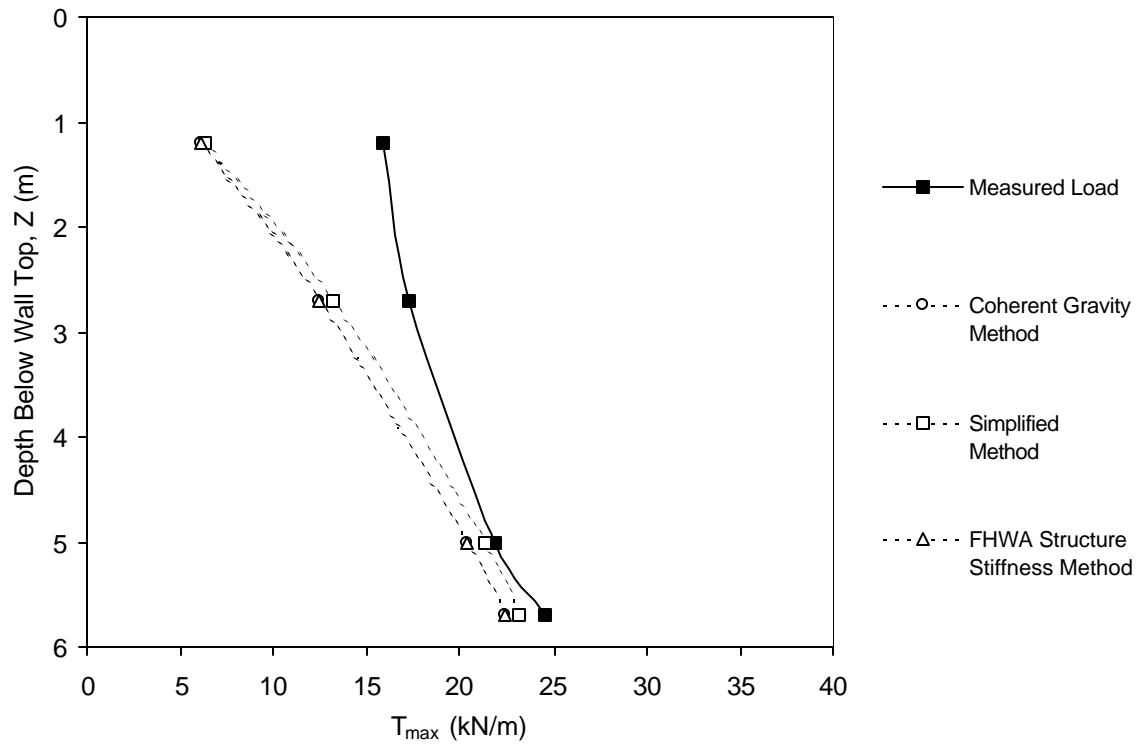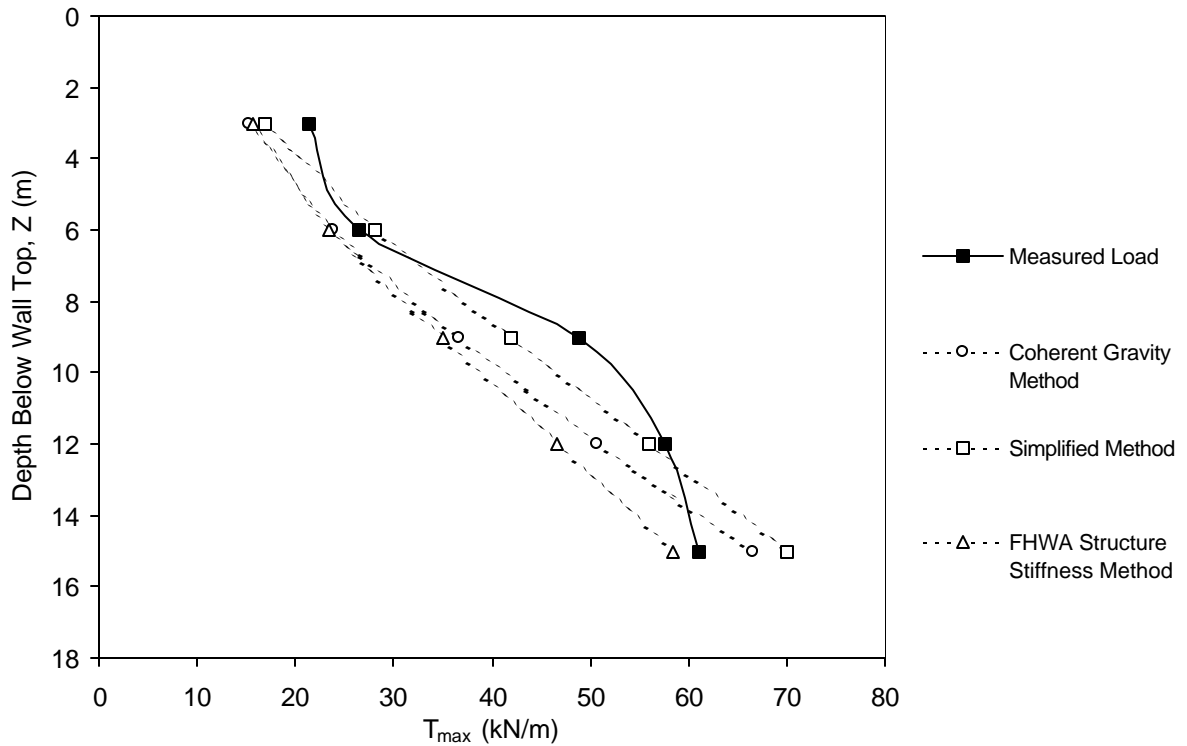

Figure A-8.   Predicted and measured reinforcement peak loads for Waltham Cross steel strip reinforced wall (SS5).
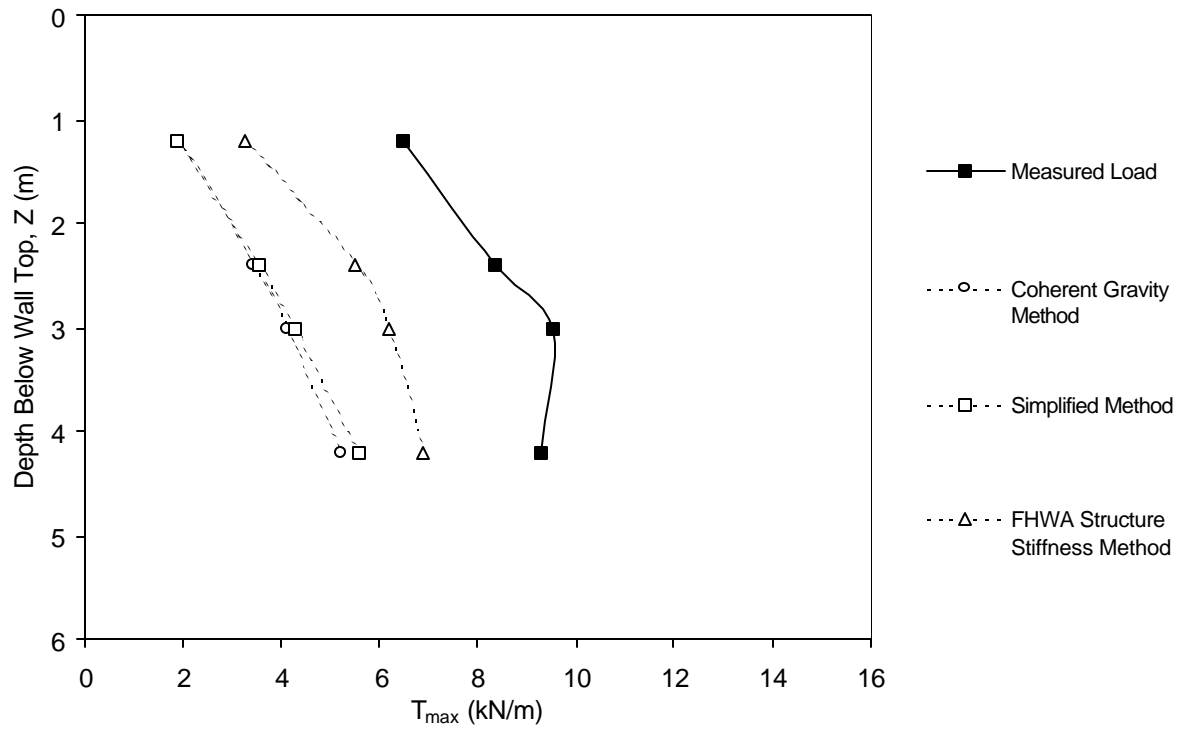
Figure A-9. Predicted and measured reinforcement peak loads for Guildford Bypass steel strip reinforced wall, Section A (SS6).
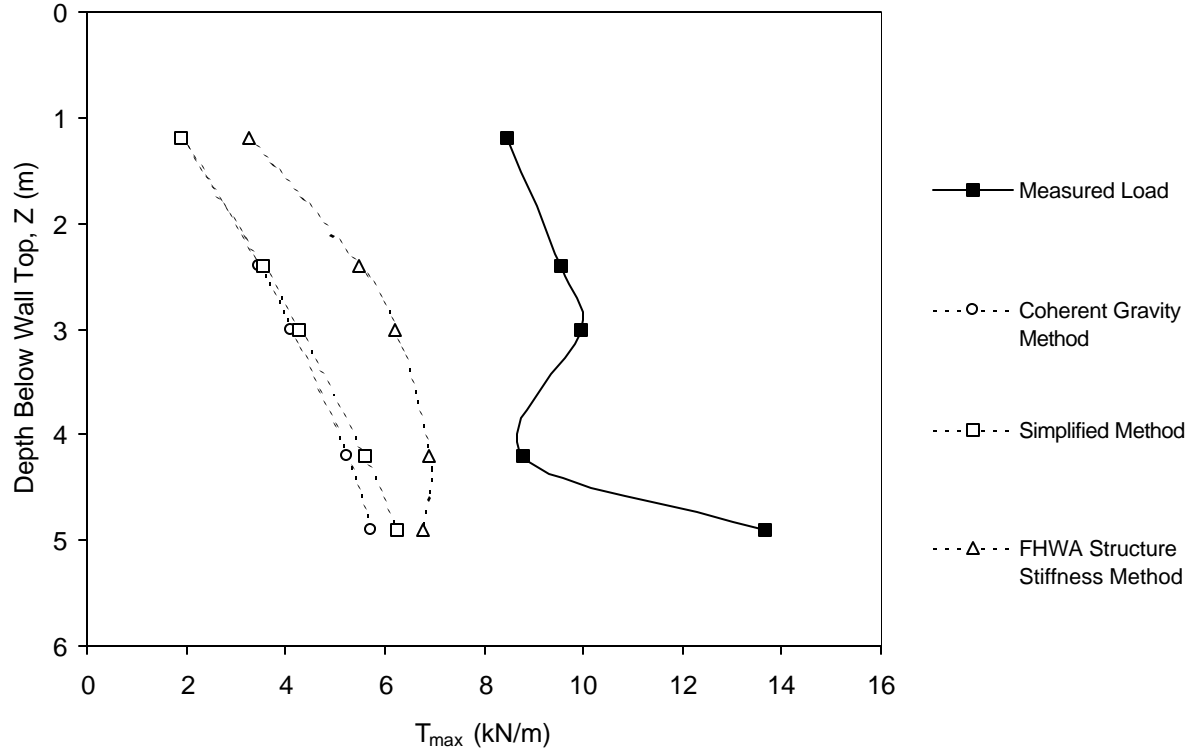
Figure A-10. Predicted and measured reinforcement peak loads for Guildford Bypass steel strip reinforced wall, Section B (SS6).
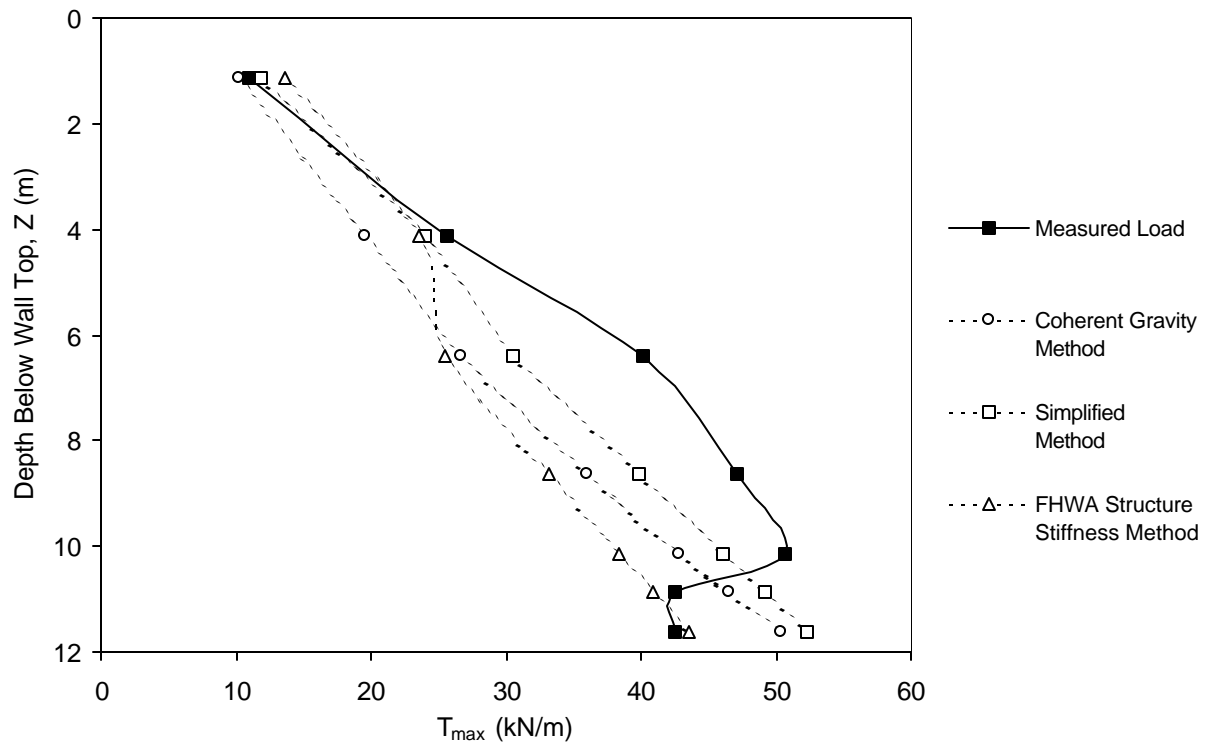
Figure A-11.   Predicted and measured reinforcement peak loads for Asahigaoka, Japan, steel strip reinforced wall (SS7).

Figure A-12.   Predicted and measured reinforcement peak loads for Ngauranga, New Zealand, steel strip reinforced wall (SS10).
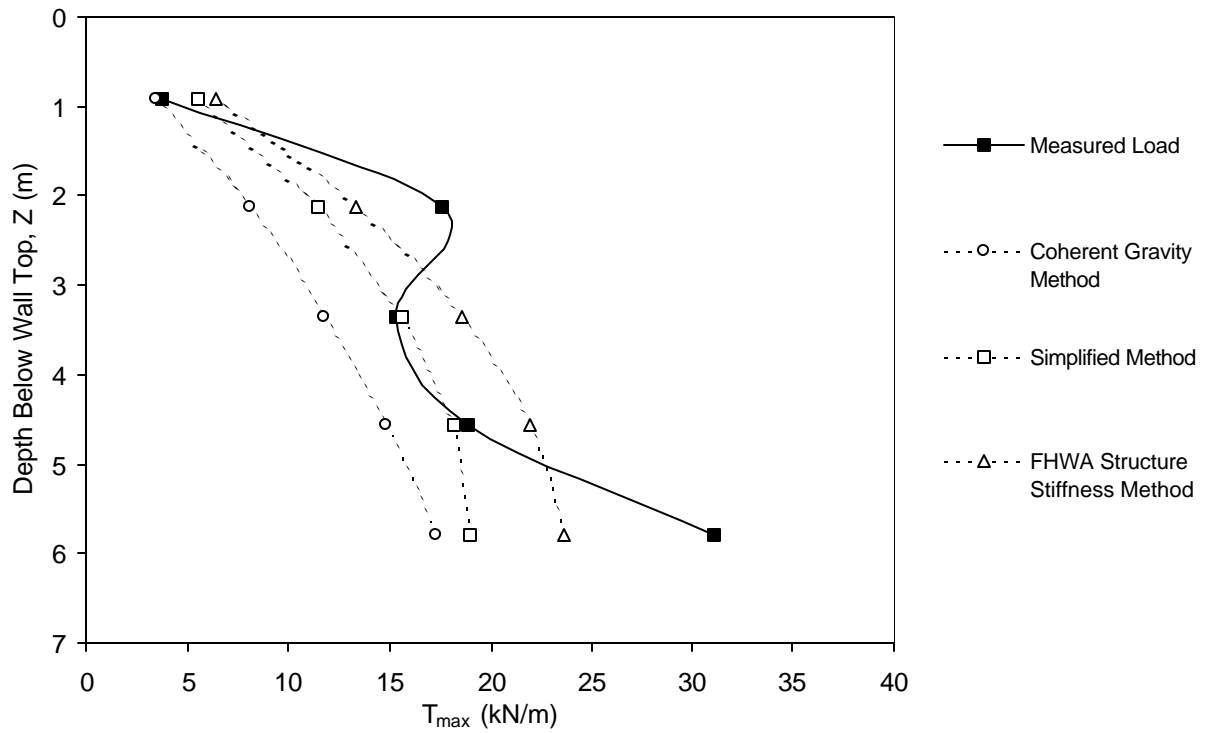
Figure A-13.   Predicted and measured reinforcement peak loads for Gjovik, Norway, steel strip reinforced wall, without surcharge (SS12).

Figure A-14.   Predicted and measured reinforcement peak loads for Gjovik, Norway, steel strip reinforced wall, with surcharge (SS12).

Figure A-15.   Predicted and measured reinforcement peak loads for Bouron Marlotte steel strip reinforced wall, rectangular section (SS13).
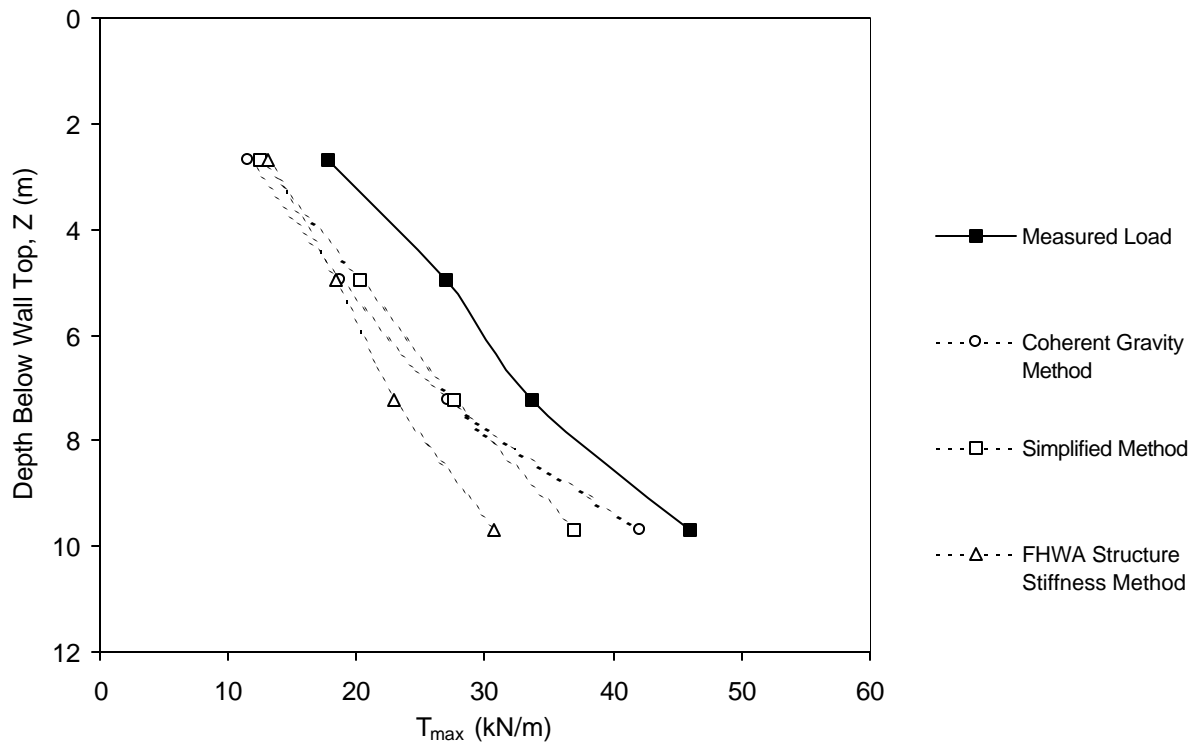
Figure A-16.   Predicted and measured reinforcement peak loads for Bouron Marlotte steel strip reinforced wall, trapezoidal section (SS14).

Figure A-17. Predicted and measured reinforcement peak loads for Algonquin steel strip reinforced wall (SS11).

Figure A-18. Predicted and measured reinforcement peak loads for INDOT Minnow Creek steel strip reinforced wall (SS15).

Figure A-19. Predicted and measured reinforcement peak loads for Hayward bar mat wall, Section 1, no soil surcharge (BM1).
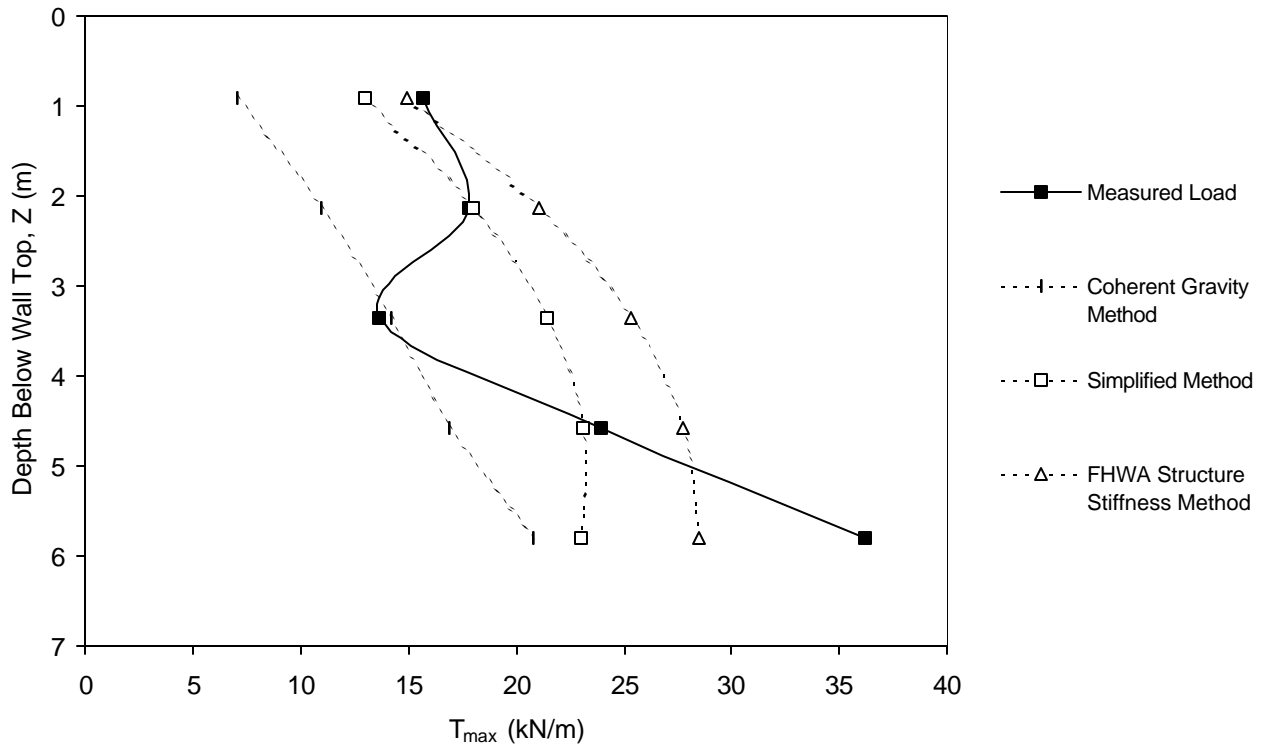
Figure A-20. Predicted and measured reinforcement peak loads for Hayward bar mat wall, Section 1, with soil surcharge (BM1).
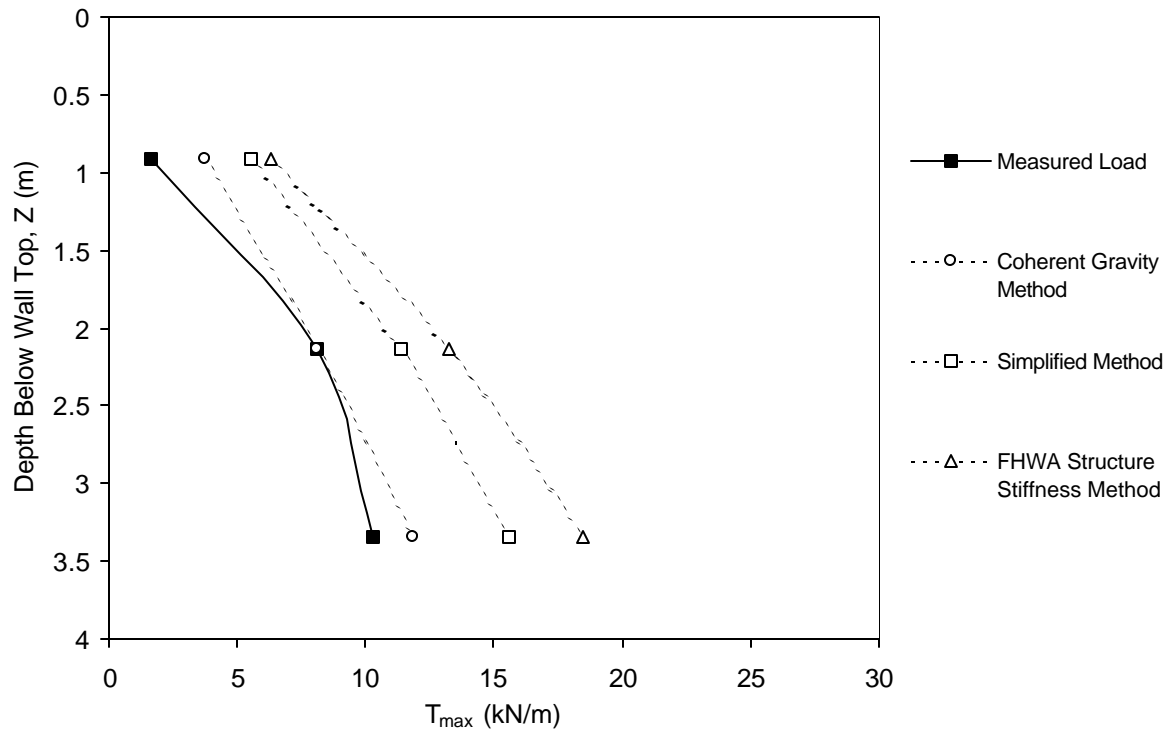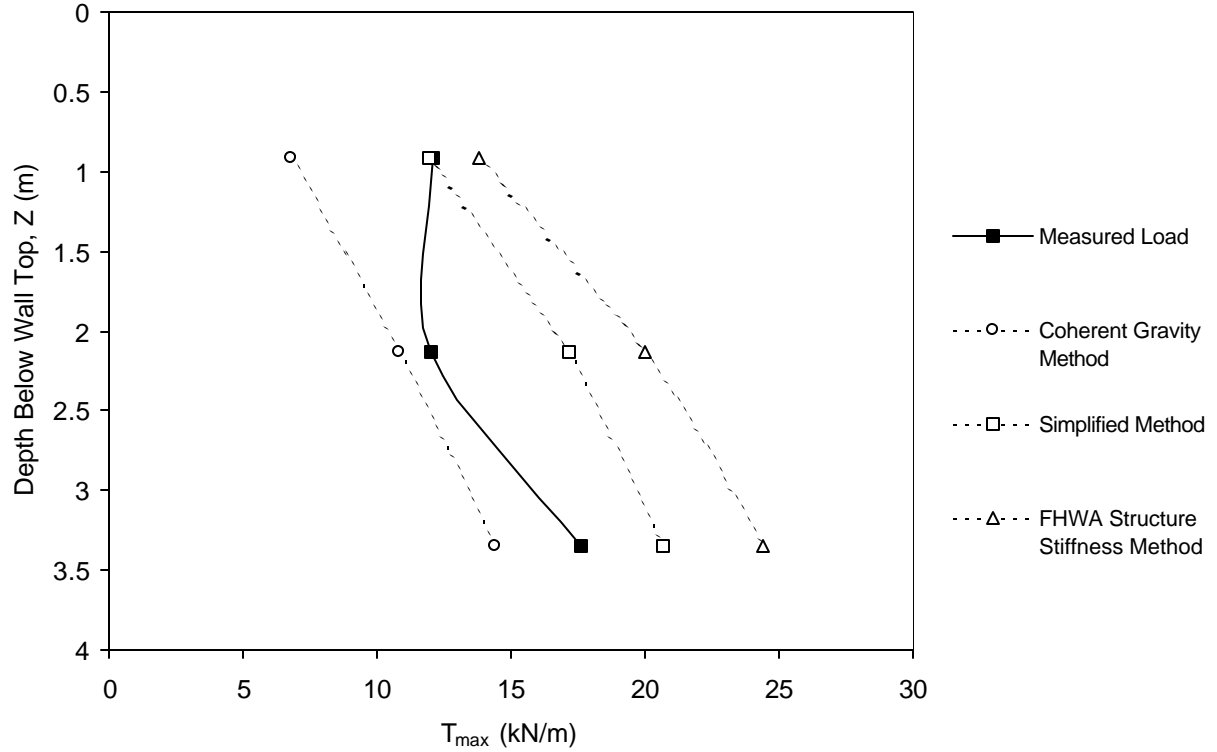
Figure A-21. Predicted and measured reinforcement peak loads for Hayward bar mat reinforced wall, Section 2, no surcharge (BM2).
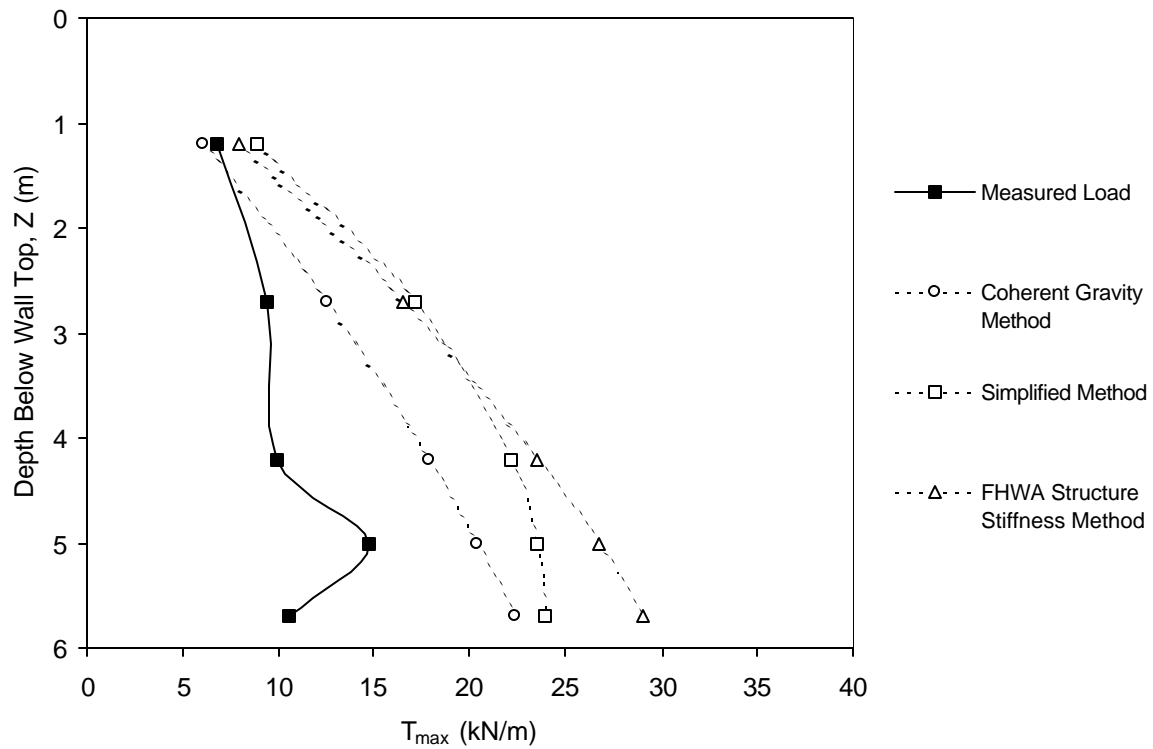

Figure A-22. Predicted and measured reinforcement peak loads for Hayward bar mat reinforced wall, Section 2, with surcharge (BM2).

Figure A-23.   Predicted and measured reinforcement peak loads for Algonquin sand backfill bar mat reinforced wall (BM3).
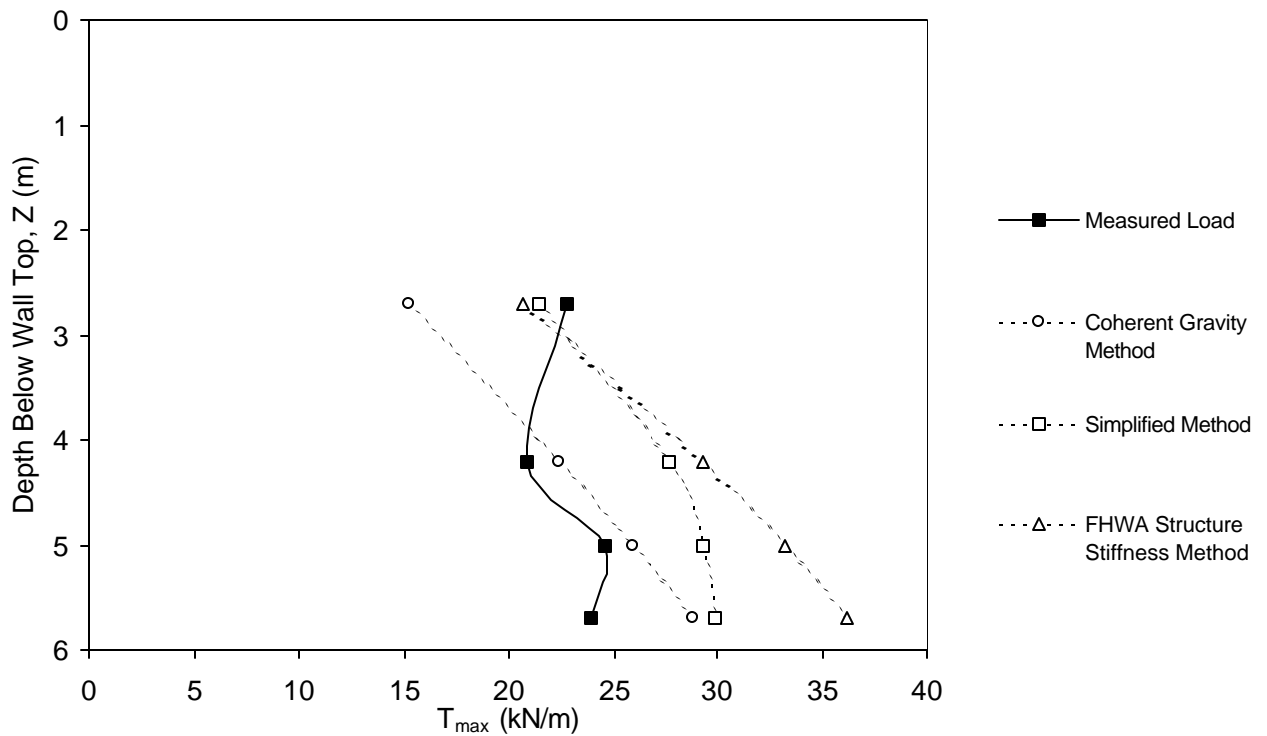

Figure A-24.   Predicted and measured reinforcement peak loads for Algonquin silt backfill bar mat reinforced wall (BM4).
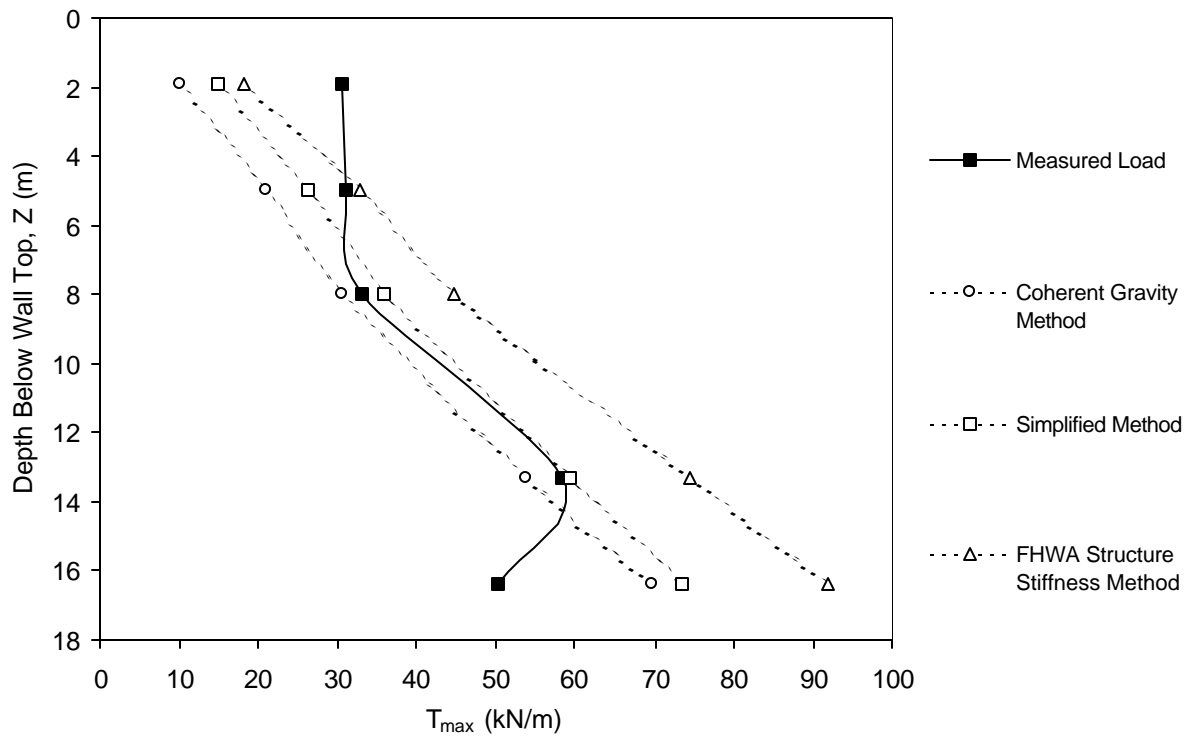
Figure A-25.   Predicted and measured reinforcement peak loads for Cloverdale, California, bar mat reinforced wall (BM5).
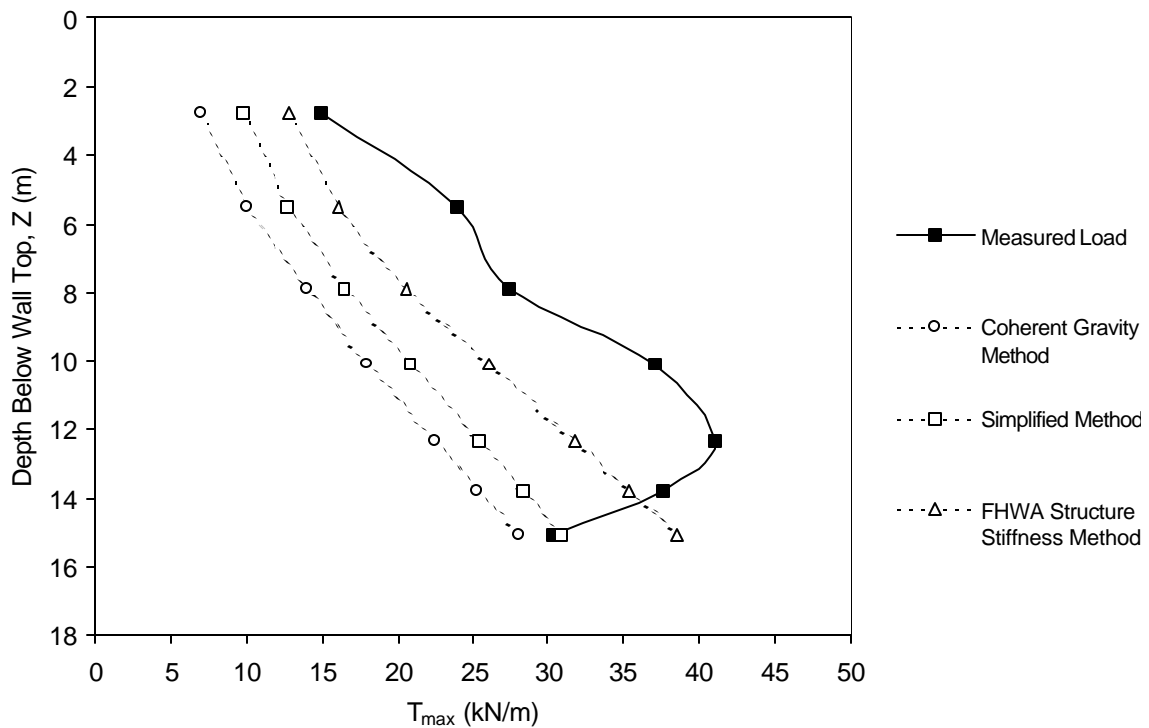

Figure A-26. Predicted and measured reinforcement peak loads for Rainier Avenue, Washington, welded wire wall (WW1).
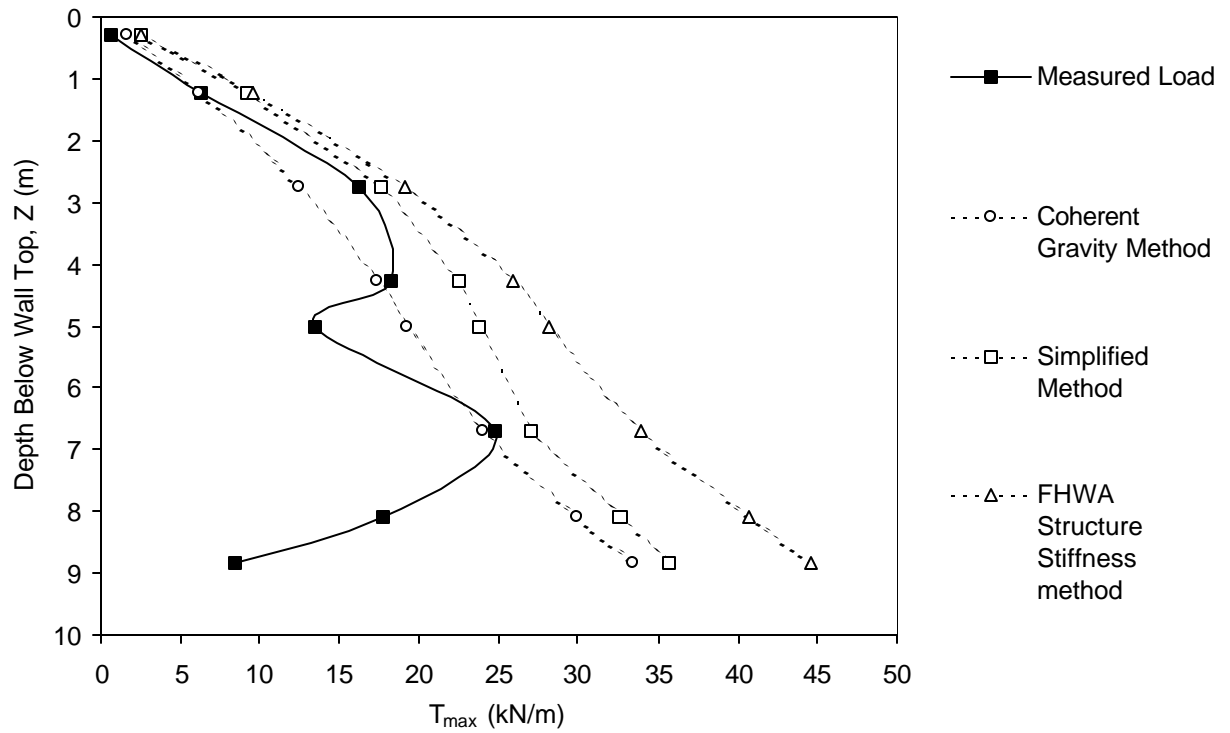
Figure A-27. Predicted and measured reinforcement peak loads for Texas welded wire wall (WW2).